STYRELSEN FÖR

VINTERSJÖFARTSFORSKNING

WINTER NAVIGATION RESEARCH BOARD

Research Report No 125

Ikka Perälä, Kai Katajamäki, Ville Valtonen

DIRECT CALCULATIONS METHODS FOR ICE STRENGTHENED HULLS IN THE FINNISH-SWEDISH ICE CLASS RULES

Finnish Transport and Communications Agency
Finnish Transport Infrastructure Agency
Finland

Swedish Maritime Administration
Swedish Transport Agency
Sweden

Talvimerenkulun tutkimusraportit — Winter Navigation Research Reports
ISSN 2342-4303
ISBN 978-952-311-873-7

FOREWORD

In this report no 125, the Winter Navigation Research Board presents the results of research project Direct calculations methods for ice strengthened hulls in the Finnish-Swedish Ice Class Rules. The project prepared the foundations for rule development of Finnish-Swedish ice class rules direct hull strength calculations. Effects of different modeling parameters were analyzed for different vessels.

The Winter Navigation Research Board warmly thanks Ikka Perälä, Kai Katajamäki and Ville Valtonen for this report.

Helsinki

August 2023

Ville Häyrynen

Finnish Transport and Communications Agency

Anders Dahl

Swedish Maritime Administration

Helena Orädd

Finnish Transport Infrastructure Agency

Stefan Eriksson

Swedish Transport Agency

RESEARCH REPORT

AKER ARCTIC K-523, VTT-R-01039-22

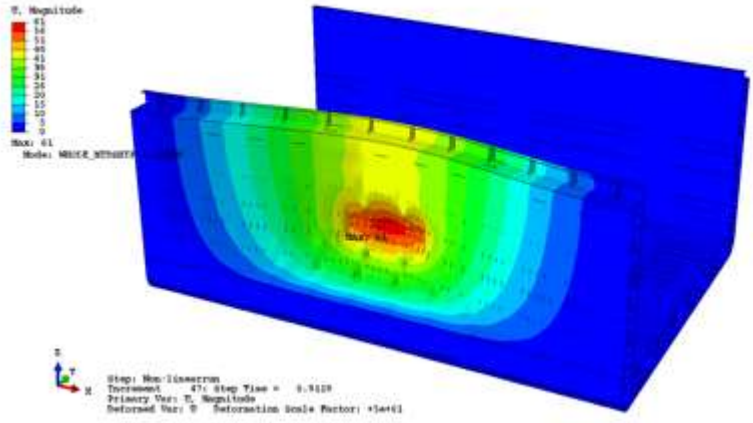

Direct calculations methods for ice strengthened hulls in the Finnish-Swedish Ice Class Rules

Authors:	Ilkka Perälä, VTT
	Kai Katajamäki, VTT
	Ville Valtonen, Aker Arctic

Confidentiality:	Public
Version:	30.12.2022

VTT Aker Arctic

beyond the obvious

Report's title Direct calculations methods for ice strengthened hulls in the Finnish-Swedish Ice Class Rules	
Customer, contact person, address Lauri Kuuliala Finnish Transport and Communications Agency, PO Box 320, FI-00101 Helsinki, Finland	**Order reference** W22-5 HULLFEM
Project name Direct calculations methods for ice strengthened hulls	**Project number/Short name** 132824 / HullFem_2022
Author(s) Ilkka Perälä (VTT), Kai Katajamäki (VTT), Ville Valtonen (Aker Arctic)	**Pages** 89
Keywords Non-linear; FEM; FSICR	**Report identification code** VTT-R-01039-22

Summary

The goal of the study was to lay groundwork for implementing guidelines in the Finnish-Swedish Ice Class Rules (FSICR) for using direct calculation methods (e.g. Finite Element Method, FEM) for assessing hull structural strength in the case of ice loads.

Major part of the work was to study in practice with FE analysis how the proposed concepts on modelling and criteria would work on different sized vessels with different ice class. It was decided to focus on general / bulk cargo vessels as these are most frequent ship type operating in ice in the Baltic Sea. Three different sizes (3000 DWT, 10 000 DWT and 58 000 DWT) of vessels, corresponding to typical sizes on the Baltic Sea, were designed and modelled. From 10 000 DWT ship three different ice class (IA, IASuper and IC) versions were modelled.

The Baseline 10 000 DWT IA model worked as test model for testing how mesh size, model size, boundary conditions and different material models affect the results. From these studies, results were gathered for suitable proposals for the future guideline text.

For determining the plastic capacity of the structure, criteria were chosen to be to limit the permanent deformation of the structure to remain below limits of IACS newbuilding quality standard [1]. All chosen vessels were loaded with various load patches to understand the capacity of the structure against the chosen criteria, and to find the most onerous load patch locations and sizes. The load patches followed the FSICR. In general, the plastic capacity of the shell and framing was found to be about 300 to 400 % of elastic rule design load. For stringers and web frames, the typical double side construction resulted in structure where capacity is not limited by bending capacity, but rather by buckling, and clear conclusions of capacity of structures according to current rules could not be drawn. For this, further research with single skin type vessels is recommended.

Finally, some recommendations for future rule formulation are given. However, further research is required before the final rule formulation can be given.

Confidentiality	Public

Espoo 30.12.2022

Written by	**Reviewed by**
Ilkka Perälä Research Scientist	Katajamäki Kai Principal Scientist

VTT's contact address
VTT Technical Research Centre of Finland Ltd. P.O Box 1000, FI-02044 VTT, Finland

Distribution (customer and VTT)

Approval

VTT TECHNICAL RESEARCH CENTRE OF FINLAND LTD

Date:	
Signature:	
Name:	
Title:	

Aker Arctic

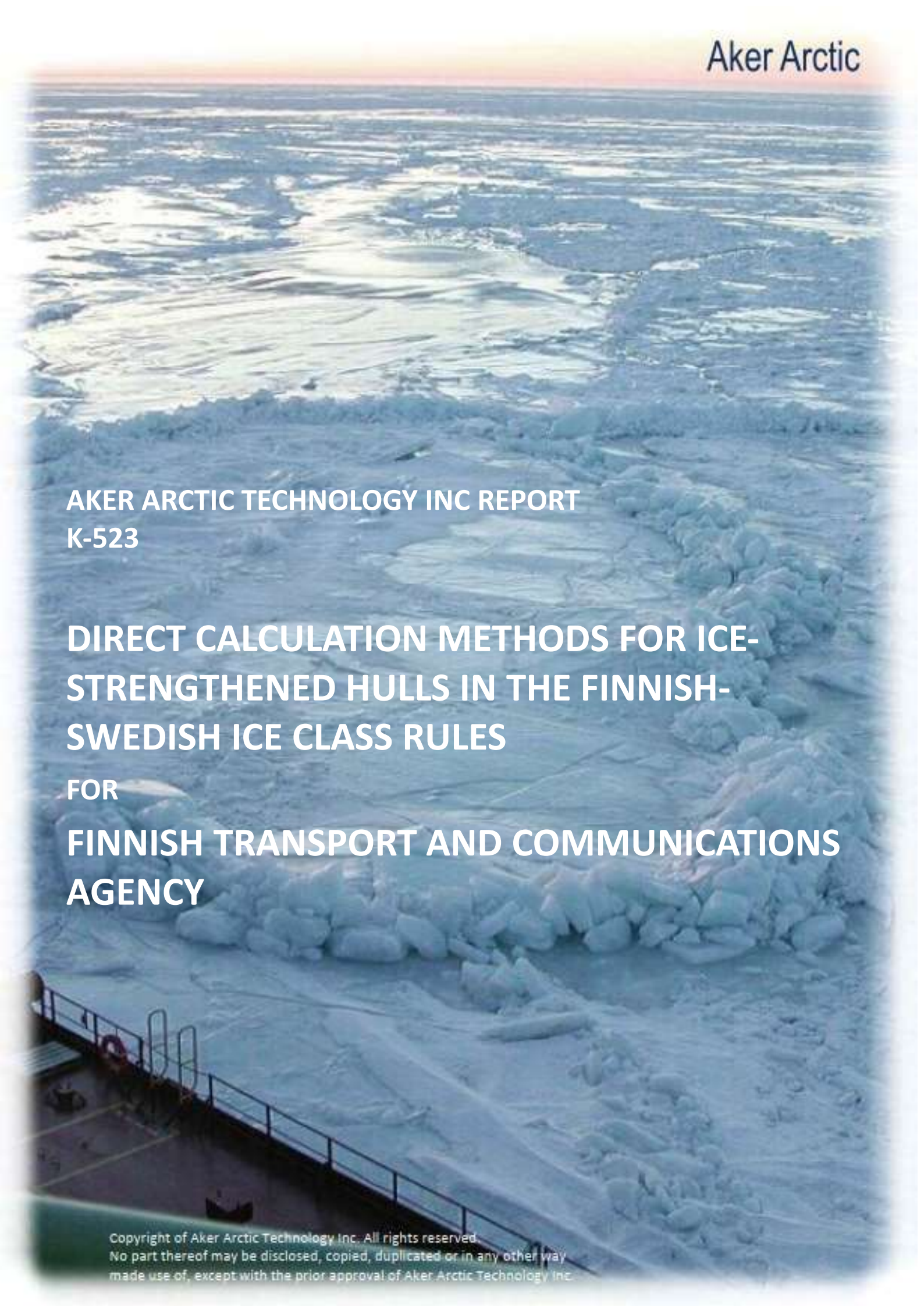

AKER ARCTIC TECHNOLOGY INC REPORT
K-523

DIRECT CALCULATION METHODS FOR ICE-STRENGTHENED HULLS IN THE FINNISH-SWEDISH ICE CLASS RULES

FOR

FINNISH TRANSPORT AND COMMUNICATIONS AGENCY

Name of document: Direct calculation methods for ice-strengthened hulls in the Finnish-Swedish Ice Class Rules	
Document Responsible: Valtonen Ville	**Document Co-Author(s):** Ilkka Perälä, VTT Kai Katajamäki, VTT
Document Reviewer: Hindley Rob	**Document Approver:** Valtonen Ville
Report number / Revision: K523 / A	**Status / Status Date:** 30.12.2022
Client: Finnish Transport and Communications Agency / Lauri Kuuliala	
Revision remarks:	

Summary:
The goal of the study was to lay groundwork for implementing guidelines in the Finnish-Swedish Ice Class Rules (FSICR) for using direct calculation methods (e.g. Finite Element Method, FEM) for assessing hull structural strength in the case of ice loads.

Major part of the work was to study in practice with FE analysis how the proposed concepts on modelling and criteria would work on different sized vessels with different ice class. It was decided to focus on general / bulk cargo vessels as these are most frequent ship type operating in ice in the Baltic Sea. Three different sizes (3000 DWT, 10 000 DWT and 58 000 DWT) of vessels, corresponding to typical sizes on the Baltic Sea, were designed and modelled. From 10 000 DWT ship three different ice class (IA, IASuper and IC) versions were modelled.

The Baseline 10 000 DWT IA model worked as test model for testing how mesh size, model size, boundary conditions and different material models affect the results. From these studies, results were gathered for suitable proposals for the future guideline text.

For determining the plastic capacity of the structure, criteria were chosen to be to limit the permanent deformation of the structure to remain below limits of IACS newbuilding quality standard [1]. All chosen vessels were loaded with various load patches to understand the capacity of the structure against the chosen criteria, and to find the most onerous load patch locations and sizes. The load patches followed the FSICR. In general, the plastic capacity of the shell and framing was found to be about 300 to 400 % of elastic rule design load. For stringers and web frames, the typical double side construction resulted in structure where capacity is not limited by bending capacity, but rather by buckling, and clear conclusions of capacity of structures according to current rules could not be drawn. For this, further research with single skin type vessels is recommended.

Finally, some recommendations for future rule formulation are given. However, further research is required before the final rule formulation can be given.

Keywords:
Non-linear; FEM; FSICR

Client reference: W22-5 HULLFEM		**Project number:** 30864	**Language:** English
Pages, total: 89	**Attachments:** 6	**Distribution list:**	**Confidentiality:** Public

Contents

1. Introduction

In recent years there has been a need for guidelines in the Finnish-Swedish Ice Class Rules (FSICR) for using direct calculation methods (e.g. Finite Element Method, FEM) for assessing hull structural strength in the case of ice loads. This need mainly comes from industry (shipyards) where the current rules and prescriptive rule formulas are seen as somewhat limiting. Rule limitations with respect to allowable structural arrangements are derived from operational experience, and by limiting the allowed structural arrangements to follow the guidelines, design can be made with simple prescriptive formulas. However, a thorough FE analysis with well-defined criteria would offer more options for structural design but still maintain safety in operation.

Direct calculation methods are nowadays frequently used in the ship design process to optimize the strength of the hull against different kinds of loads. In case of open water loads, for example, fatigue loads are an important case. Classification societies usually have detailed guidelines regarding the analysis methodology for direct calculation methods. However, in the case of application of ice loads, and especially considering the FSICR, there is still a lack of guidelines for direct calculation methods.

Ice loads are somewhat different from open water loads because they are very local, and highest loads are not repeated as often, making fatigue a less of a concern. In addition, the magnitude of the highest loads is very high, up to and beyond yield. There is also a higher level of uncertainty regarding the load magnitude and load patch size/shape. The design target in practice is that there should not be such denting of hull that repairs would be necessary, and obviously any larger damages that would endanger the load-carrying capability or tightness of the structure need to be avoided with a margin of safety, but it is generally accepted that small local denting of the shell plating is acceptable as long as there is sufficient margin against other more severe failure modes, such as rupture, tripping of frames and buckling of plate structures.

Earlier, direct calculation has practically meant either linear FE analysis or grillage analysis. In recent years, research has been published (for example, [2] and [3]) and some guidelines on direct calculation methods for ice loads have been issued by classification societies for the PC Rules, such as [4], [5] and [6] using non-linear FE, which allows for evaluating the response of the structure beyond yield and is thus better suited for analysing structures under ice loads. However, there is still on-going discussion on the modelling methods and chosen criteria.

In the FSICR the scantlings for beams, stiffeners and webs and thicknesses for plating come from a simple prescriptive rule formula which are validated by operational experience. Complementing the strength requirements are structural arrangement / structural detail required for the structural members. For example, the use of brackets is mandatory for many structures. These rules work well but are somewhat limiting for the hull designer.

The use of direct calculation is a much more accurate way of understanding how the structure behaves under load. However, the results are dependent on modelling techniques, application of loads and acceptance criteria. Thus, all these must be taken into account carefully by the designer. It is important that the rules and guidelines for direct calculation are made understandable and easy to use. The criteria for structural strength must be conservative enough for safe design. However, too conservative criteria will lead to excess weight and will be economically demanding for the ship owners.

2. Goal

The goal of the HULLFEM project is to gather a better understanding of using direct calculation methods in the case of ice loads. This is important background knowledge for future ice class rule development work.

To understand and study the criteria for use in calculation methods and allowable structural capacity, the project will incorporate example calculations with direct calculation methods.

The main tasks of the present study is to set ground what kind of FE modelling methods should be used by the designer, what are the loads and how the loads are set up in the model.

3. Background

3.1 Linear and non-linear finite element analysis

Currently, all requirements for hull scantlings in the Finnish-Swedish Ice Class Rules are based on prescriptive rule formulas and requirements. The formulas are based on linear elastic analysis and elastic limit state.

If alternative designs with direct calculations, in practice finite element method, would be taken into rules, it could be done with either linear or non-linear FE. While linear FE would bring some additional design freedom compared to prescriptive requirements, it is seen that much of the potential of direct calculation would be missed. Moreover, as the actual target is to limit permanent deformation to remain small during service and ensure that the structure has sufficient margin against larger permanent deformation, using linear analysis and assuming some plastic reserve could lead to erroneous results in some cases, if only elastic capacity would be assessed and constraints on the structural arrangement would be relaxed.

Therefore, non-linear finite element analysis would be preferable option, as that will give information of the actual margin, instead of assumption that certain amount of plastic margin exists. [7] Especially, non-linear analysis gives much improved insight into actual reserve capacity of nonconventional structural arrangements, such as leaving out brackets that support the ice frames. Thus, non-linear analysis is used in this study.

Earlier, there was a tentative note for using non-linear FE for designing longitudinally framed structures for the FSICR by ABS [8]. However, that method required modelling first the rule compliant structure and then the proposed alternative arrangement, requiring double work. It would be desirable to formulate a set of criteria that would not require two models but modelling only the proposed structure and showing that it has adequate capacity against ice loads. For formulating those criteria, several vessels complying with the current rules are modelled in this study, and the plastic capacity of those structures is analysed.

3.2 Design point in the Finnish-Swedish Ice Class Rules

The design point in the Finnish-Swedish Ice Class Rules is discussed in [9]. Essentially, the current formulations assume a design load that occurs relatively often, and the structure is designed remain below yield limit at that load. Then, it is assumed that since typical shipbuilding steel is ductile and structural arrangement is dictated by the rules, the structure will have sufficient plastic reserve to cope with more rarely occurring loads that exceed the rule design load [8]. Similar scantlings could also be achieved by using a higher design load with longer return period together with higher limit state, such as some defined amount of permanent deformation. This is illustrated in Figure 1.

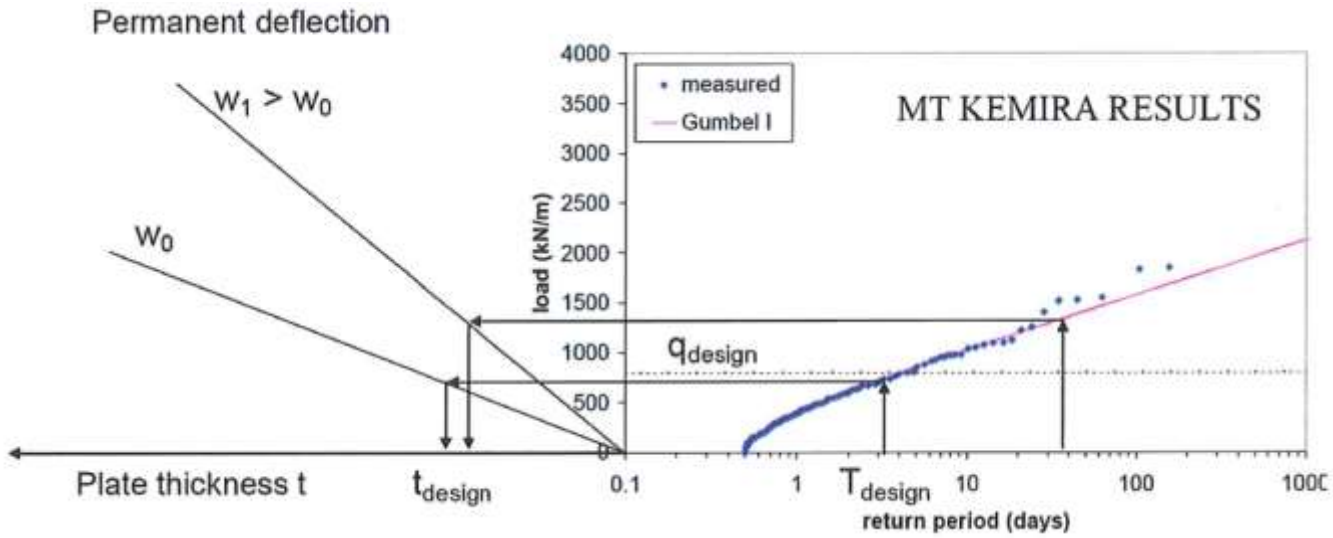

Figure 1 Design point in the Finnish-Swedish Ice Class Rules. [9]

The underlying aim of the design load and the scantling calculations that follow from the design load is to ensure structure that has sufficient strength for the expected loads in service. The main targets are to ensure safety and serviceability, i.e. that even if small dents are allowed and happen occasionally, repairs are not needed due to denting, and that there is sufficient margin against larger damage. To achieve these targets, the Rules are based on load measurements and research, and damage studies have been made to calibrate the rule loads to the loads encountered in service.

Two large damage studies have been made into the fleet of ships that have a Finnish-Swedish ice class. First study was made by Kujala in 1984 to 1987 [10], and later one by Hänninen in 2003 to 2003 [11]. The damages to shell of the vessel from both reports are collected into Table 1.

As a background info to this table, it should be noted that hull rules were completely reformatted in 1985 [12] [13], and these apply to ships which have their keel laid in 1986 and forwards. From the table, it can be concluded that after the introduction of 1985 rules, the damages are limited to dented shell plates, and all damages to framing and primary members have happened to ships built to previous rules. Thus, the maximum expected ice loads should be tied to the typical maximum plate damages observed.

The rules for shell plate design have not been changed between 1985 and 2008. In the 2010 rules, the design pressure for longitudinally framed vessels was increased by removing the factor of 0.75 in calculation of the design pressure [6] [7] [8] [9]. The reason for removing this factor for longitudinal framing is explained by Riska and Kämäräinen to follow from that the concept of varying pressure is more relevant to transverse than longitudinal framing [9]. Later studies have proven that ice pressure does not vary appreciably along transversally framed shell plate regardless of stiffness difference between shell plate and framing [17] [18].

The origin of the higher design load for framing was to compensate for the larger plastic reserve of the plate compared to a frame, as a means to achieve a balanced design in plastic region while using elastic capacity formulas in the design [9]. Based on the damages observed for ships built to the 1985 and later rules, the structures designed with the rules seem to have proper hierarchy, so that tertiary member (shell plate) is deformed before secondary (frames).

Table 1 Ice damages on shell from winters 1984-87 and 2002-2003

Ship	Ice class	Ship type	Built	DWT / BRT	Framing	frame spacing	plate dents	Plate dent, % of spacing	Location	frame deformation	frame span	Frame deformation, % of span
2002-2003 study by Hänninen												
Ship 98	1A	Bulk carrier	1976	10980	transv.	800	50	6.3 %	Ice belt	-	-	-
Ship 66	1A	Tug	1968	240	transv.	270	10	3.7 %	Ice belt	30	2400	1.3 %
Ship 76	1C	Oil tanker	1993	95000	longit.	800	30	3.8 %	Ice belt	-	-	-
Ship 55	1A super	Bulk carrier	1986	3900	longit.	1300	50	3.8 %	Below	-	-	-
Ship 30	1A	Passenger-car ferry	1966	10500	transv.	750	50	6.7 %	Below	-	-	-
Ship 44	1A	Chemical tanker	1984	22700	transv.	600	30	5.0 %	Below	-	-	-
					longit.	800	30	3.8 %	Below	-	-	-
Ship 100	1A	Cruise ship	1992	25600	transv.	800	40	5.0 %	Below	-	-	-
Ships 89 & 90	1A super	Oil tanker	1976	16420	Not relevant, damage from Arctic voyages							
1984-1987 study by Kujala												
Ship 4	1A super	Dry cargo	1978	14931	transv.	400	20	5.0 %	Ice belt	10	3000	0.3 %
Ship 7	1A super	Dry cargo	1972	7214	transv.	380	10	2.6 %	Ice belt	33	3000	1.1 %
					longit.	450	10	2.2 %	Ice belt	-	-	-
					transv.	600	23	3.8 %	Below	-	-	-
Ship 13	1A super	Chemical tanker	1980	8145	transv.	350	20	5.7 %	Ice belt	10	3200	0.3 %
					longit.	350	20	5.7 %	Ice belt	-	-	-
					longit.	700	15	2.1 %	Below	-	-	-
Ship 14	1A	Bulk carrier	1976	10935	Lots of damage below ice strenghtening, due to insufficient ballast capacity and too low draught. Not relevant here.							
Ship 16	1A	Dry cargo	1972	5915	transv.	350	25	7.1 %	Below	70	3500	2.0 %
Ship 21	1A super	Cargo ferry	1982	13090	transv.	400	10	2.5 %	Below	-	-	-
					transv.	800	15	1.9 %	Below	-	-	-
Ships 22-25	1A	Bulk carrier	1977	16560	longit.	400	30	7.5 %	Ice belt	30	3300	0.9 %
Ship 35	1A	Bulk carrier	1985	4693	transv.	350	15	4.3 %	Ice belt	50	2500	2.0 %
					transv.	700	10	1.4 %	Below	-	-	-
Ship 37	1A	Bulk carrier	1980	31850	transv.	-	-	-	Ice belt	200	2500	8.0 %
Ship 39	1A	Bulk carrier	1977	7885	Complete collapse of web frames & framing in compressive ice, max. Deflection 500 mm							
Ships 43 & 44	1A	Passenger ferry	1980	10604	transv.	400	25	6.3 %	Below	-	-	-
					transv.	800	30	3.8 %	Below	-	-	-
Ship 45	1A super	Cargo ferry	1982	7000	longit.	300	30	10.0 %	Ice belt	55	2800	2.0 %
Ships 48-50	1A super	Tanker	1976	15954	transv.	343	30	8.7 %	Ice belt	-	-	-
					transv.	350	50	14.3 %	Above	-	-	-
Ship 51	1A super	Tanker	1974	6863	transv.	350	15	4.3 %	Ice belt	-	-	-
					transv.	700	15	2.1 %	Above	-	-	-

Significant portion of the damages have occurred on the lower hull regions where the FSICR are not applied and fall outside the scope of this study. For the damages occurred on the ice strengthened region of the hull for vessels built to 1985 rules or later, the plate deformation is 5 % of frame spacing or less, and no framing damages have been observed.

For defining the required capacity for the non-linearly analysed alternative structure, there is two main aims. First, it should be ensured that amount of ice damages (denting of plates, bending of frames) that need repairs will not increase, and the structures remain serviceable and able to carry the design load after being subjected to ice loads. Second, it should be ensured that if subjected to highest loads measured, the structure may dent and require repairs, but should remain safe, i.e. watertightness of the hull should not be compromised, and the structure should retain load-carrying capacity, i.e. buckling and tripping should be limited so that sudden loss of load-carrying capacity is prevented. Based on the damage data above, the second criteria should be met at load that cause permanent plate deformation of 5 % of the frame spacing.

4. Chosen example vessels

Major part of the study is to examine example vessels with direct calculation methods. This enables testing of different modelling methods for realistic vessel designs used in the Baltic Sea.

4.1 General

The example vessels for this study were selected to represent typical Finnish-Swedish Ice Class ships as well as possible. Based on the traffic statistics from winter 2018-2019 in the Bay of Bothnia, the most common ship type is a general cargo vessel, as shown in Figure 2.

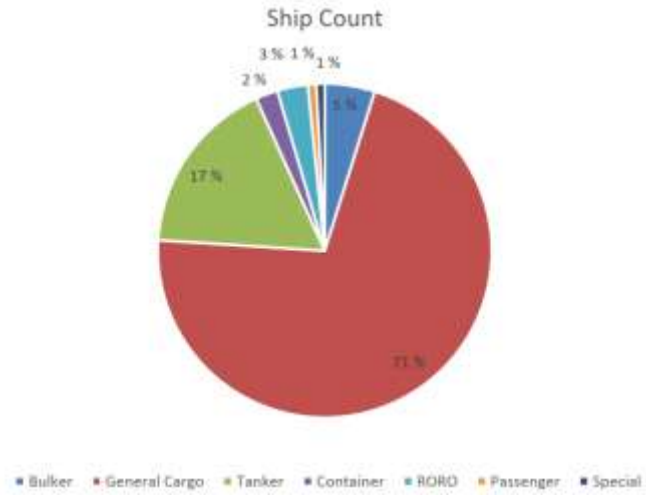

Figure 2. Ships that have visited in the Bay of Bothnia in winter 2019, categorized by type. [19]

Ship size, measured in DWT, is shown in Figure 3. From this data, it was concluded that most typical ship size is around 10 000 DWT, which was selected as the baseline vessel. It should represent well the most common ships that are sized between 5 000 DWT and 15 000 DWT.

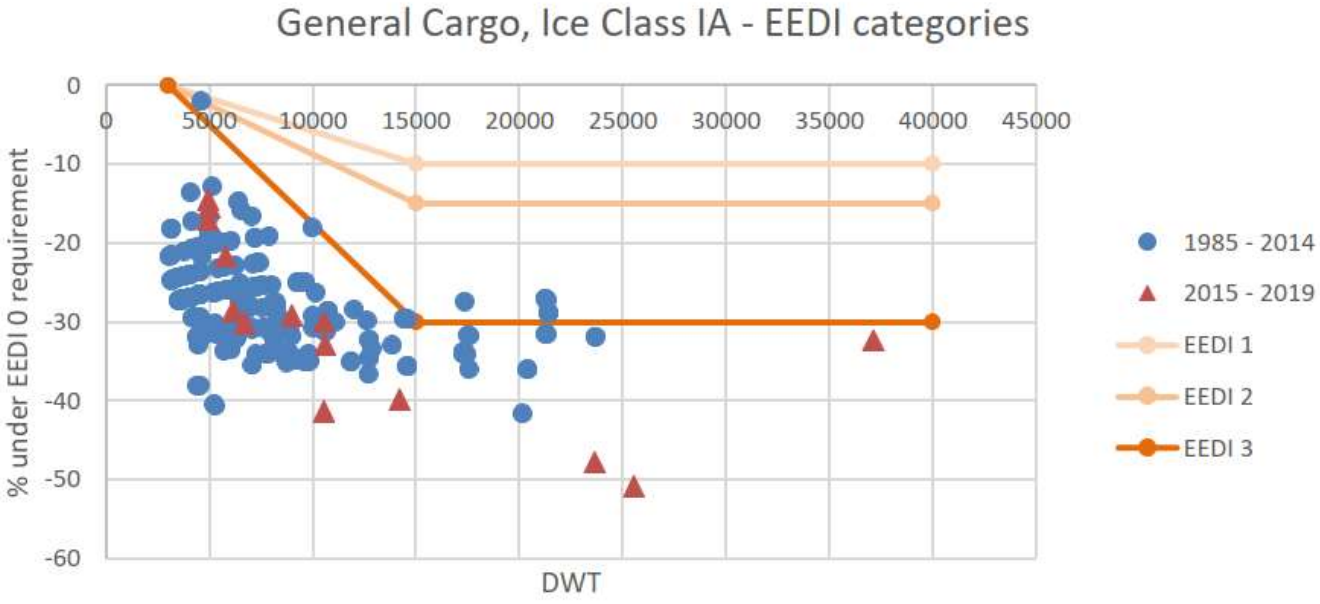

Figure 3. General cargo ships that have visited Bay of Bothnia in winter 2019. Y-axis represents the difference of calculated EEDI and phase 0 EEDI in percentage. Lines show the EEDI phase 1 - 3 requirements. New ships built after 2014 are highlighted. [19]

In addition, a smaller and larger vessel were studied to cover the different structural configurations and particulars of the vessels that typically trade in the Baltic Sea in winter. The smaller end of the range is limited by icebreaker assistance, which is in winter provided to vessels that have a minimum DWT ranging from 2 000 to 4 000 DWT depending on ice conditions. To cover this category, a 3 000 DWT vessel was selected. It is also noted that typical Saimax vessel has a DWT capacity of about 2 500 DWT on Saimaa channel draft and about 3 500 DWT on seagoing draft [20], so this vessel covers Saimaa vessels as well.

On bigger end of the range, it is anticipated that vessel size is going to increase somewhat, as Sweden plans for larger vessels to visit Luleå port. To represent the maximum typical size of vessels on the Baltic Sea, a 58 500 DWT vessel was selected, corresponding roughly to typical old Panamax size vessel.

Based on the traffic statistics from [19], shown in Figure 4, the most common ice class is IA, and thus that was selected as the base ice class for this study. In addition, ice classes IC and IA super will be studied to ensure good coverage. Main data of all the example vessels is shown in Table 2. Summary of shell plate and frame scantlings is shown in Table 3. Full scantling calculations are presented in Appendix F.

Table 2 Main data for example vessels.

	10 000 DWT 1A	**10 000 DWT 1C**	**10 000 DWT 1Asuper**	**3 000 DWT 1A**	**58 500 DWT 1A**		
DWT	10000	10000	10000	3000	58500	t	*Deadweight*
L	121	120.2	122.6	84.0	196	m	*Length*
B	20.3	20.3	20.3	14.0	32.26	m	*Breadth*
D	10.7	10.7	10.7	7.0	18.6	m	*Depth*
T	7.4	7.4	7.4	5.7	13.0	m	*Draught*
LS	4200	4100	4360	1960	11430	t	*Lightship weight*
Δ	14200	14100	14360	4960	69930	t	*Displacement*
Cb	0.75	0.75	0.75	0.758	0.83		*Block coefficient*
v	12	12	12	12	12	kn	*Service speed*
P	4000	3000	5500	1650	14750	kW	*Shaft power*
Framing	Transv.	Longit.	Transv.	Transv.	Longit.		*Framing orientation*
s	0.4	0.6	0.4	0.4	0.7	m	*Frame spacing*

Table 3 Summary of ice class scantlings for the example vessels.

			Shell		**Frames**				
Ship	**Framing**	**s** (m)	$t_{req.}$ (mm)	t_{actual} (mm)	**Profile**	$A_{req.}$ (cm^2)	A_{actual} (cm^2)	$Z_{req.}$ (cm^3)	Z_{actual} (cm^3)
3 000 DWT IA	Transv.	0.4	12.5	12.5	HP 180x10	4.0	18	173	177
10 000 DWT IC	Longit.	0.6	14.3	15.0	HP 140x9	9.6	12.6	93	98
10 000 DWT IA	Transv.	0.4	13.3	14.0	HP 160x9	4.6	14.4	123	128
10 000 DWT IAsuper	Transv.	0.4	15.1	15.5	HP 180x9	6.5	16.2	171	171
58 500 DWT IA	Longit.	0.7	23.7	23.5	HP 260x12	28.8	31.2	278	520

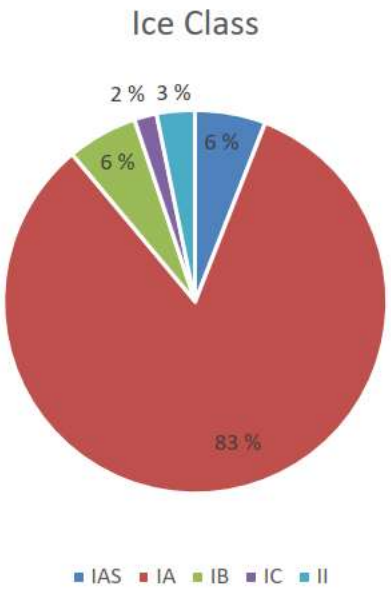

Figure 4. Ships that have visited in the Bay of Bothia in winter 2019, categorized by ice class. [19]

4.2 Baseline vessel, 10 000 DWT IA

The baseline vessel for this study was selected to be a dry cargo vessel with deadweight capacity of 10 000 t and ice class IA. The main dimensions for the vessel were selected based on [21], and are shown in Table 4. The midship section is shown in Figure 5.

Table 4 Main dimensions for 10 000 DWT IA dry cargo vessel.

DWT	10000	t	*Deadweight*
L	121	m	*Length*
B	20.3	m	*Breadth*
D	10.7	m	*Depth*
T	7.4	m	*Draught*
LS	4200	t	*Lightship weight*
Δ	14200	t	*Displacement*
Cb	0.75		*Block coefficient*
v	12	kn	*Service speed*
P	4000	kW	*Shaft power*

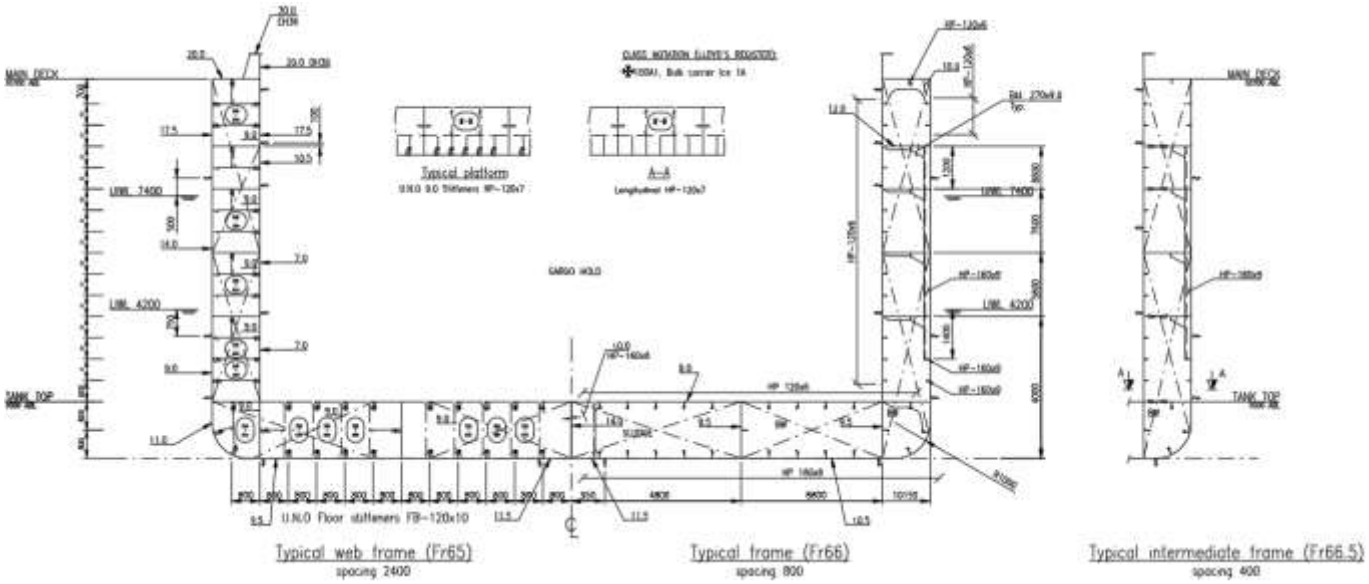

Figure 5. Midship section for 10 000 DWT IA vessel.

Ice loads for the 10 000 DWT IA cargo vessel were calculated according to the current (2017) FSICR. The different load cases are listed in Table 5 below. It should be noted that the loads listed are not meant for direct calculation, but they are used as a starting point.

Table 5. Load patch size and pressure for different load cases for 10 000 DWT IA vessel.

Structural part	**Load patch size**			
	Height [m]	**Width [m]**	**Pressure [MPa]**	**Tot. force [kN]**
Shell plating	0.30	0.40	1.306	157
Frame	0.30	0.40	1.306	157
Stringer	0.30	2.40	0.653	470
Web frame	0.30	4.80	0.462	665

Two finite element models were made of the baseline vessel. One model was used for studying effect of various modeling aspects, such as mesh density, material model and boundary conditions. This model included the double bottom and it was duplicated and mirrored to study different sizes of models. These models are shown in Figure 40.

The other model of the baseline vessel was made to study the most onerous locations for the load patch and to find out the capacity of the structure according to the limits defined in 5.3.3. This finite element model of the baseline vessel is shown in Figure 6, Figure 7, Figure 8. For this model, the double bottom was left out of the model, as it has been earlier found out that typically it does not have a significant effect on the results for a typical icebreaker, and as quite many (44 in total) load patch locations were studied, model size was limited to reduce the calculation time. For a few load cases on stringers and web frames, it was found out that the model size was slightly too small and boundary conditions had some effect on the results, but none of these load cases were the limiting ones, and thus this had no effect on the results.

The load application and boundary conditions are shown in Figure 9. For this vessel, a wide selection of load patch sizes and locations was tested to find the most onerous ones. All tested locations are shown in Figure 10, Figure 11, Figure 12 and Figure 13.

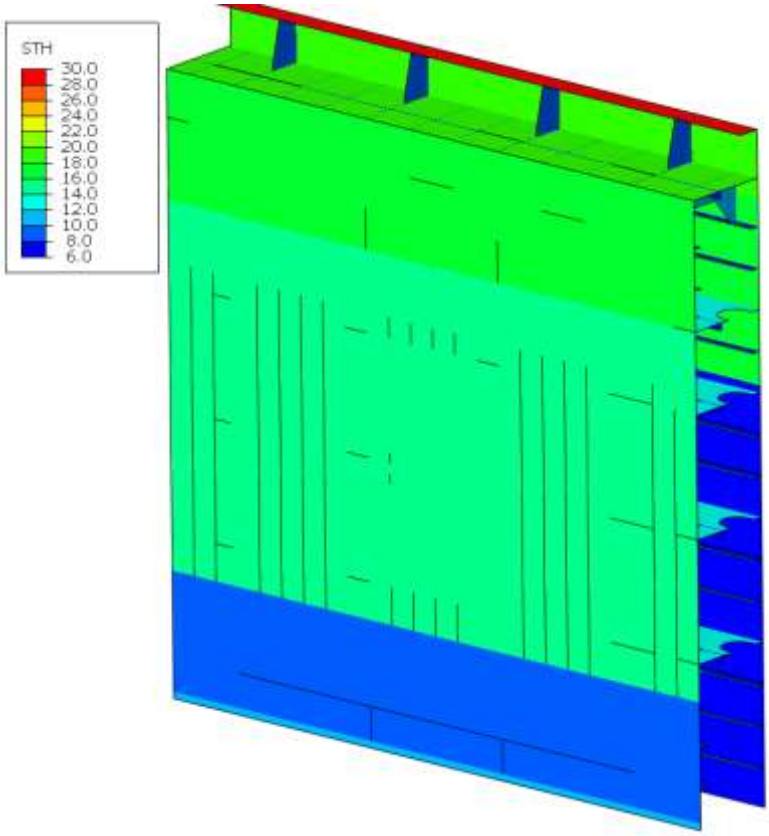

Figure 6 Shell element thicknesses, whole model.

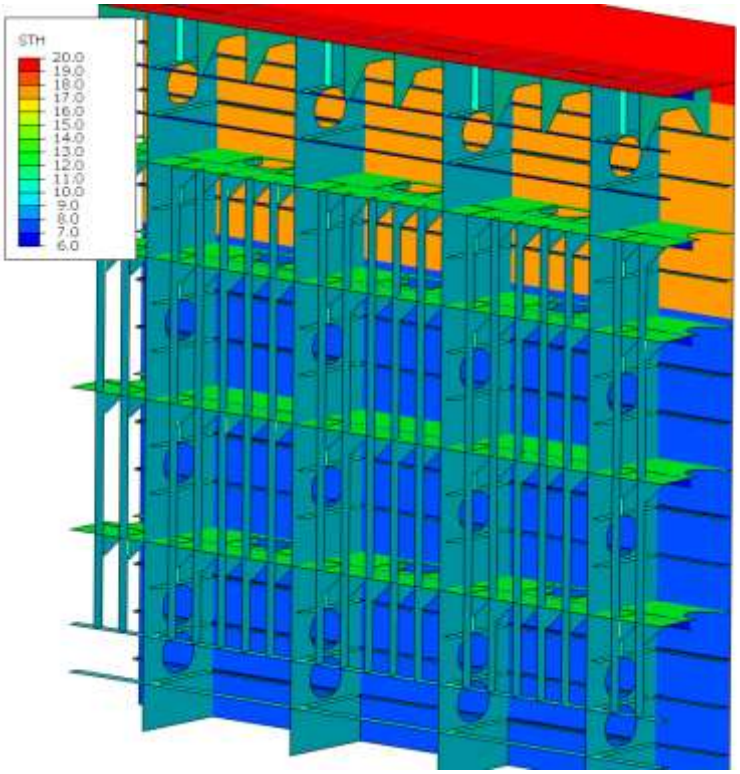

Figure 7 Shell element thicknesses, inside structures.

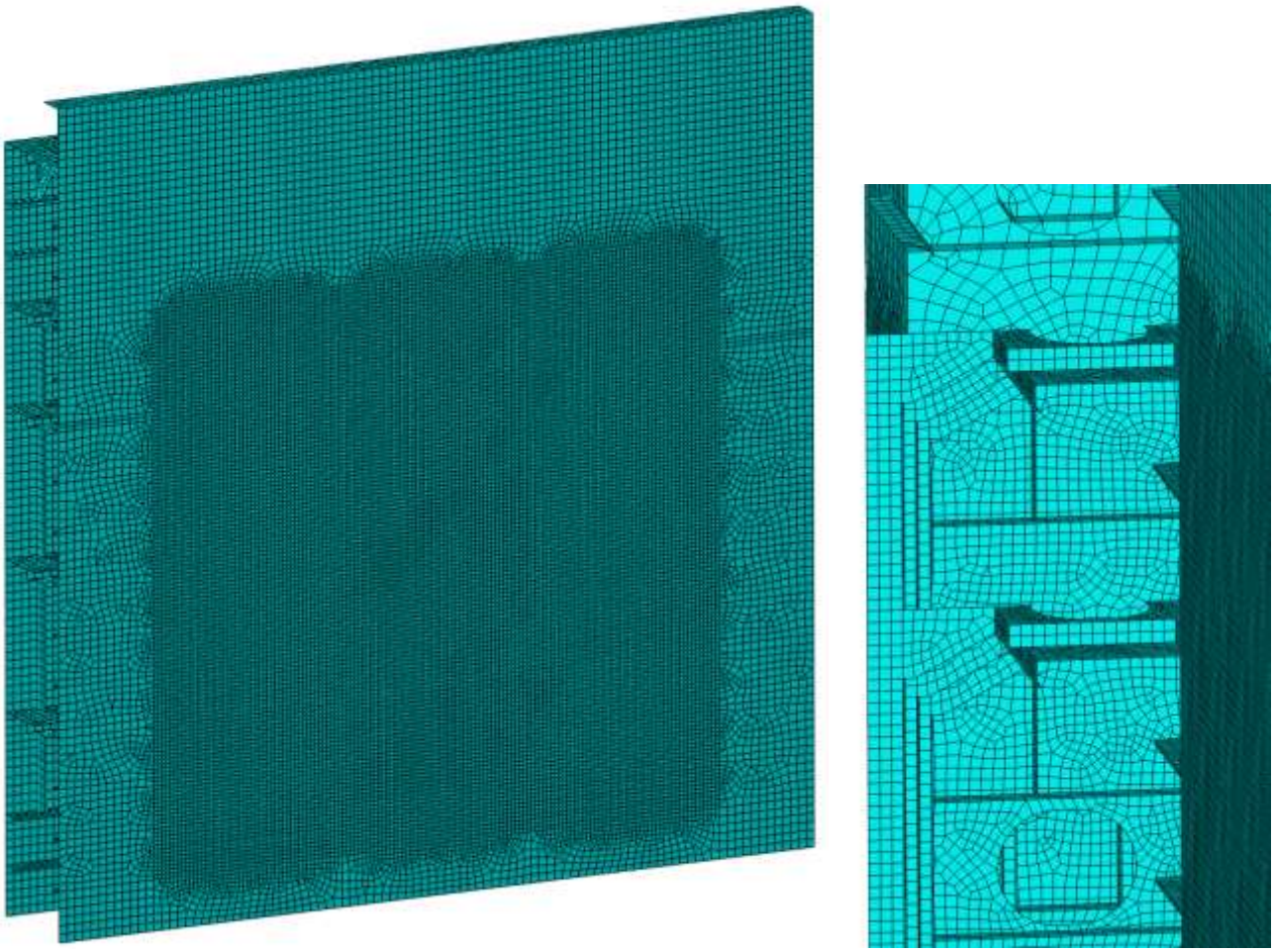

Figure 8 Finite element mesh.

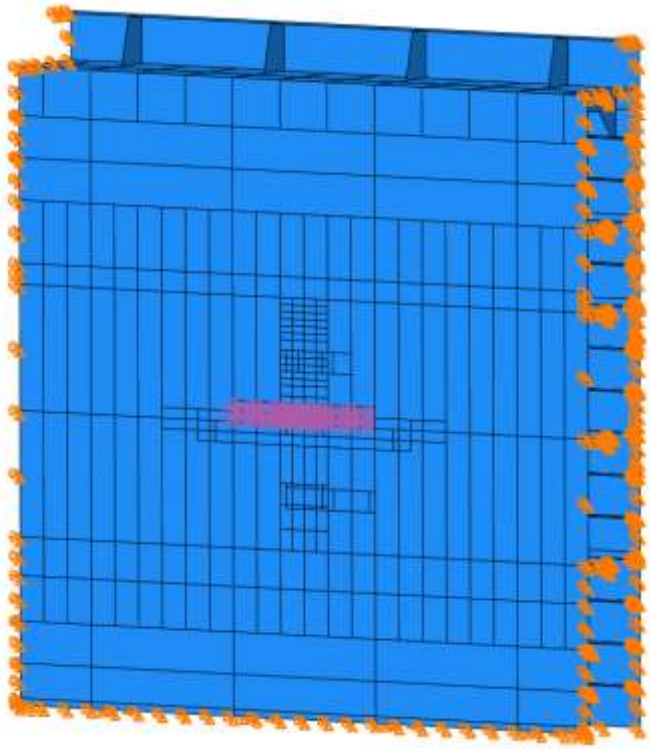

Figure 9 Typical load application, load patch in magenta and pinned boundary conditions in orange.

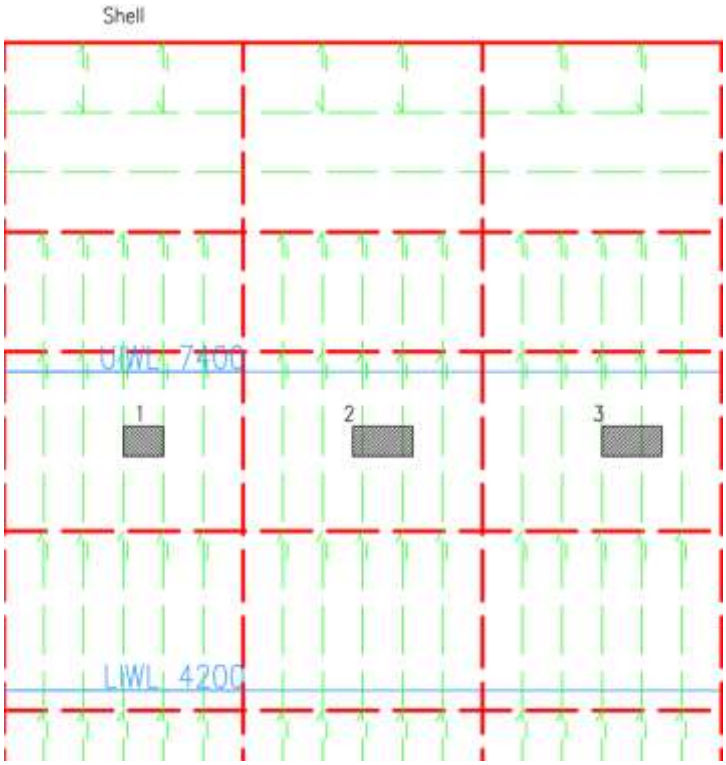

Figure 10 Load patch locations for checking the capacity of the side shell.

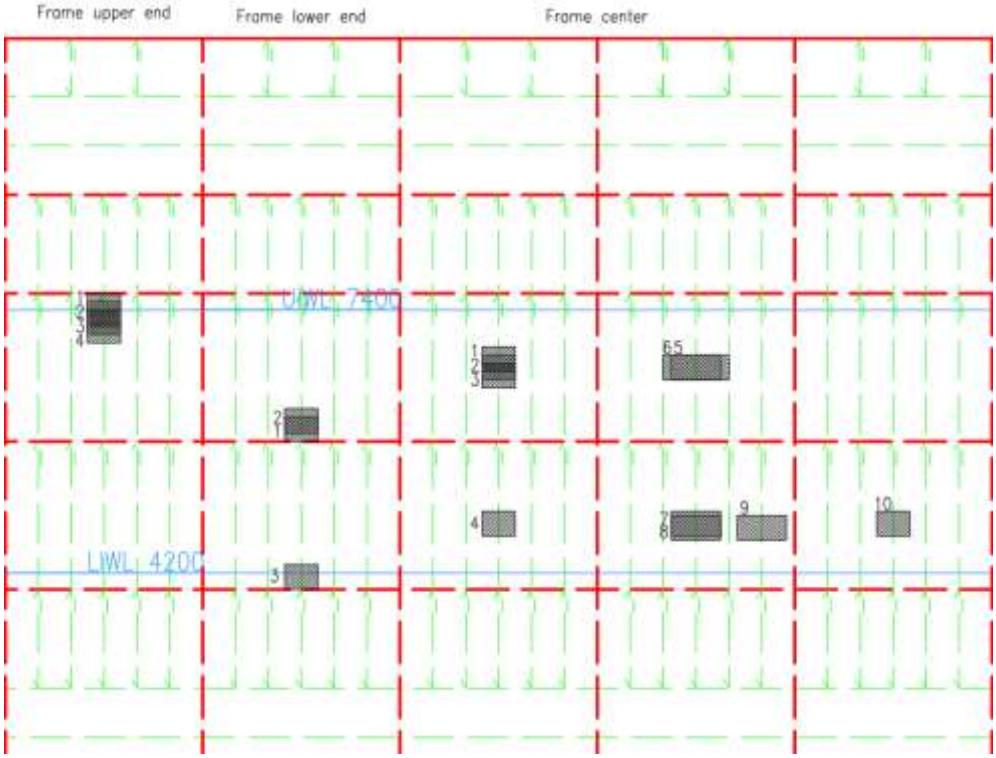

Figure 11 Load patch locations for checking the capacity of the frames.

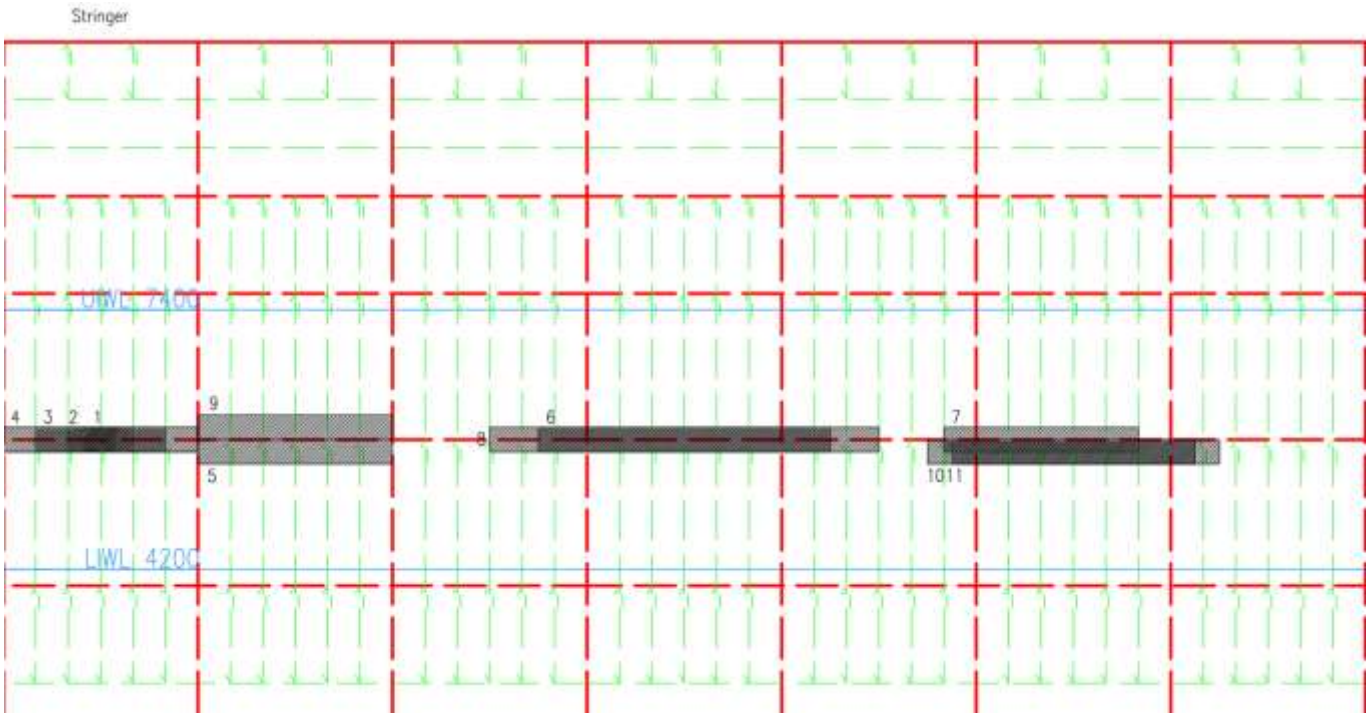

Figure 12 Load patch locations for checking the capacity of the stringer platforms.

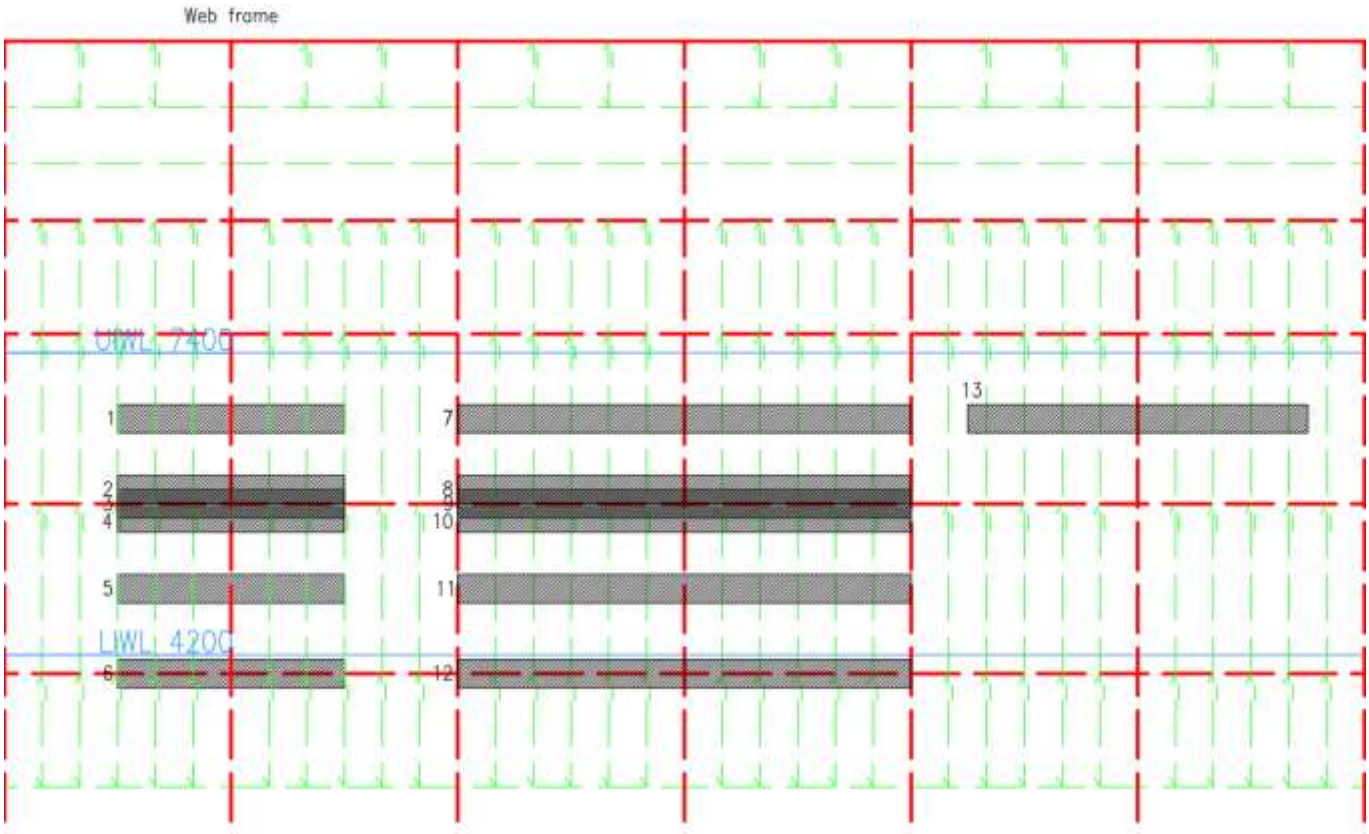

Figure 13 Load patch locations for checking the capacity of the web frames.

4.3 10 000 DWT IC vessel

To cover lower ice classes, IC variant of the baseline vessel was made. The main dimensions for the vessel were selected based on [21], and are shown in Table 6. The midship section is shown in Figure 14. Rule ice loads are shown in Table 7.

Table 6 Main dimensions for 10 000 DWT IC dry cargo vessel.

DWT	10000	t	*Deadweight*
L	120.2	m	*Length*
B	20.3	m	*Breadth*
D	10.7	m	*Depth*
T	7.4	m	*Draught*
LS	4100	t	*Lightship weight*
Δ	14100	t	*Displacement*
Cb	0.75		*Block coefficient*
v	12	kn	*Service speed*
P	3000	kW	*Shaft power*

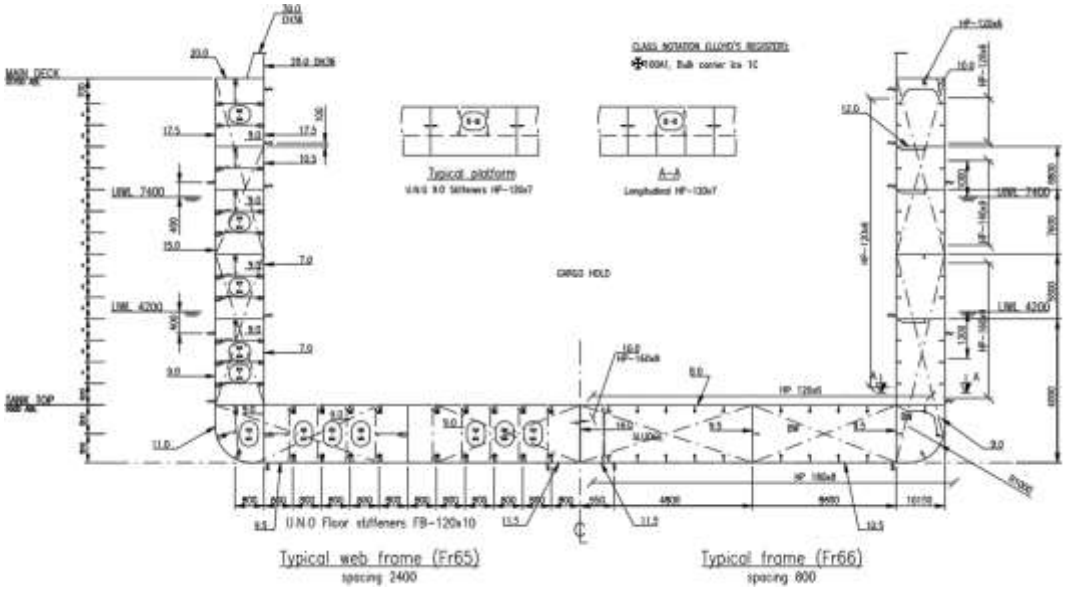

Figure 14. Midship section for 10 000 DWT IC vessel.

Table 7. Load patch size and pressure for different load cases for 10 000 DWT IC vessel.

Structural part	**Load patch size**			
	Height [m]	**Width [m]**	**Pressure [MPa]**	**Tot. force [kN]**
Shell plating	0.22	1.02	0.767	172
Longitudinal	0.22	2.40	0.372	197
Web frame	0.22	4.80	0.263	278

Finite element model of the IC 10 000 DWT vessel is shown in Figure 15, Figure 16 and Figure 17. The load application and boundary conditions are shown in Figure 18. The tested load patch locations are shown in Figure 19.

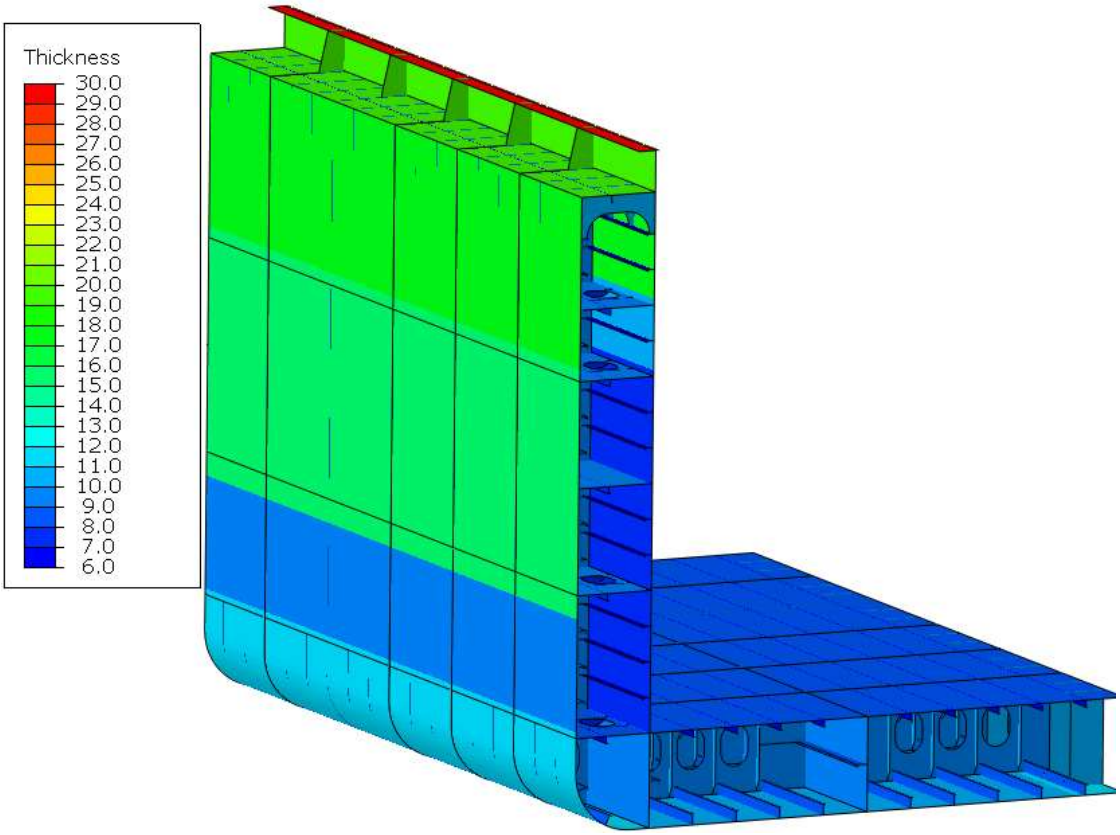

Figure 15 Shell element thickness.

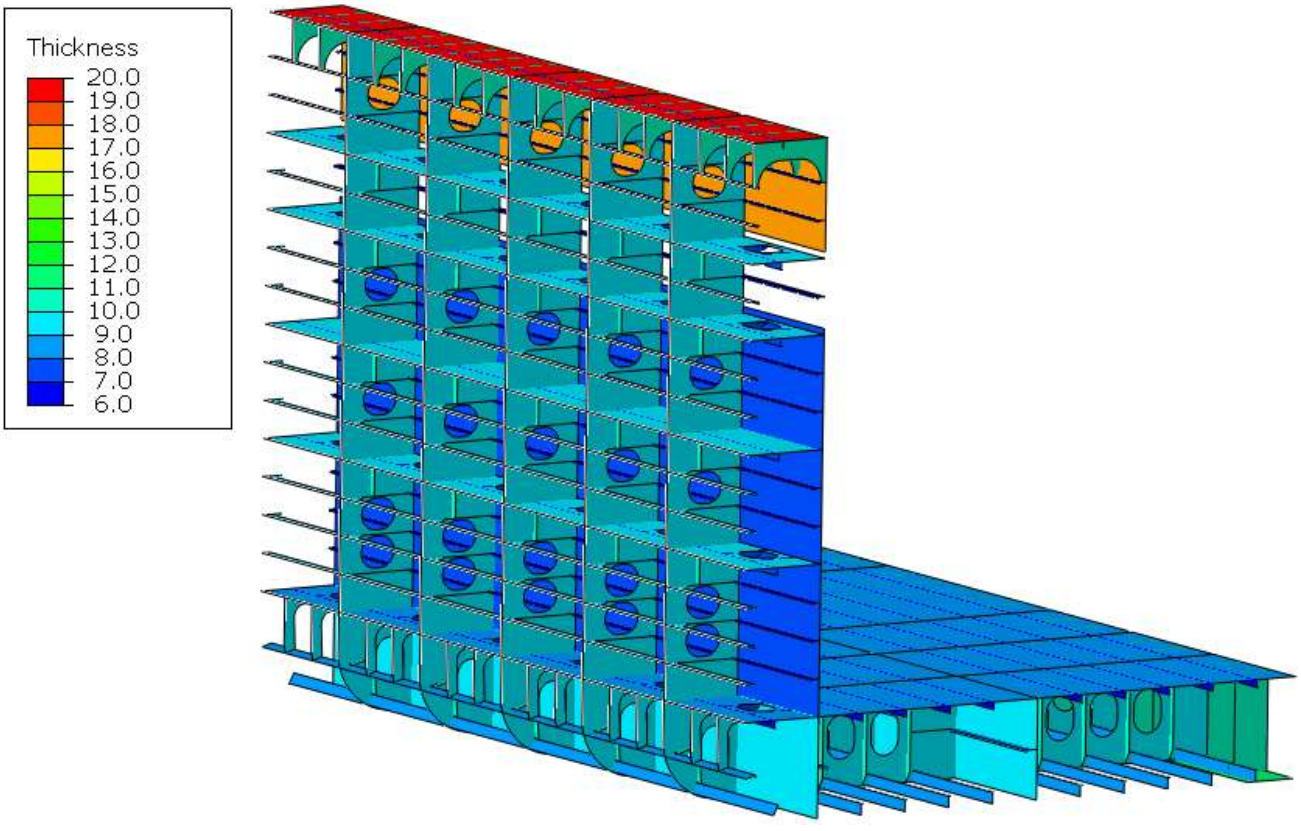

Figure 16 Shell element thickness, inside structures.

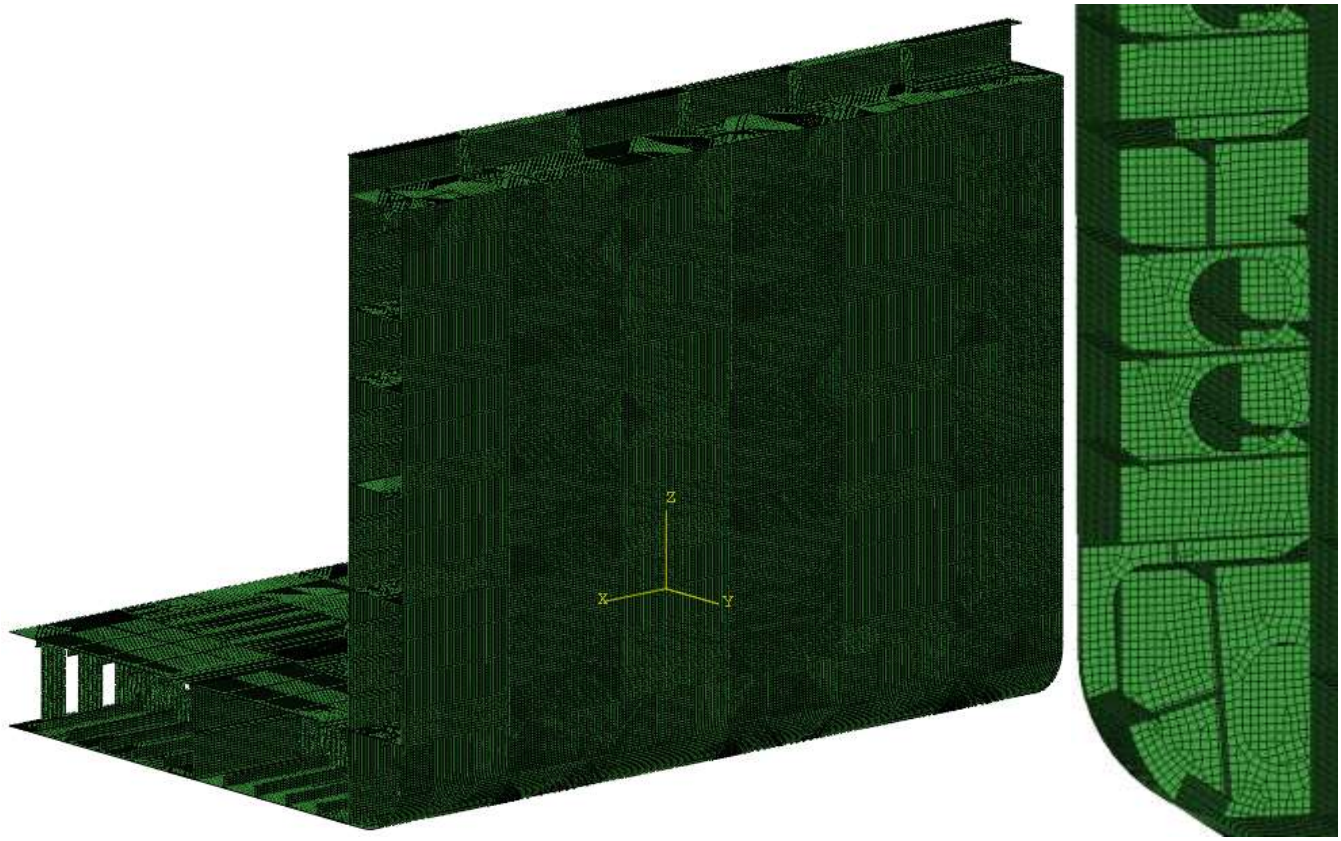

Figure 17 Finite element mesh.

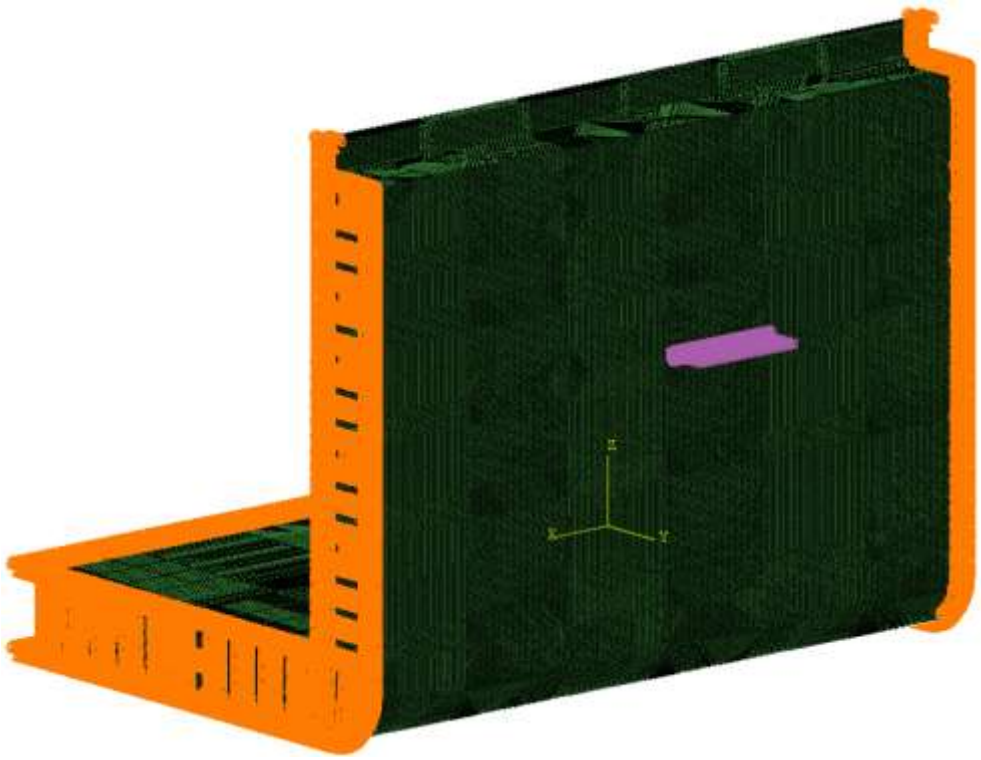

Figure 18 Typical load application, load patch in magenta and pinned boundary conditions in orange.

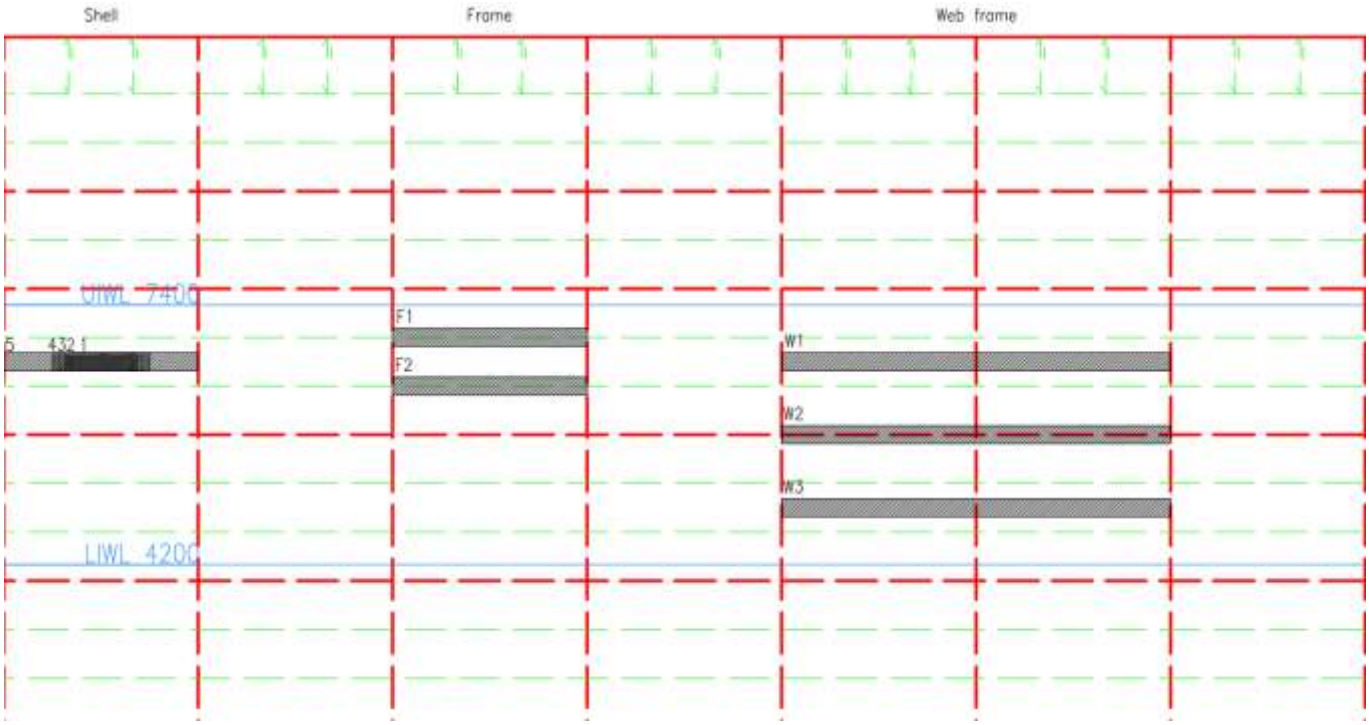

Figure 19 Load patch locations.

4.4 10 000 DWT IAsuper vessel

To cover highest ice class, IAsuper variant of the baseline vessel was made. The main dimensions for the vessel were selected based on [21], and are shown in Table 8. The midship section is shown in Figure 20. Rule ice loads are shown in Table 9.

Table 8 Main dimensions for 10 000 DWT IAsuper dry cargo vessel.

DWT	10000	t	*Deadweight*
L	122.6	m	*Length*
B	20.3	m	*Breadth*
D	10.7	m	*Depth*
T	7.4	m	*Draught*
LS	4360	t	*Lightship weight*
Δ	14360	t	*Displacement*
Cb	0.75		*Block coefficient*
v	12	kn	*Service speed*
P	5500	kW	*Shaft power*

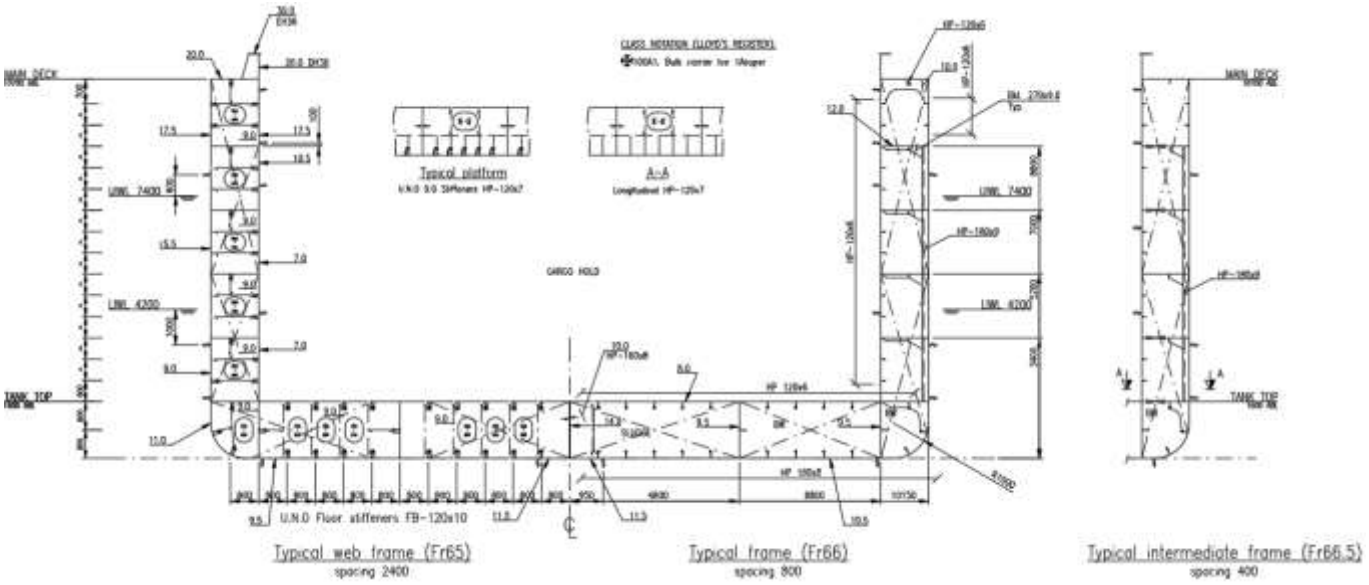

Figure 20. Midship section for 10 000 DWT IAsuper vessel.

Table 9. Load patch size and pressure for different load cases for 10 000 DWT IAsuper vessel.

Structural part	**Load patch size**			
	Height [m]	**Width [m]**	**Pressure [MPa]**	**Tot. force [kN]**
Shell plating	0.35	0.40	1.597	224
Frame	0.35	0.40	1.597	224
Stringer	0.35	2.40	0.798	671
Web frame	0.35	4.80	0.564	948

Finite element model of the IAsuper 10 000 DWT vessel is shown in Figure 21, Figure 22, Figure 23 and Figure 24. The load application and boundary conditions are shown in Figure 25. The tested load patch locations are shown in Figure 26.

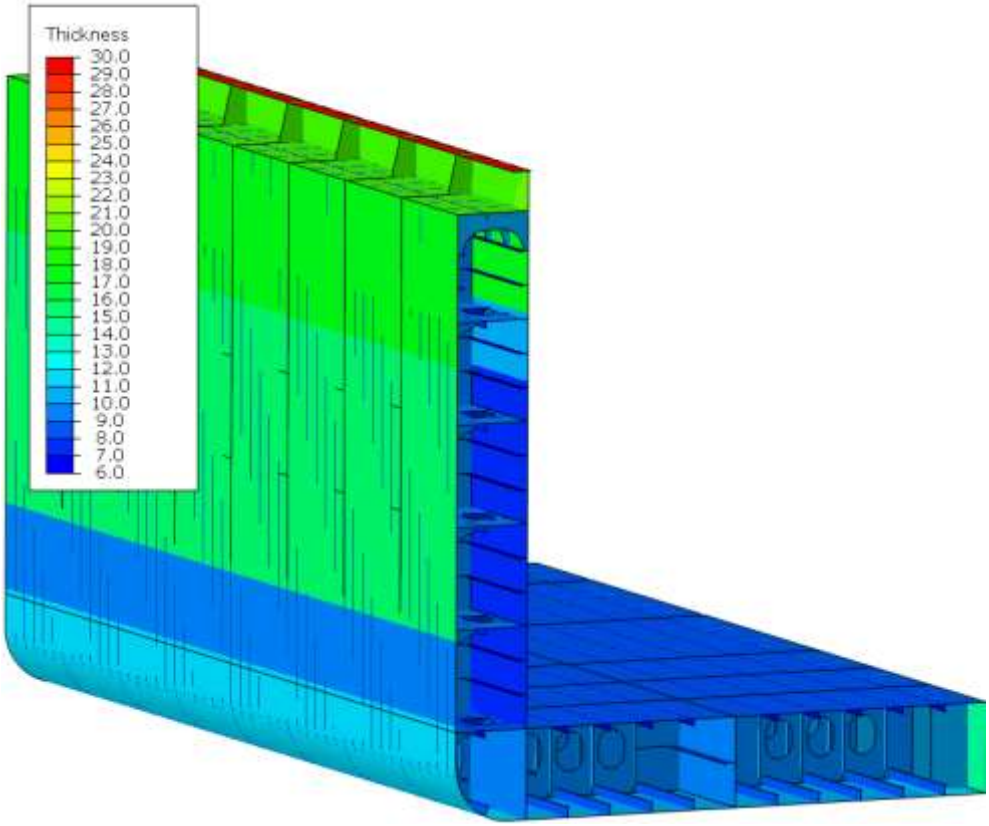

Figure 21 Shell element thickness.

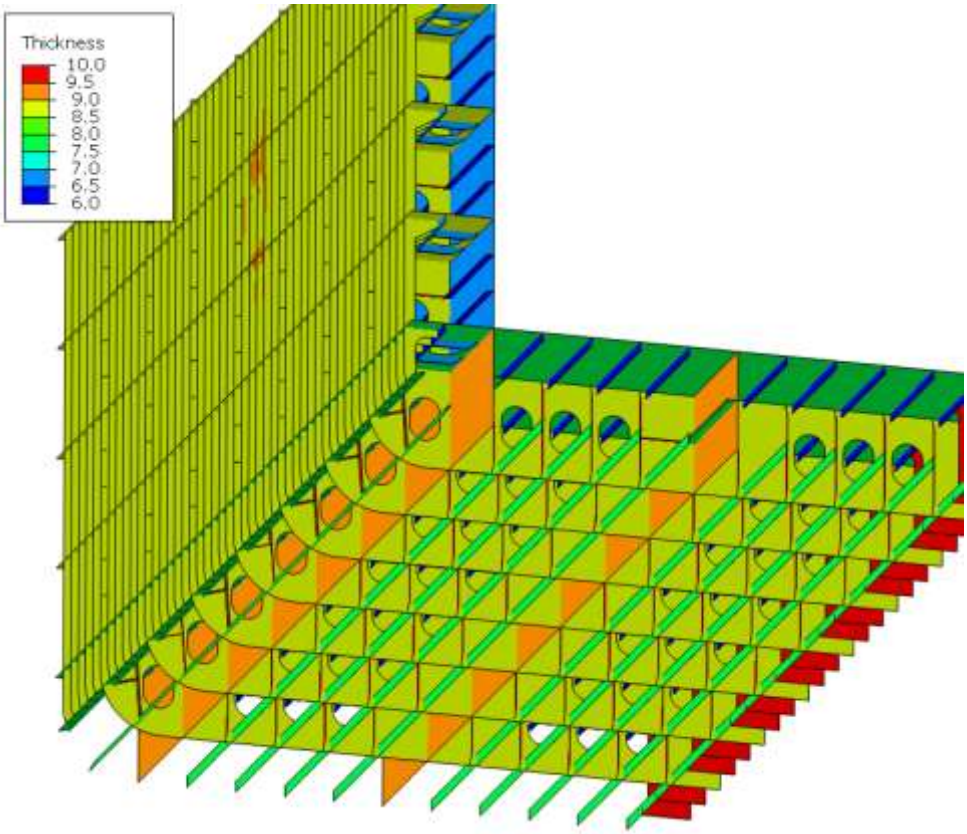

Figure 22 Shell element thickness, inside structures.

Figure 23 Finite element mesh, overall view.

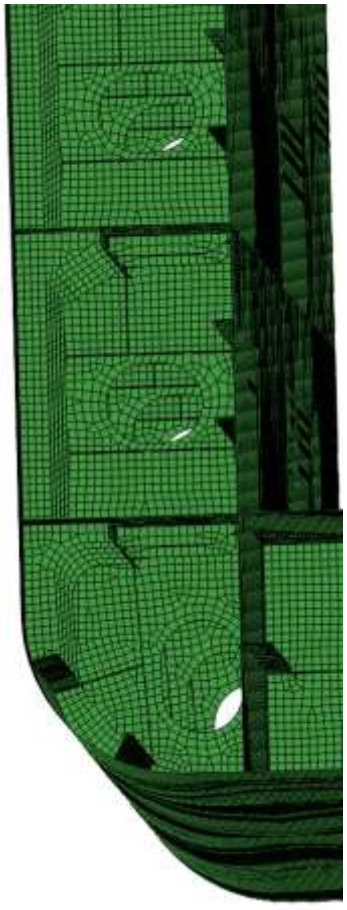

Figure 24 Finite element mesh, detail.

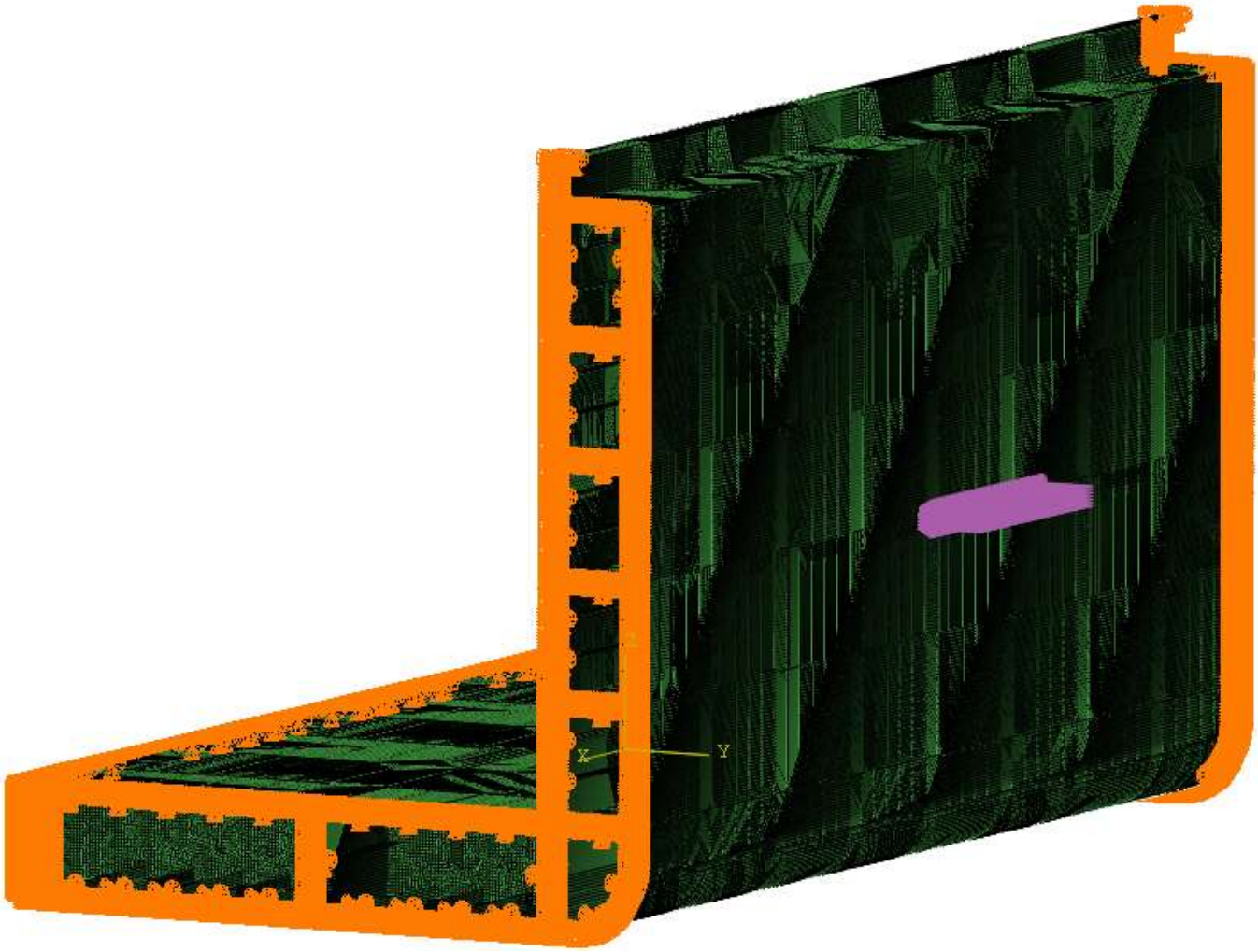

Figure 25 Pinned boundary conditions (orange) and typical load patch (magenta).

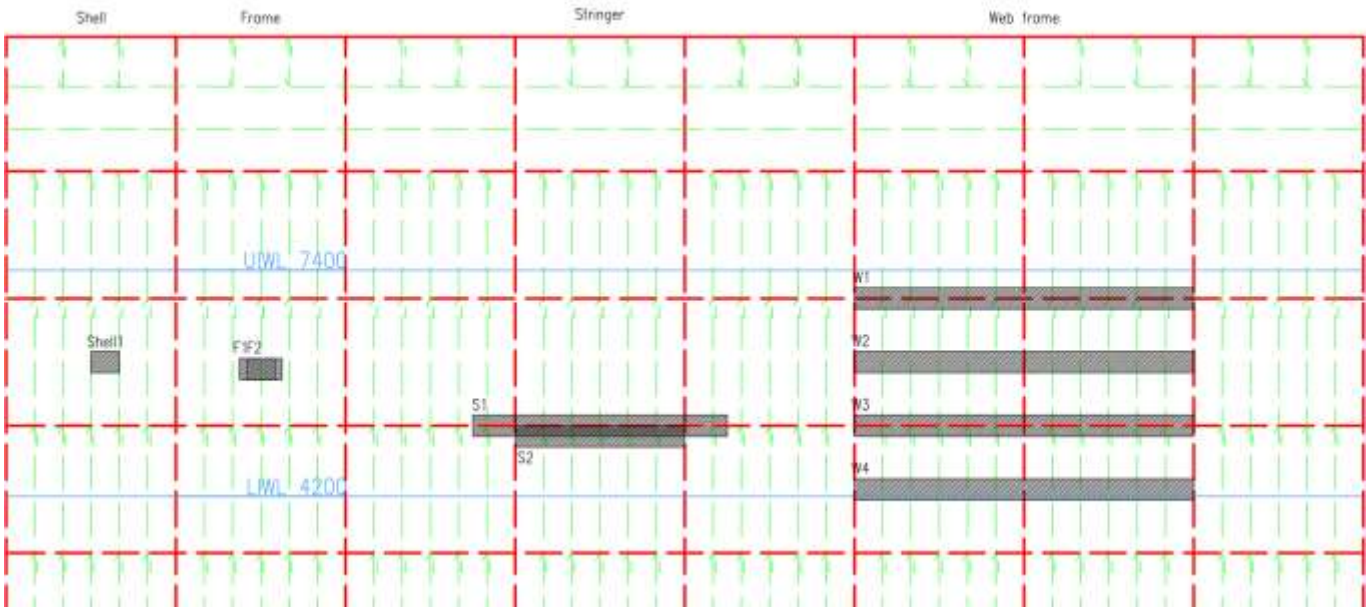

Figure 26 Load patch locations.

4.5 3 000 DWT IAvessel

To study the behaviour of a typical smaller vessel, a 3 000 DWT dry cargo ship with the most typical ice class, IA, was modelled. The main dimensions for the vessel were selected based on [21], and are shown in Table 10. The midship section is shown in Figure 27. Rule ice loads are shown in Table 11.

Table 10 Main dimensions for 3 000 DWT IA dry cargo vessel.

DWT	3000	t	*Deadweight*
L	84.0	m	*Length*
B	14.0	m	*Breadth*
D	7.0	m	*Depth*
T	5.7	m	*Draught*
LS	1960	t	*Lightship weight*
Δ	4960	t	*Displacement*
Cb	0.758		*Block coefficient*
v	12	kn	*Service speed*
P	1650	kW	*Shaft power*

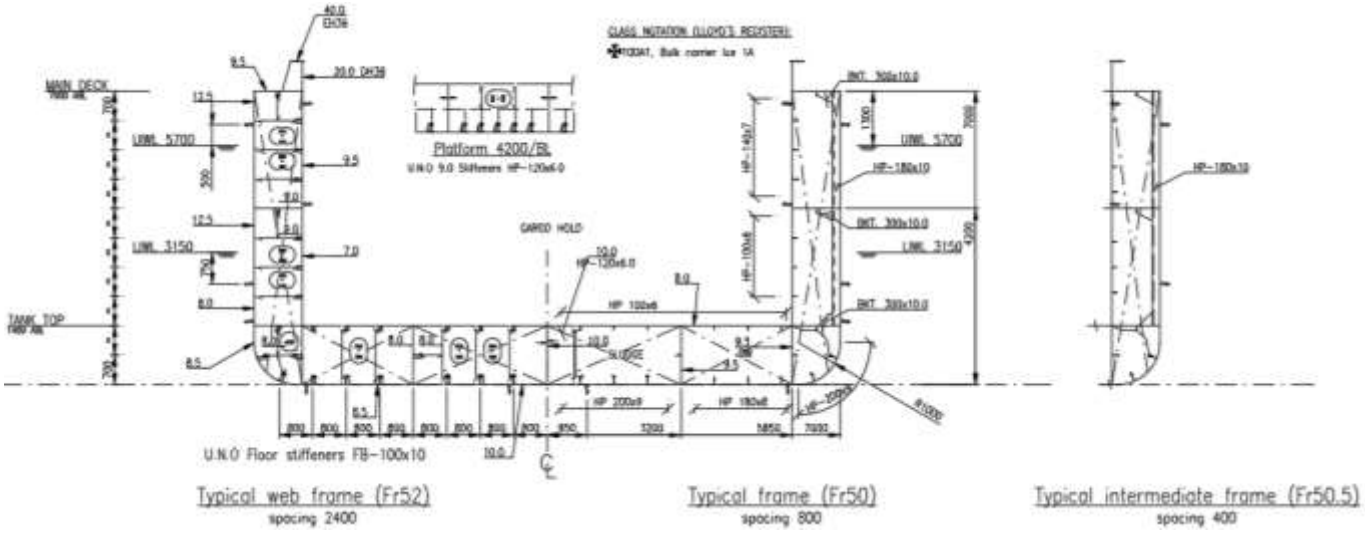

Figure 27. Midship section for 3 000 DWT IA vessel.

Table 11. Load patch size and pressure for different load cases for 3 000 DWT IA vessel.

Structural part	**Load patch size**			
	Height [m]	**Width [m]**	**Pressure [MPa]**	**Tot. force [kN]**
Shell plating	0.30	0.40	1.128	135
Frame	0.30	0.40	1.128	135
Stringer	0.30	2.40	0.564	406
Web frame	0.30	4.80	0.399	574

Finite element model of the IA 3 000 DWT vessel is shown in Figure 28, Figure 29 and Figure 30. The load application and boundary conditions are shown in Figure 31. The tested load patch locations are shown in Figure 32.

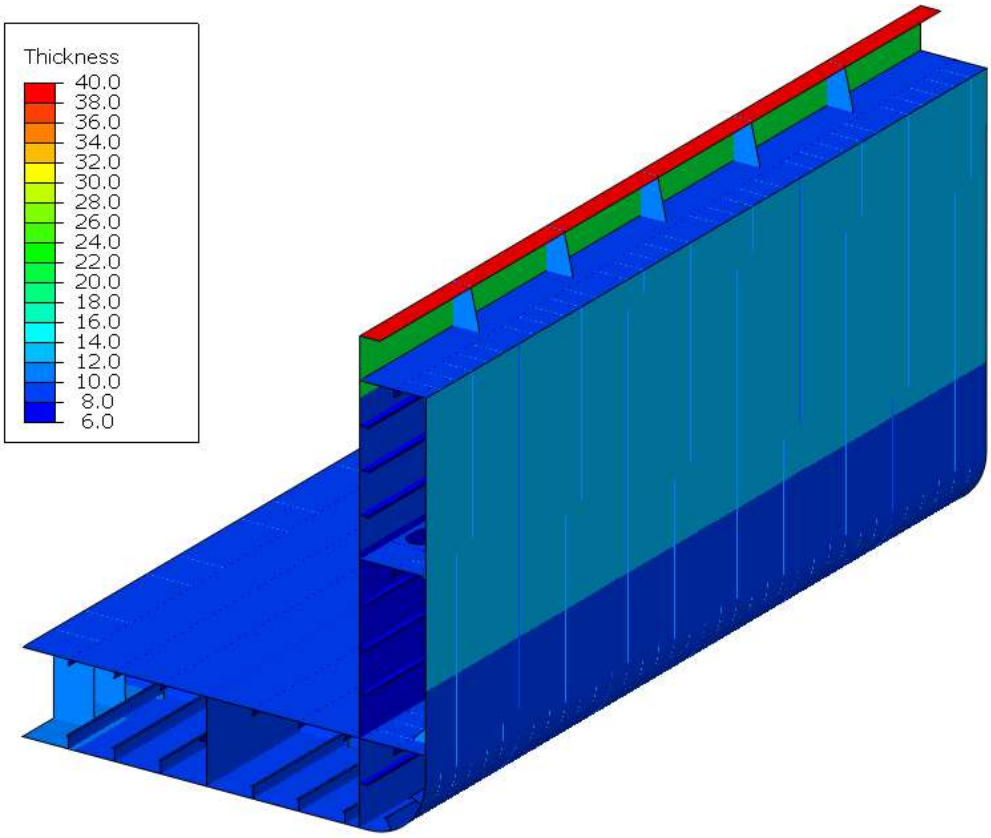

Figure 28 Shell element thickness.

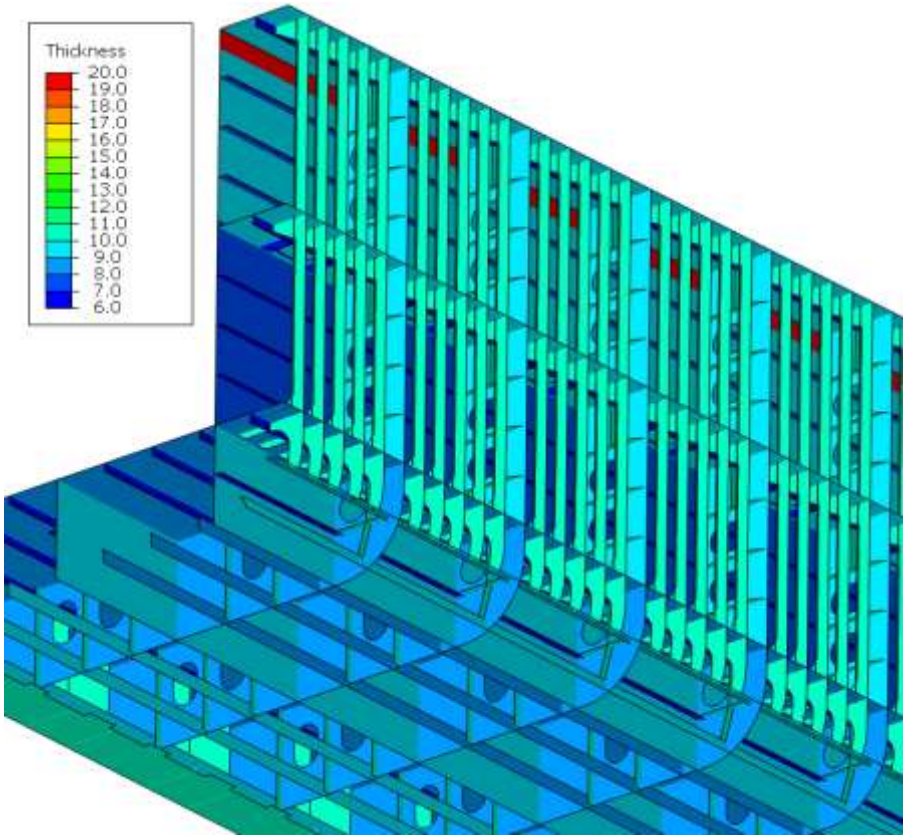

Figure 29 Shell element thickness, inside structures.

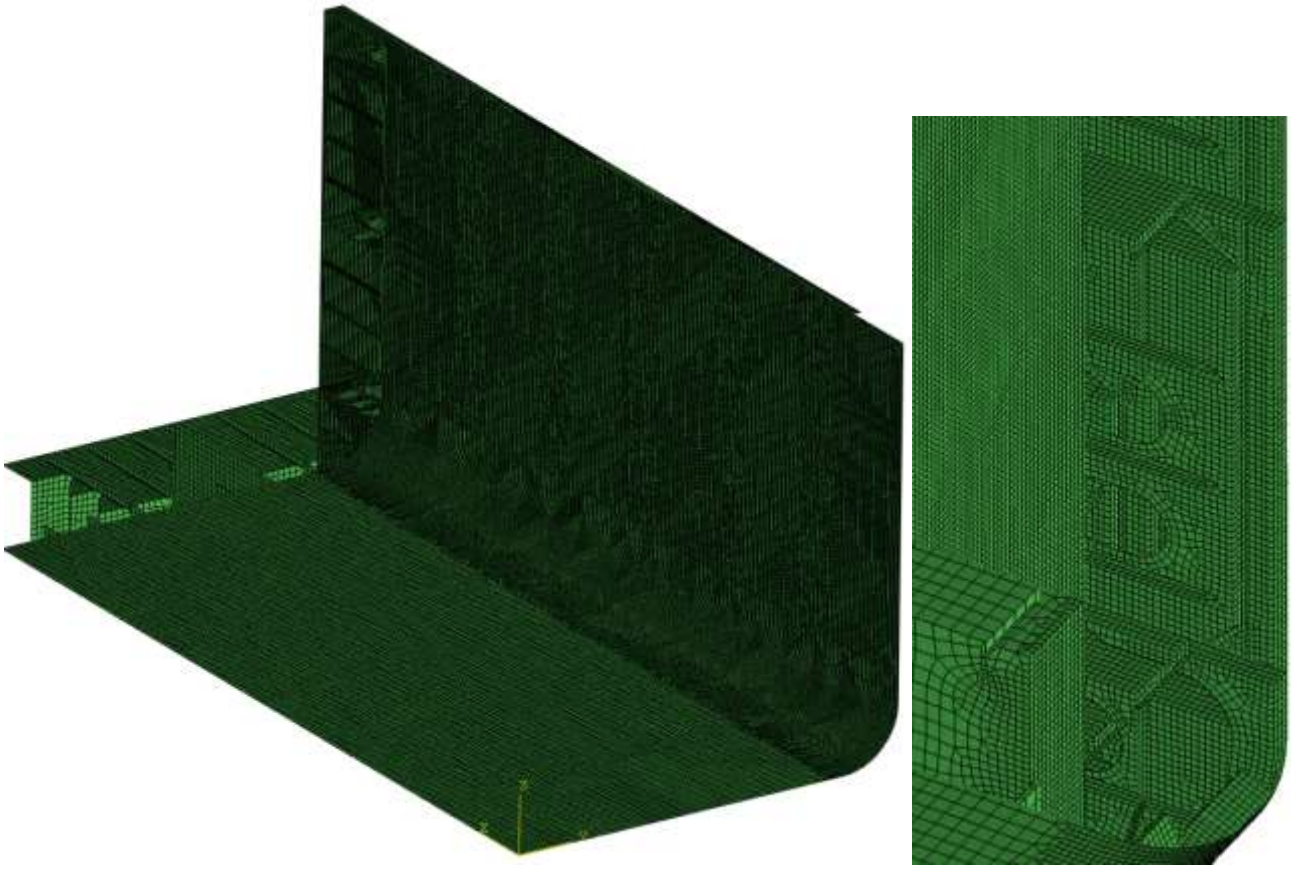

Figure 30 Finite element mesh.

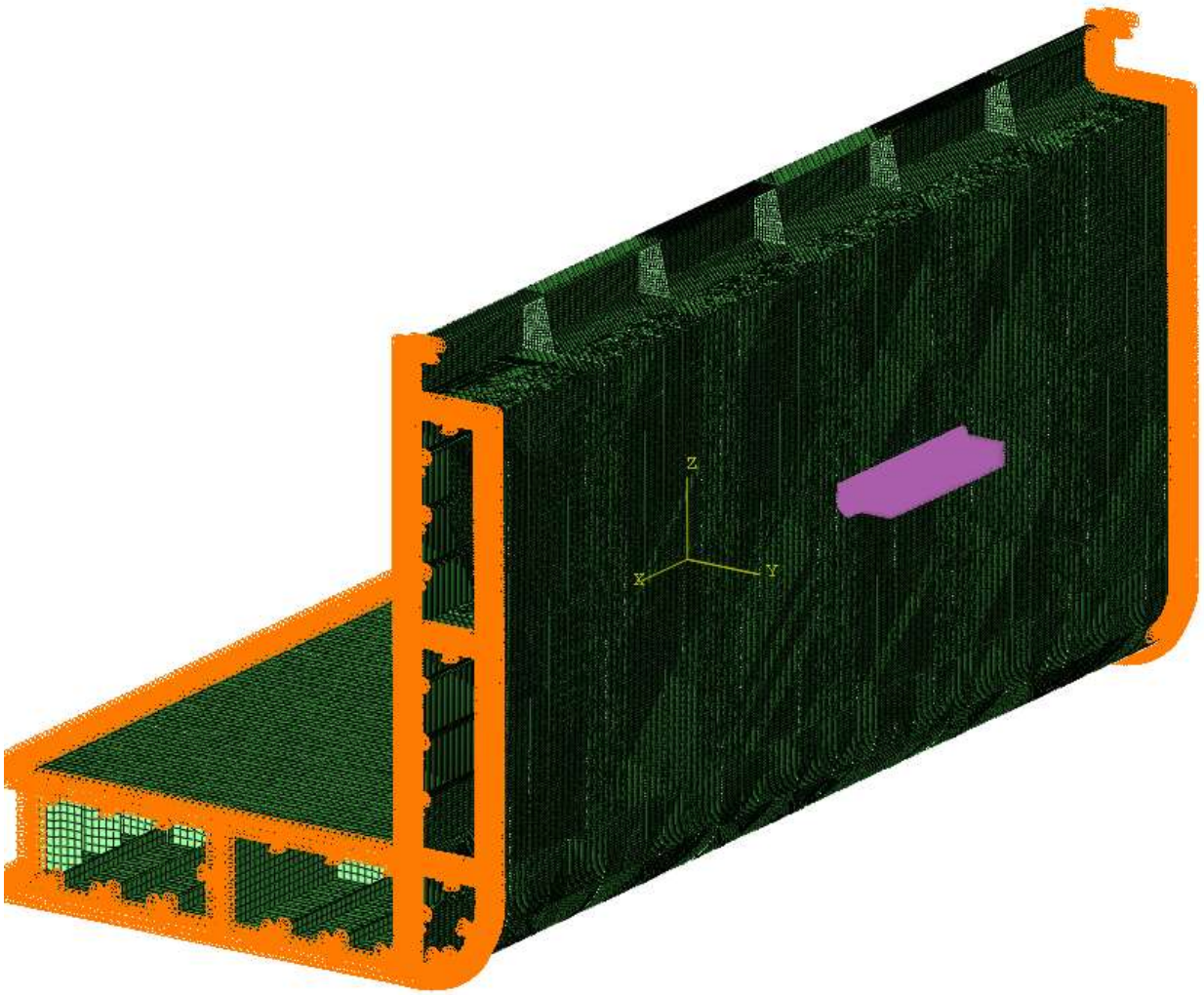

Figure 31 Typical load application, load patch in magenta and pinned boundary conditions in orange.

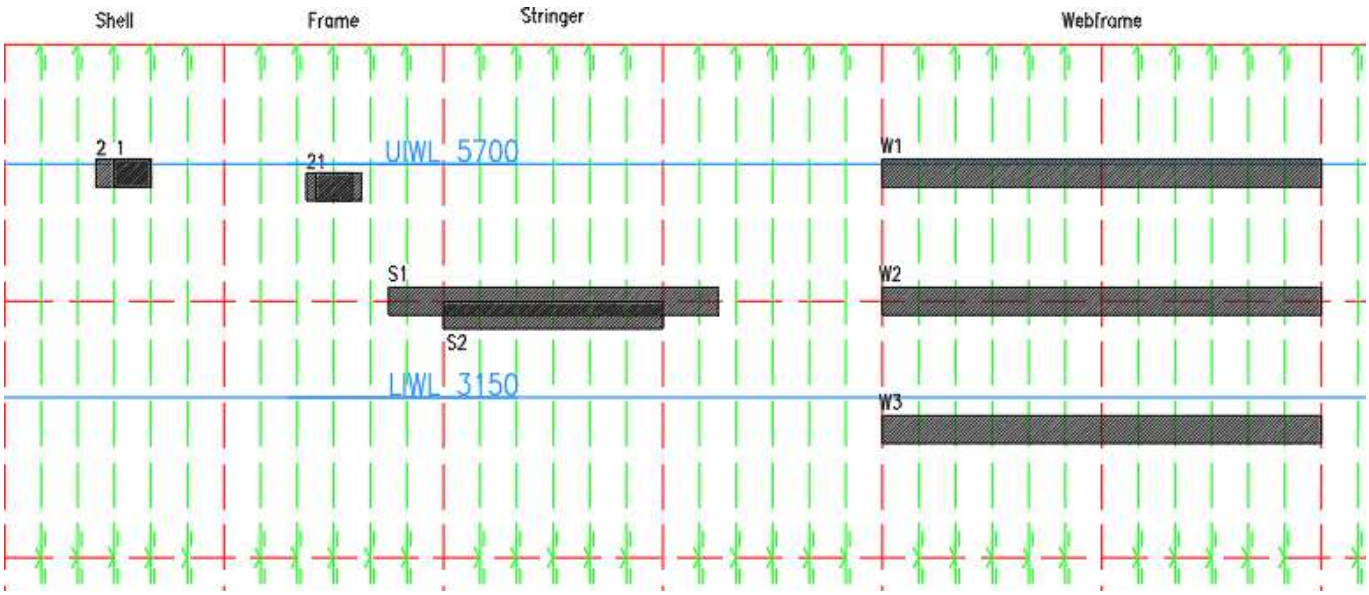

Figure 32 Load patch locations.

4.6 58 500 DWT IA vessel

To study the behaviour of a typical large vessel, a 58 500 DWT dry cargo ship with the most typical ice class, IA, was modelled. The main dimensions for the vessel were selected based on [21], and are shown in Table 12. The midship section is shown in Figure 33. Rule ice loads are shown in Table 13.

Table 12 Main dimensions for 58 500 DWT IA dry cargo vessel.

DWT	58500	t	*Deadweight*
L	196	m	*Length*
B	32.26	m	*Breadth*
D	18.6	m	*Depth*
T	13.0	m	*Draught*
LS	11430	t	*Lightship weight*
Δ	69930	t	*Displacement*
Cb	0.83		*Block coefficient*
v	12	kn	*Service speed*
P	14750	kW	*Shaft power*

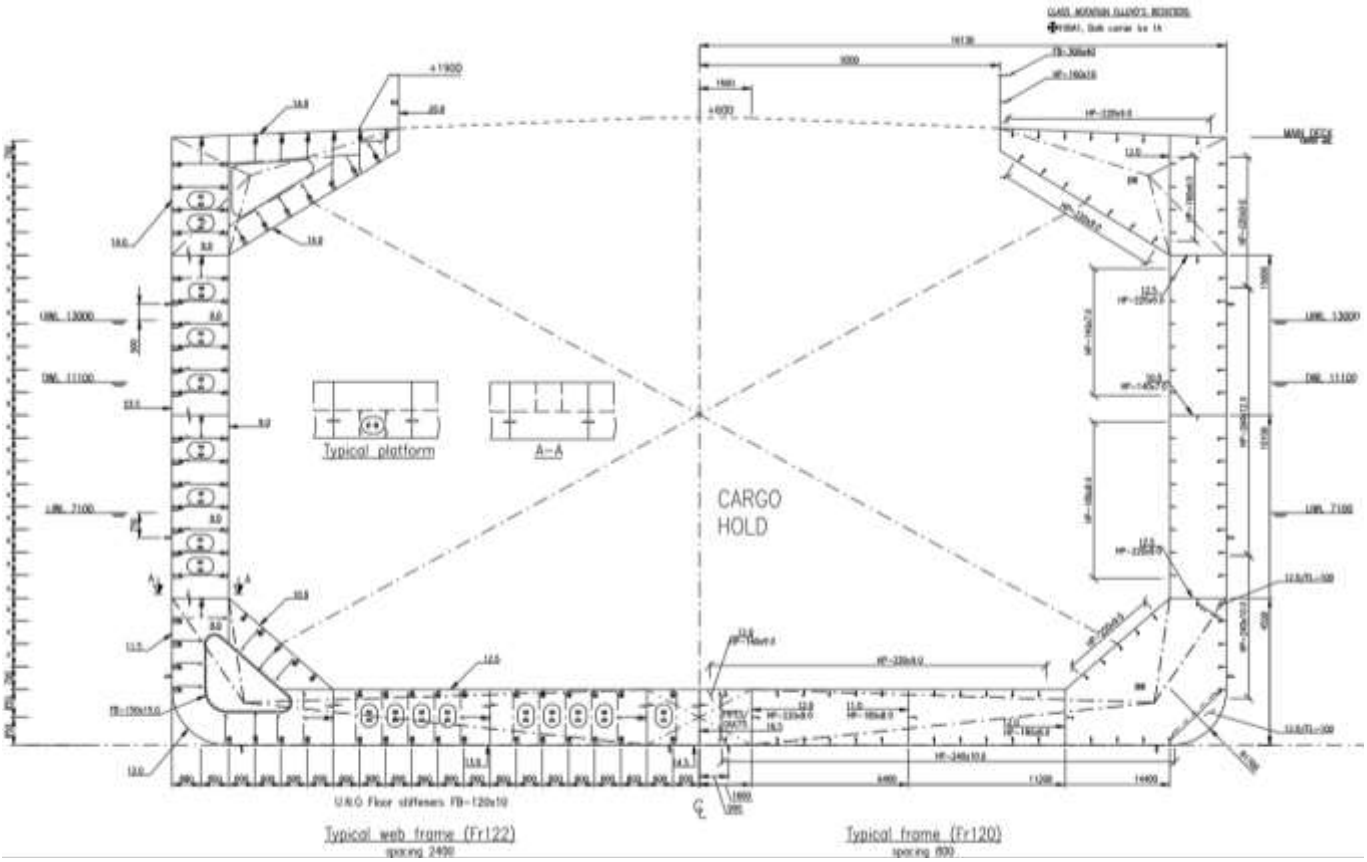

Figure 33. Midship section for 58 500 DWT IA vessel.

Table 13. Load patch size and pressure for different load cases for 58 500 DWT IA vessel.

Structural part	Load patch size			
	Height [m]	Width [m]	Pressure [MPa]	Tot. force [kN]
Shell plating	0.30	1.19	1.180	421
Longitudinal	0.30	2.40	0.831	598
Web frame	0.30	4.80	0.588	846

Finite element model of the IA 58 500 DWT vessel is shown in Figure 34, Figure 35, Figure 36 and Figure 37. The load application and boundary conditions are shown in Figure 38Figure 9. The tested load patch locations are shown in Figure 39.

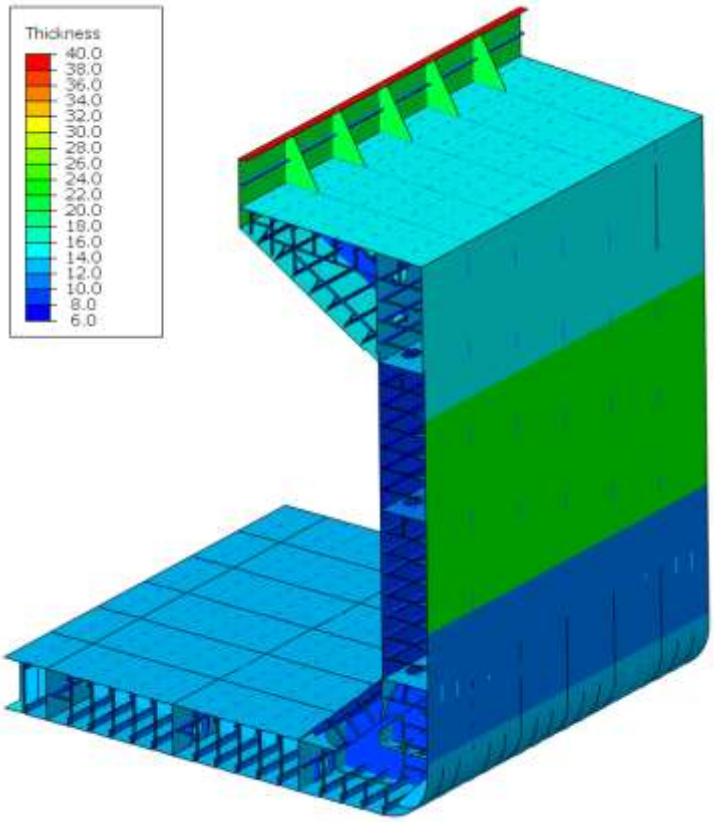

Figure 34 Shell element thicknesses.

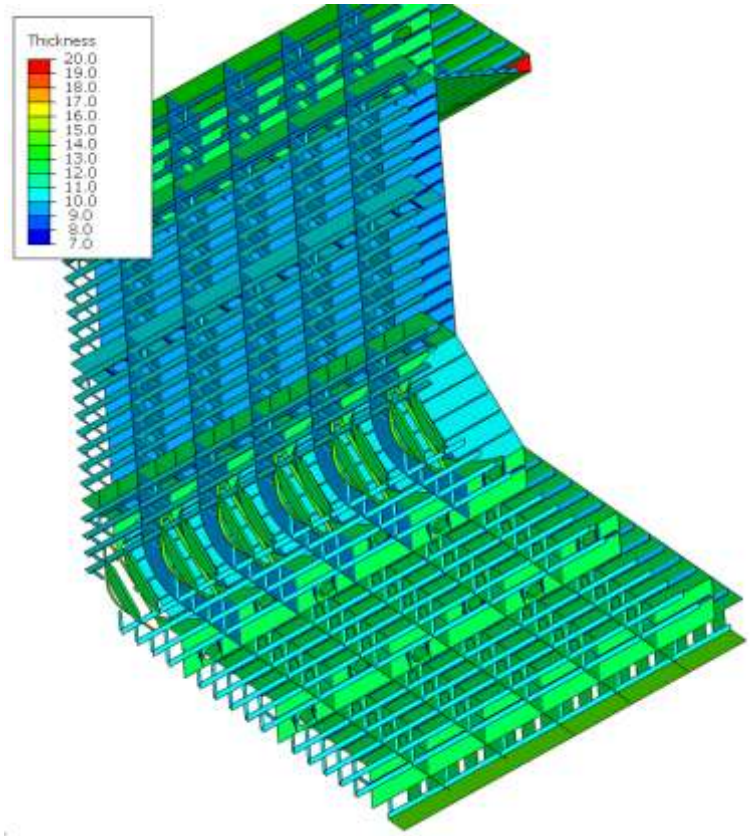

Figure 35 Shell element thicknesses, inside structures.

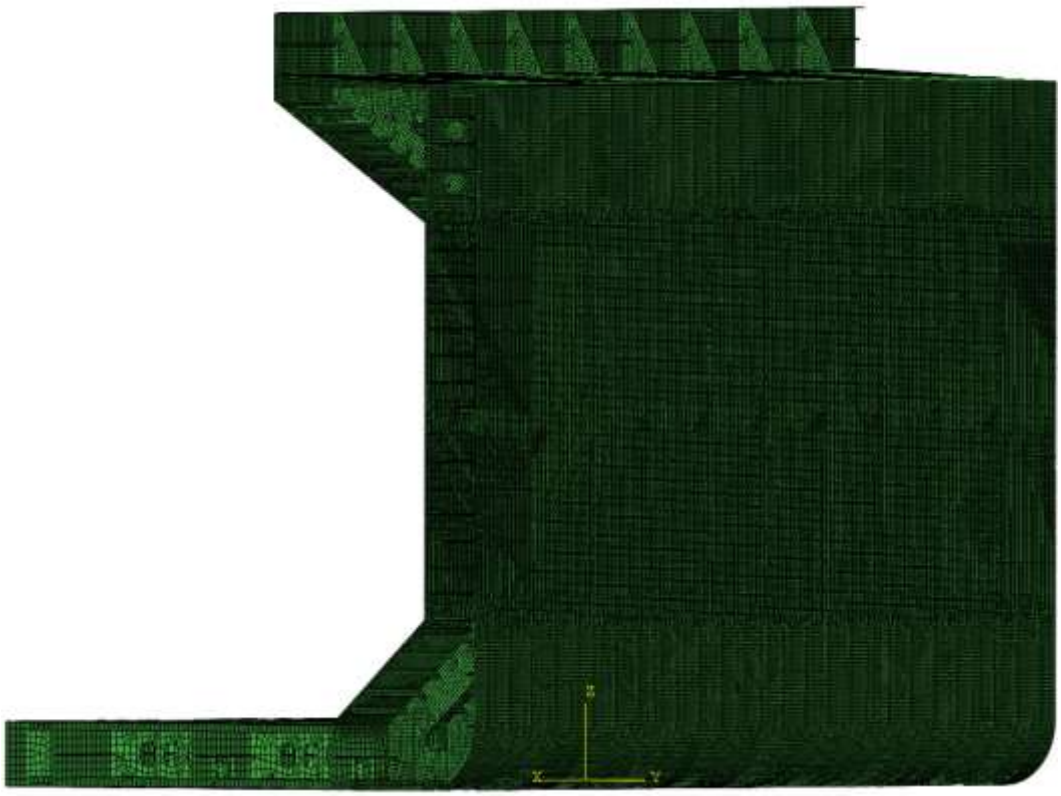

Figure 36 Finite element mesh.

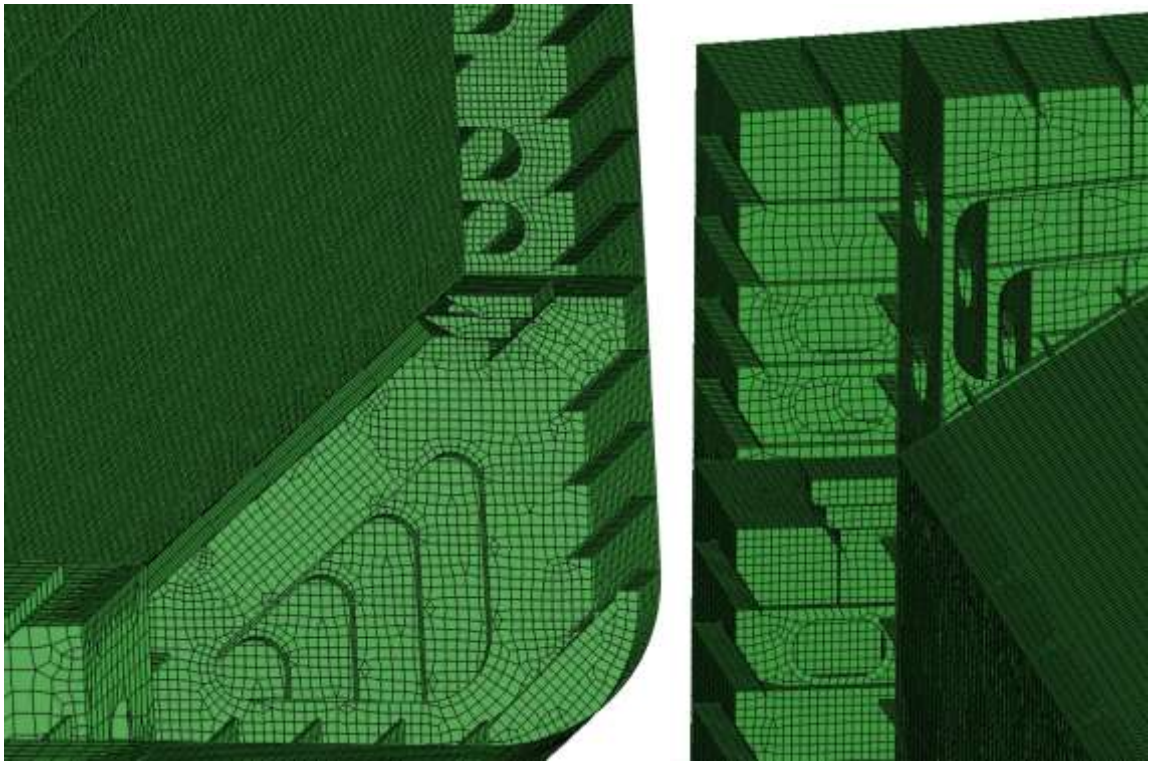

Figure 37 Finite element mesh, details.

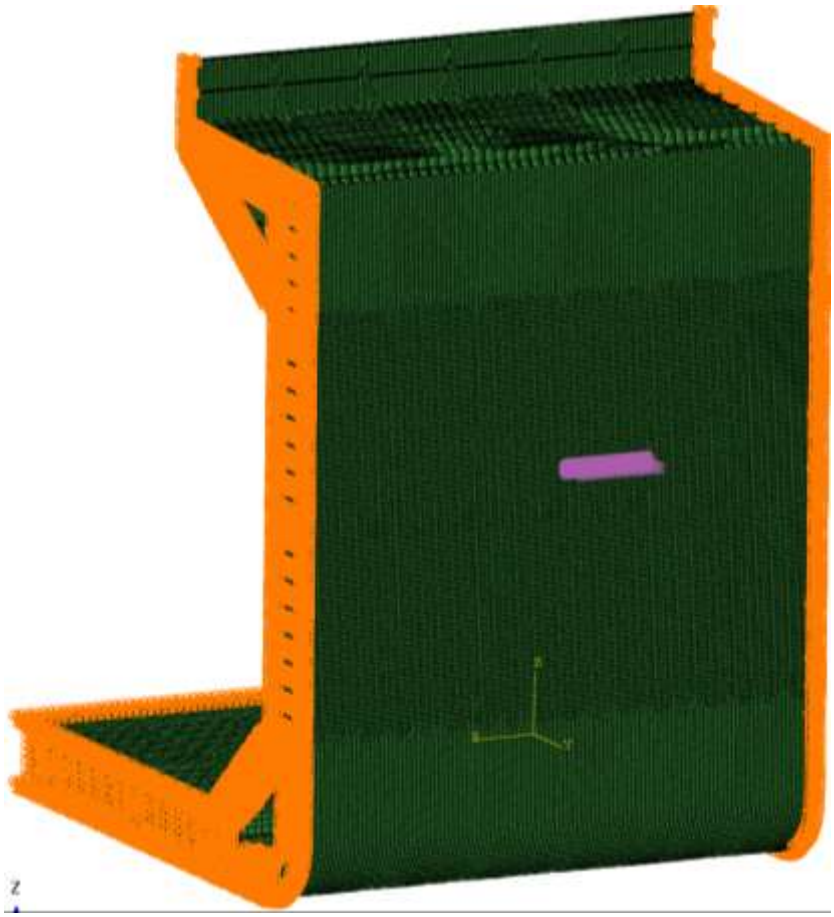

Figure 38 Typical load application, load patch in magenta and pinned boundary conditions in orange.

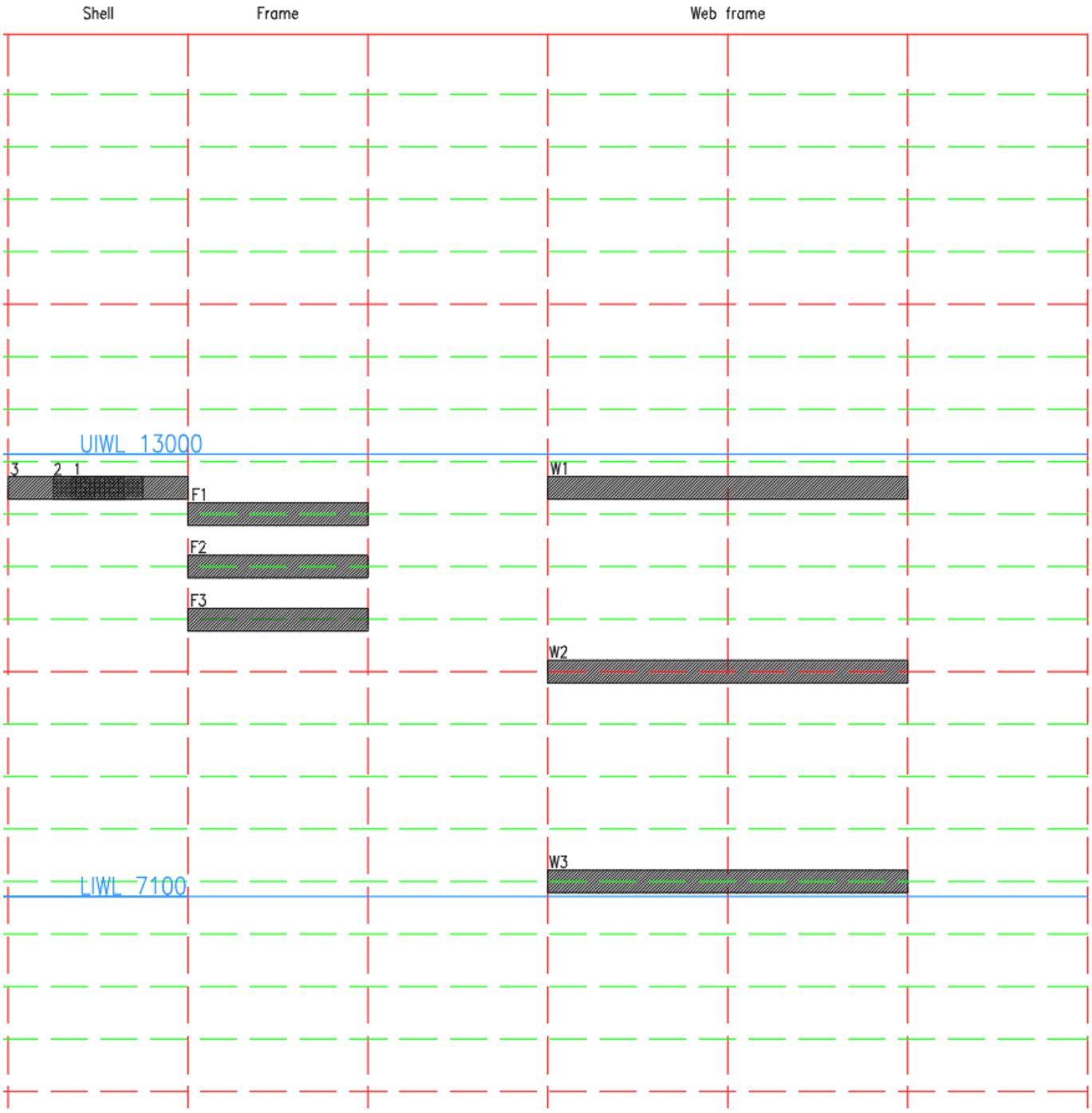

Figure 39 Load patch locations.

5. Modelling

FE modelling of the baseline vessel described in chapter 4 was carried out with Abaqus CAE 2022 software. The purpose was to achieve a parametric model that could be easily modified for studying effects of different modelling and analysis techniques, such as mesh size, element type, model side, boundary conditions etc.

The rest of the vessels were modelled and meshed in NAPA Designer and then exported to Abaqus, to obtain quick and accurate models. The upside is that modelling a ship geometry in NAPA Designer is very quick and efficient compared to modelling in Abaqus. The downside of this process is that the model cannot be modified as freely as in Abaqus, and the export process would need to be repeated every time the geometry is changed. However, for this study, this was not an issue, as the goal was to study the capacity of an existing structure.

5.1 Size of the model

First, four different models of the 10 000 DWT IA cargo vessel midship were created to test the effect of size of the model and boundary conditions. These are shown in Figure 40 below. Results from the largest model is compared to the smaller ones to understand what would be a suitable size for the model to capture all relevant phenomena. Obviously, larger and more accurate model gives more realistic results but also increases modelling effort for the designer and calculation time for the analysis. Goal is to keep the modelling effort reasonable without decreasing the accuracy too much.

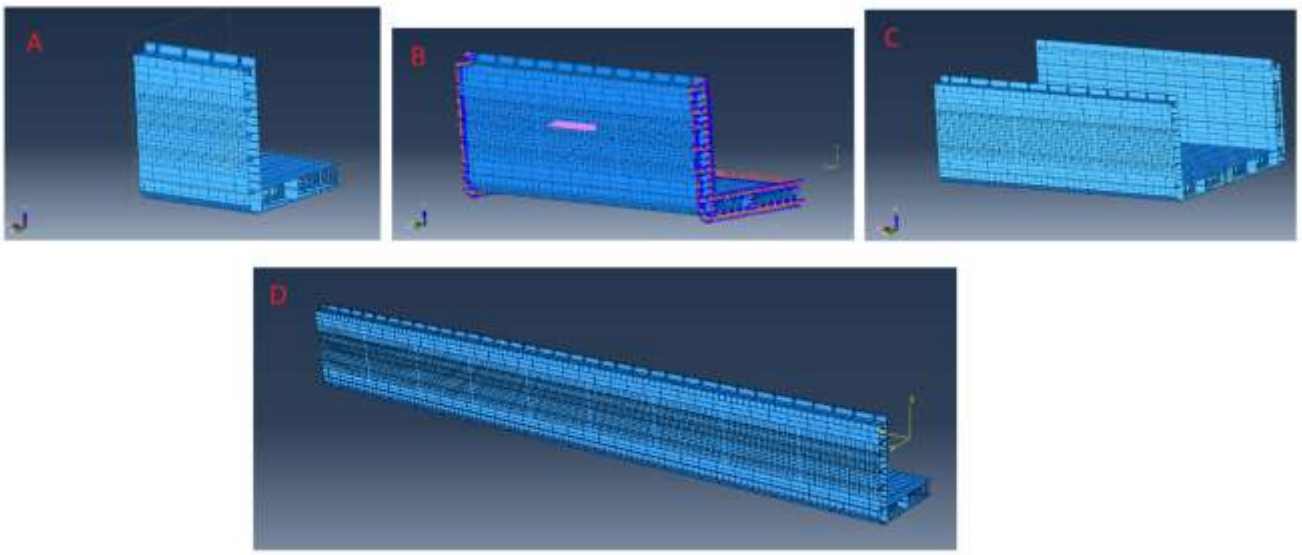

Figure 40. Four different models of baseline vessel (10 000 DWT IA cargo vessel) used in the initial analysis to test for example the boundary conditions. Only geometry is visible, no mesh is applied at this stage. The model B also shows the boundary conditions and load patch.

5.2 Modelling techniques

5.2.1 Element type

The initial models were chosen to be modelled fully with linear shell elements. This is standard practice in ship design nowadays, although there are other options as well. Beam elements could be used for some stiffeners to model the whole stiffener or only part of it, for example the flange. However, at this stage it is a straightforward choice to use shell elements, because with sufficient fine mesh they can capture all relevant phenomena such as buckling. Shell elements also enable modelling of the stiffener end connections quite accurately, especially brackets. Because ships are thin shell structures, solid elements are rarely used in FE modelling of ship structures.

One specific question, when using shell elements, is how to model the bulb stiffeners with shell elements? In this case an equivalent L profile was used, which is also a standard practice in ship design. Figure 41 shows the transformation.

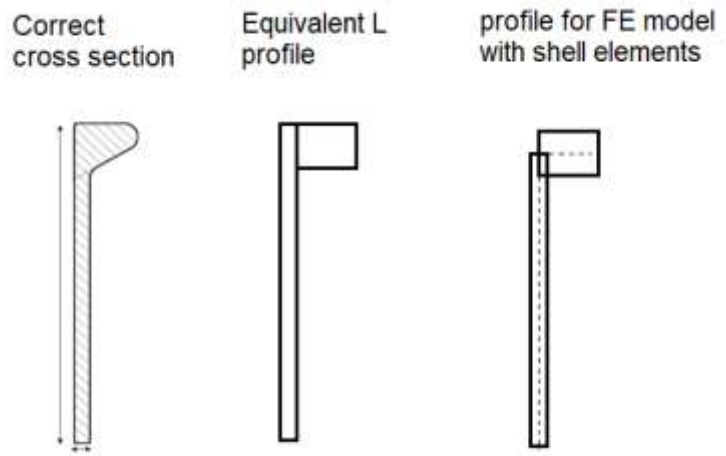

Figure 41. Equivalent L profile used in the modelling of bulb profiles with shell elements.

Usually, linear elements are sufficient, but higher order parabolic elements are also available. This might have an effect when large deformations are present. In Abaqus documentation, element types S4R and S3R, which are quadrilateral (4-node) and triangular (3-node) general- purpose shell elements with reduced integration, hourglass control, and finite strain, are recommended for this type of analysis and these element types were used in this study [22].

5.2.2 Mesh size

Mesh size is also an important parameter in all FE-models. With too coarse mesh the results can be inaccurate but on the other hand fine mesh model takes more computational resources. However, with today's computer calculation capacity the mesh size is not so much of a problem anymore.

In currently available Class Rules for nonlinear finite element analysis for ice loads, there are some guidelines for mesh sizes. In the Lloyd's Register Rules [5], the mesh size is recommended to be as minimum 8 elements between stiffeners. In addition, element size should not exceed 10 times the plate thickness and 50 mm, whichever is the smaller. In the ABS Rules [23], the mesh size is recommended to be as minimum 6 to 8 elements between stiffeners, 3 to 6 elements across stiffener web, 2 elements across full stiffener flange and minimum 3 elements on bracket. In the DNV Rules [6], the mesh size is recommended to be as minimum 6 elements between stiffeners.

Because the mesh size is fairly easy to vary it is one of the parameters to test to have better understanding on how it affects the end results. This was studied with the parametric model of the baseline vessel.

For analyzing the structural capacity of the example vessels, the mesh density was chosen to obtain as minimum 8 elements on shell plate between each stiffener.

5.2.3 Material model

When non-linear analysis is carried out with large deformations, the material model plays a significant role. For analysis in the elastic region (no plastic deformation) the linear material model with constant modulus of elasticity is sufficient. However, with large strain values the stress-strain curve must be wider than the elastic region considering the non-linear material behaviour in the plastic region. A bi-linear stress-strain curve is often used where the plastic region has a different modulus of elasticity due to

strain hardening. Even more sophisticated models can be used, and those will be tested out to understand the effect on the end results. Especially description of the onset of yielding might have some effect on the amount of permanent deformation of the structure after the loading is removed.

The material for the studied ship structures was chosen to be S355. This is a very typical choice for ice-strengthened ship. The material has the nominal yield stress of 355 MPa.

Four different material models were studied. These included two simple models having bi-linear stress-strain curves. In the elastic portion the Young's modulus of elasticity *E* defines the stress-strain ratio up to the nominal yield point. After that the material behaves plastically and this region is described in the simpler models with tangential or plastic modulus E_t. Two different values of plastic modulus were studied. In the first model it has a value of 1000 MPa and in the second model of 0 MPa. The latter material model describes ideal-plastic behaviour. Because in some cases numerical solution algorithms may not converge to the correct solution if ideal-plastic model is used some classification societies recommend the use of small plastic modulus in the used material model. Value of 1000 MPa has been most widely proposed for the plastic modulus [3], [2], [5] and [6].

Both DNV [24] and ABS [23] recommend somewhat more sophisticated material models which are composed of several linear parts. Specially the yield plateau which is characteristic to some steels has been described in these models more precisely. DNV's model includes five straight lines. The ABS model is defined with equations describing stress-strain relations in the plastic range. There are also readily calculated tables for different materials including current HS36 steel.

The studied material models had the same linear-elastic part defined by the Young's modulus of 210 MPa. The models differ in how the plastic portion of the stress-strain curve was described. The studied material models described the plastic portion using:

1. ideal-plastic model having E_t = 0 MPa in plastic region
2. plastic model having plastic E_t = 1000 MPa in plastic region
3. DNV proposed material model [24], [25] and [26]
4. ABS material model [23]

When large strains are considered then in defining the material model logarithmic strain and true Cauchy stress, which is defined as force per current area, must be used.

True strain is defined by [27]:

$$\varepsilon_t = \int_{l_0}^{l} \frac{dl}{l} = ln\left(\frac{l}{l_0}\right) \quad (1)$$

In the equation l_0 is the original length and *l* is the loaded length of the tensile test specimen respectively. Assuming that the material is incompressible and the distribution of strain along the specimen length is homogeneous, the true stresses and strains can be expressed in terms of commonly used engineering stresses and strains using the equations:

$$\varepsilon_t = ln(1 + \varepsilon_e) \quad (2)$$

$$\sigma_t = \sigma_e(1 + \varepsilon_e) \quad (3)$$

It should be noted that these equations apply only until the onset of the specimen necking.

True stresses are always higher than engineering stresses. The difference between these two stresses becomes noticeable after a couple of percent's strain levels.

ABS gives the stress-strain relation in tabulated form both for the true total strain and true plastic strains. These are related by the equation

$$\varepsilon_p = \varepsilon - \frac{\sigma}{E} \qquad (4)$$

The DNV material model depends on the plate thickness as shown in Figure 42 for material S355. For thick plates the true stresses are somewhat lower in the plastic region.

Figure 43 and Figure 44 show all the studied material models. The latter figure shows how the behaviour just after the first yielding differs in different material models.

For calculating the plastic capacity of the example vessels, ABS material model was used.

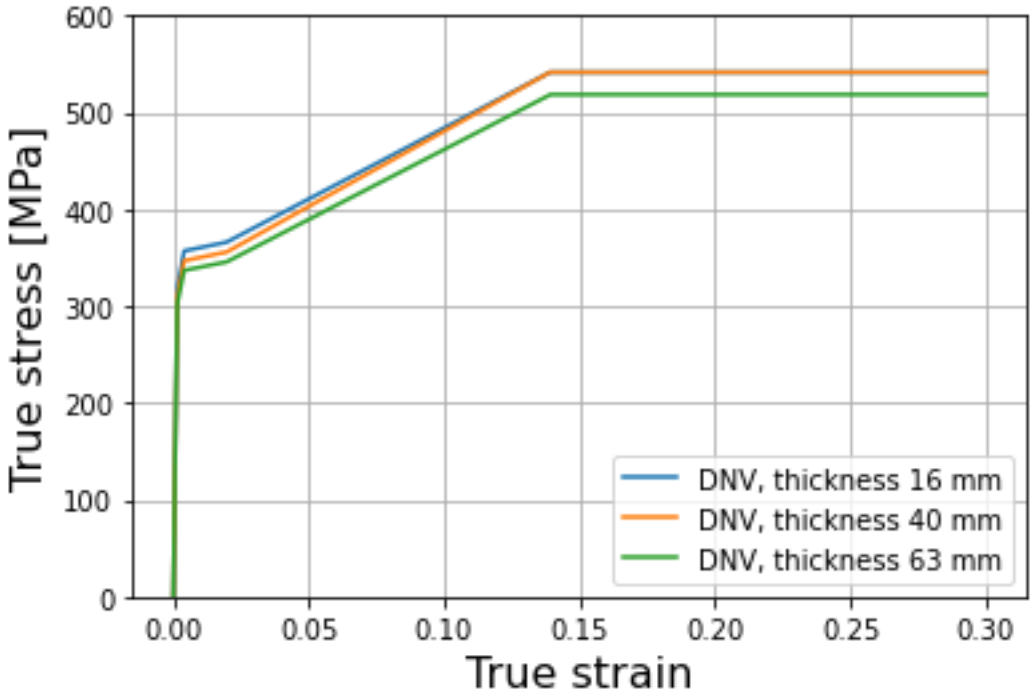

Figure 42. DNV proposed material mode for steel S355 [24].

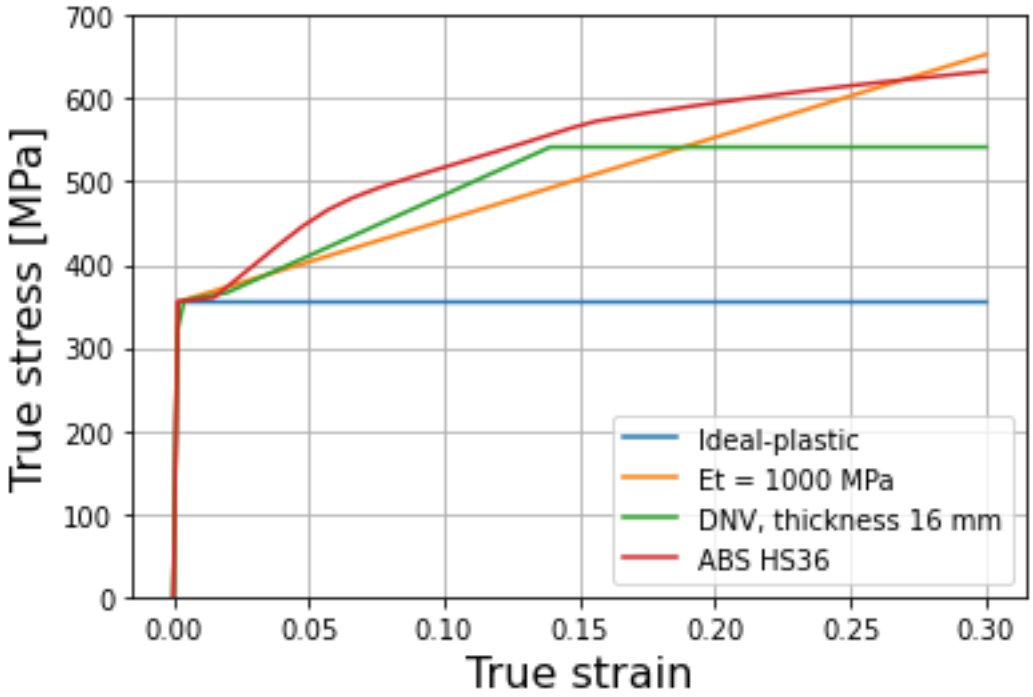

Figure 43. Comparison between different material models.

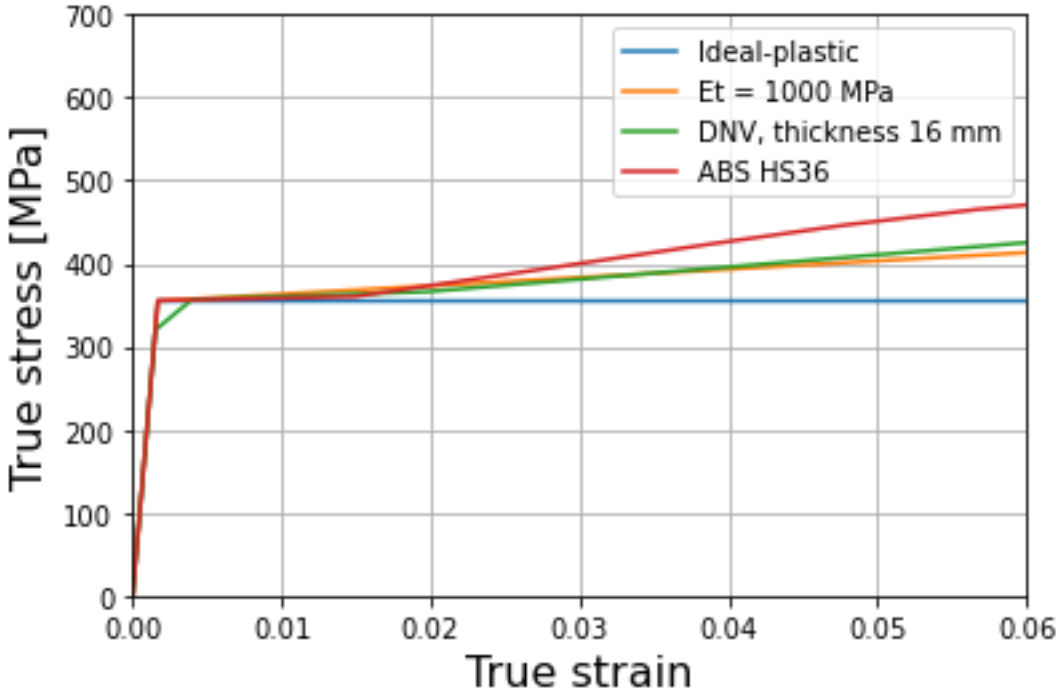

Figure 44. Comparison between different material models. Start of yielding.

The following tables 14 - 16 give the true stress – true plastic strain relations in tabular forms. This is the format in which the material plastic behaviour is usually given in finite element software.

Table 14. True stress – true plastic strain for ideal-plastic, E_t =0 and for E_t = 1000 MPa.

	E_t = 0 MPa	E_t = 1000 MPa
True strain	True stress [MPa]	True stress [MPa]
0.000	355.0	355.0
0.298	355.0	653.3

Table 15. True stress – true plastic strain according to DNV for plate thicknesses below 16 mm [24].

True strain	True stress [MPa]
0.000	320.0
0.002	357.0
0.018	366.1
0.138	541.6
0.298	541.6

Table 16. True stress – true plastic strain according to ABS.

True strain	True stress [MPa]	True strain	True stress [MPa]
0.000	355.6	0.135	555.2
0.003	356.8	0.144	564.6
0.007	358.0	0.153	572.6
0.010	359.1	0.162	577.6
0.013	360.3	0.171	582.3
0.017	370.0	0.180	586.8
0.021	379.7	0.189	591.1
0.024	389.6	0.198	595.3
0.028	399.5	0.207	599.3
0.037	423.6	0.216	603.2
0.046	446.4	0.225	606.9
0.055	465.5	0.234	610.5
0.064	480.0	0.243	614.0
0.072	491.3	0.252	617.4
0.081	501.1	0.261	620.7
0.090	510.2	0.270	623.9
0.099	519.1	0.279	627.0
0.108	528.0	0.288	630.0
0.117	537.0	0.297	633.0
0.126	546.0		

5.2.4 Boundary conditions

Used boundary conditions of a FEM model are very important for accurate results. Especially if the model is limited in size the boundary conditions have large impact. In case of ice loads on a ship the

loads are somewhat local and it is not feasible or necessary to model the whole ship. The analysed ship part is thought to be cut from the whole ship model. Consequently, the displacements at these cut boundaries must be constrained in a proper way to reflect the true behaviour. Without properly defined boundary conditions, the solution to the finite element problem may not accurately enough forecast the behaviour of the ship due to the ice loads. The extent and location of the loaded area must be also considered when defining the boundary conditions.

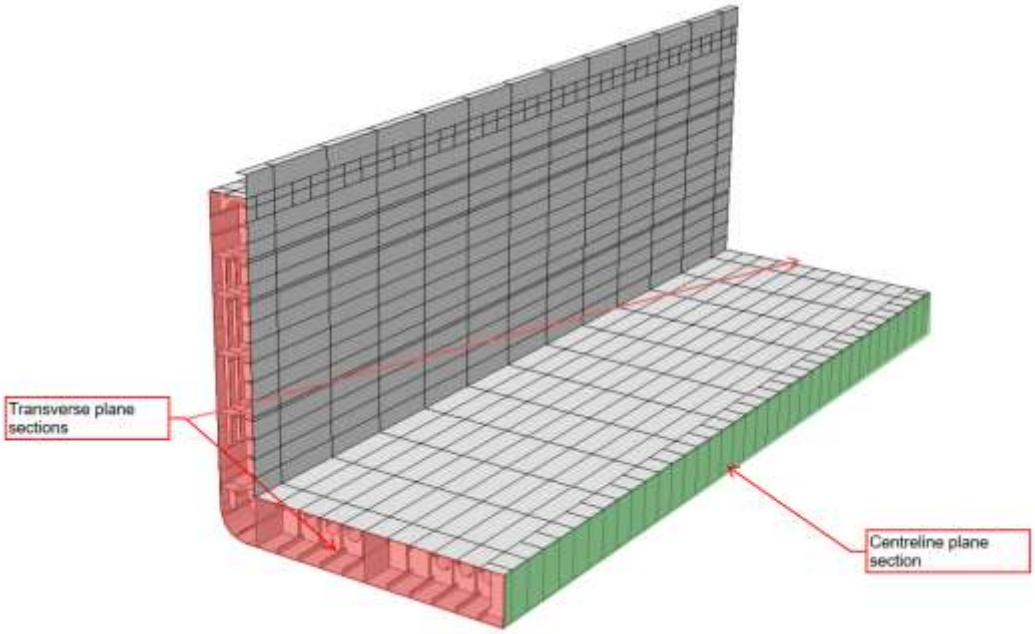

Figure 45. Definitions of planes where boundary conditions are set.

In classification societies guidelines there exists examples on what boundary conditions to use. ABS guideline [8] from 2014 proposes a much smaller local model without upper decks and double bottom to study the ice loads. The guideline lists boundary conditions for this kind of model. However, the size of the model is deemed too small for the purposes of the analysis proposed in this study. Thus, these boundary conditions are not further studied here. Lloyds guidelines for non-linear FE analysis [5] also give boundary conditions for a local half-breadth model similar to ones used in this study, as well as for a full-breadth model. These are investigated in this study and compared to more rigid boundary conditions.

Location	Translation			Rotation		
	δ_x	δ_y	δ_z	θ_x	θ_y	θ_z
Aft End and Fore End						
Cross-section (local and full breadth FE model)	Fixed	-	Fixed	-	Fixed	Fixed
CL Elevation						
Centreline (local FE model)	-	Fixed	Fixed	Fixed	-	Fixed

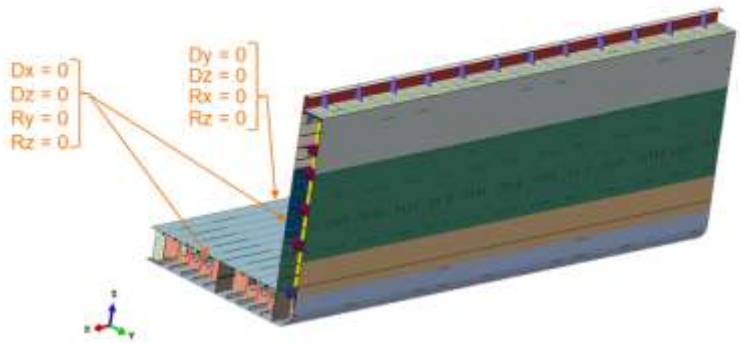

Figure 46. Lloyds boundary conditions [5].

Chosen boundary conditions should of course reflect the structural behaviour at the point where they are applied. When boundary condition limits the translation, real structure should also be able to do that. For example, a watertight transversal bulkhead could be considered quite rigid in y and z direction. Taking into account the outer shell and stiffener structure would make this section also stiff in x direction. Thus, it can be argued that at this transverse plane section even a rigid boundary condition would be applicable.

When half-breadth model is used, a symmetrical boundary condition at the centreline (CL) plane section is a natural choice. This assumes that the ship structure as well as the loads are symmetrical. Ships usually are symmetric regarding to CL and symmetrical load essentially means a condition where the ship is in a compressive ice field, which is quite normal situation in heavy ice conditions for typical Baltic Sea vessels. The proposed boundary condition of Lloyds guideline is not strictly a symmetry boundary condition at the CL because also the z direction is fixed.

In Chapter 6 results from a study are shown on how different boundary conditions perform when compared to each other and how the size of the model affects the results.

5.2.5 Load application

The load is applied on a rectangular load patch as evenly distributed pressure. This approach has been widely used for ice loads and can be considered standard practice, see for example [23], [8], [6], [5], [2] and [3]. The load patch dimensions are taken according to the Finnish-Swedish ice class rules [16] and the pressure is varied to study the capacity and response of the structure. Load is increased incrementally.

During the study, various load patch widths were tested to understand the effect of load patch width on the capacity. The design ice pressure decreases as the load patch length in increased, but the total force increases. This effect is applied to load lengths larger than 0.6 m, and below that, the pressure is limited to a maximum value.

However, for making the rules well balanced and to work with varying structural arrangements, it is most likely best to use load patch sizes as described in the Finnish-Swedish Ice Class Rules, as shown in Table 17. These load patch sizes were used for the final results, even though in name of research and thoroughness, other patch sizes were explored as well with the baseline vessel.

Table 17 Load patch lengths for various structures [28].

Structure	Type of framing	l_a [m]
Shell	Transverse	Frame spacing
	Longitudinal	1.7×Frame spacing
Frames	Transverse	Frame spacing
	Longitudinal	Span of frame
Ice Stringer		Span of stringer
Web frame		2×Web frame spacing

5.3 Analysis techniques

5.3.1 Solution and incrementation

The analysis is made with implicit solver. Explicit analysis could be also used, but due to required rather small element size, and consequently relatively small maximum stable time increment, the computational cost would become excessive.

Incrementation is set so that Abaqus solver can vary the load increment to find optimum for obtaining stable solution with minimum computational effort. Maximum load increment is set to 10%, so that sufficient resolution for the load-displacement curve is ensured. When necessary, Abaqus Solver uses smaller load increments to find a stable solution.

5.3.2 Elastic, plastic, and total deformation

Plastic (permanent) deformation is solved from total deformation by subtracting elastic deformation to obtain the load at which the plastic deformation reaches the limit of allowed permanent deformation. This is done by

$$\delta_{plastic} = \delta_{total} - \delta_{elastic}$$

It should be noted that this is an approximation. At small displacements and strains, the approximation is relatively accurate, and as the deformations increase, the accuracy diminishes. For finding the exact load at which the allowed plastic deformation limits defined 5.3.3 in occur, linear interpolation is used between load increments. At the allowed plastic deformations defined in 5.3.3, the accuracy is typically acceptable.

5.3.3 Definition of capacity limit

There are several methods to define the capacity limit of the structure. The simplest and most widely used is the elastic limit, which requires that the stress in all parts of the structure stays below yield stress of the material. The upside of elastic limit is that analysis is linear, and thus simple and straightforward to perform. The downside is that for structures for which a small permanent set is allowed, such as ice strengthened ship structures, the linear elastic analysis cannot predict the load at which small permanent set occurs accurately and reliably. For structures made of steel, which is ductile and isotropic material, it can be assumed that a plastic reserve exists above the yield limit, but linear elastic analysis cannot predict the amount of this margin [7].

For non-linear plastic analysis, there exists several methods to define the capacity limit for the structure. The ones that have been proposed for design of ice-strengthened ship structures are discussed here.

Several methods are based on analysis of load-displacement curve. One of these is published in the Russian Maritime Register of Shipping (RS) Rules, while several others remain unpublished. The acceptance criteria used in the RS Rules for non-linear analysis of primary structures for Polar Class vessels is a modified tangent intersection method [29]. These methods are based on analysing the shape of the load-deformation curve and trying to characterize the “knee” point that is observed in curve of a typical beam structure, as shown in Figure 47. The “knee” point occurs at plastic hinge formation when the main load-carrying mechanism changes from beam to membrane stresses.

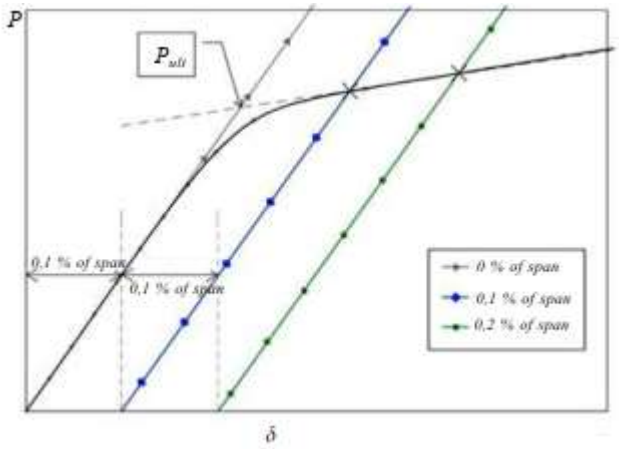

Figure 47 Definition of plastic capacity with modified tangent intersection method, from [29].

The issue with these methods is that while they work well for ideally shaped load-displacement curves, the load-displacement curves for typical ship structures often differ from that significantly as the structure is more complicated than simple beam grillage and other mechanisms such as buckling affect the behaviour of the structure. [3]

Other publicly proposed criterion is the one proposed by Pearson et al. based on study of several existing high ice class vessels. [2] They found out that typical structures of existing icebreakers were able to carry 150 % of Polar Class design load with a plastic strain of less than 2.5 % and proposed that as a design criterion. While not directly applicable to typical merchant vessels governed by the Finnish-Swedish ice class rules, the 2.5 % plastic strain, or some other strain value, could be used as criterion to define the point where structure transits from small deformation to large, and consequently as capacity limit.

Similarly, the criterion could also be based on certain stress limits. As stress is directly tied to strain by material properties, these two limits behave essentially in similar way. The issue with both is that strain, and consequently stress, is very dependent on the mesh. To ensure that the future rules would be applied similarly by all designers, very strict guidance on meshing techniques, mesh size, element shapes and element types would be required. Even with strict guidance, there would always be some degree of variation on the results even for the same structure, depending on mesh details. The required quality of mesh would also make the practical use of the method more tedious for the designers, as the effort required to achieve sufficiently good quality mesh is high.

Some tries have also been made with setting the displacement at the design load as the criteria. The issue with these is that while structures of certain ship types, such as bulk carriers and container vessels which do not have decks and are open at the top, might exhibit significant elastic deformation during ice load, the permanent deformation might still be small or nonexistent. On the other hand, other vessel types with lots of decks and bulkheads, such as ferries, might have very small elastic deformation due to dense supporting structures. Applying this sort of criteria might lead to excessively heavy scantlings on certain ship types. It should also be noted that for the vast majority of cases, there is no afterwards evidence of the elastic deformations that the structures have sustained, as these will not have any permanent consequences.

Criteria based on permanent deformation of the structure was first proposed by Bond and then developed to analysis procedure by Valtonen et al. [3] and adopted into several Classification Society Rules [4] [30] [5]. In all of these, the allowed permanent deformation of the structure at design load is tied to newbuilding quality standard IACS rec. 47 [1]. The basis of this approach is that afterwards, it is not possible to determine if the deformation that is within those limits is caused by ice load or has been there since the ship has been built. Another important consideration is that as long as permanent deformations are within those limits, the structure can be assumed to have same load-carrying capacity as a newbuilt structure, as the initial deformation is not more than what is considered acceptable for a newbuild. Additional benefits of this approach are that deformation is fairly robust against small variations in meshing and modelling practices, and that the criteria are directly linked into the design target which is to avoid excessive deformation of the structure, i.e. ice damage.

While IACS rec. 47 has fairly extensive table of limits for various structural elements [1], it has been typically simplified for this application by taking maximum deflection along span of framing members as 0.3% of span and maximum out-of-plane deformation for all members as 8 mm [4] [5] [6] [3]. Shell plating has not been considered previously, but as the allowed limit for deformation between frames is 8 mm [1], it is taken as the limit for shell plate as well.

In calculation of the 0.3 % of span limit for framing members according to rec. 47, the span should be taken as minimum 3000 mm, leading to a limit value of 9 mm [1]. On Polar Class Rules, that limit has not been specified, as the non-linear FEM is applied only to primary members, for which the spans are typically relatively long. As the same criteria is now applied also to frames, a lower limit is proposed, as

otherwise the allowed deformation for frames may become less than that for plate, which can lead into wrong balance between structures. For simplicity and good structural balance, that limit is taken as 8 mm for this study.

Due to these considerations, it is recommended that the required limit states are tied to this criterion. Following [3] [4] [30] and [5], the limits are in this study taken as 0.3% of span (but in no case less than 8 mm) for frames, stringers and webframes, and out-of-plane deformation of maximum 8 mm. For later work of writing the exact rules, these should be visited in more detail to see if there is need to refine these limits or to set additional ones.

In addition, it is recommended to set a limit requiring that stresses stay below ultimate strength of the material to avoid rupture, even though this limit is a design driver with the current shipbuilding materials. [3]

In addition, it is recommended to include criteria that requires the structure to retain positive slope of load-deflection curve up to a load that causes permanent denting of 5 % of frame spacing on the shell plate, to ensure that even when overloaded, the structure behaves in a safe way, even if it is dented to such extent that repairs are needed. The 5 % of frame spacing dent depth follows from the maximum observed damages in damage statistics, as discussed in chapter 3.

6. Results

Results from the different parametric studies are reported here. The first task was to determine the size of the model and appropriate boundary conditions.

6.1 Boundary conditions and model size

Two different boundary condition set-ups were considered:

1) All fixed: all the degrees of freedom were fixed at the centre line and model fore and aft cuts
2) Lloyd's boundary conditions, see Figure 46.

Model size was varied from small to large and from half-breadth model to full-breadth model. See Figure 40 for the different model sizes. The small model (A) had a length of 4 web frames, medium model (B) had a length of 12 web frames and the long model (D) had a length of 36 web frames. Large model (C) was the full breadth model with length of 12 web frames. The loading was the web frame load as stated in Table 5 (implemented as pressure load) positioned either at the level of platform or between two such platforms. The used material model was simple bi-linear elastic-plastic model with ideal plastic behaviour after the yield stress (Et = 0). Ultimate load was calculated, and it was assumed to be obtained at the force level where the analysis run stopped indicating that small increment in load would cause indeterminate displacement under the load.

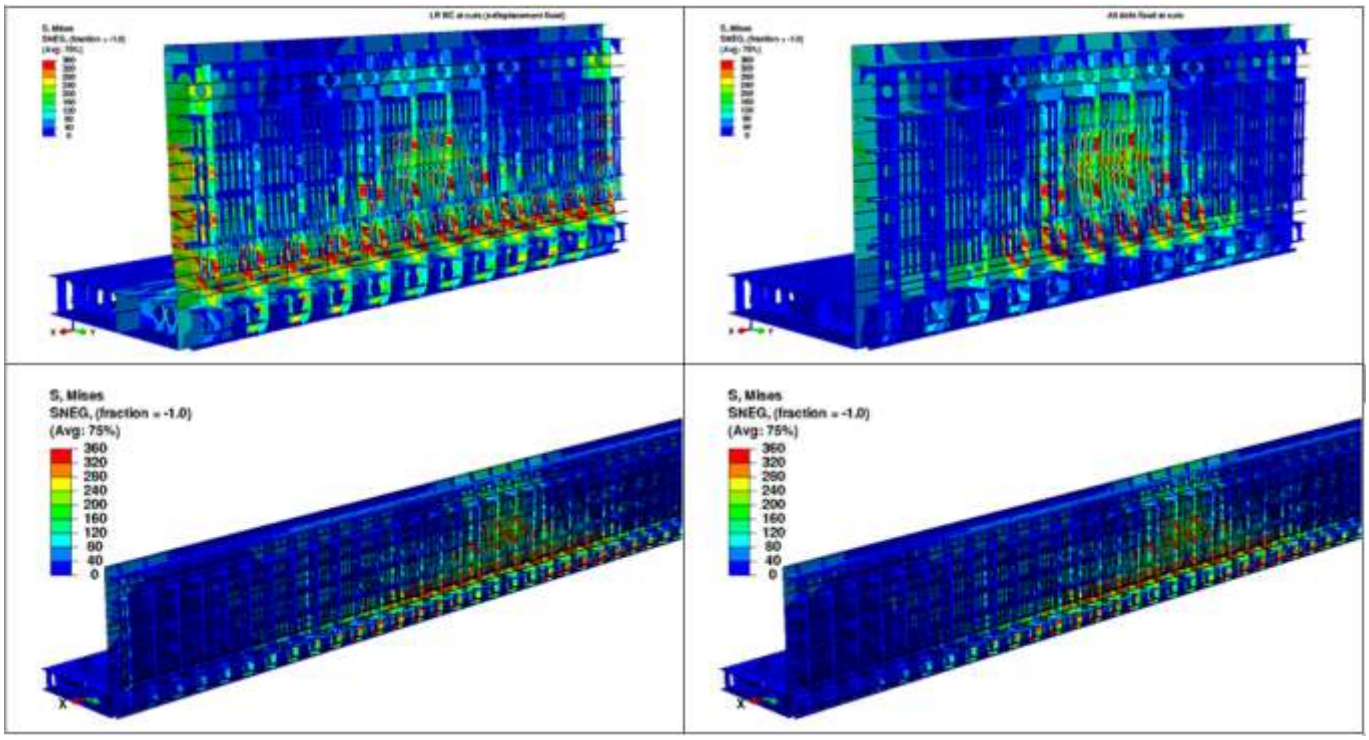

Figure 48. Stress distribution at the ultimate load level. Model with Lloyds boundary conditions on left and with all degrees of freedom fixed on right. Medium size model in the upper row and long model in the lower.

Stress results at the ultimate load level are shown in Figure 48 both obtained with the medium size and long models. It was noticed that the Lloyds boundary conditions did not work very well with this ship type. This is because the displacement in the y-direction in the transverse sections is free with Lloyds boundary conditions and thus the whole side tends to bend. The Lloyds boundary condition is obviously meant for a ship with an upper deck where the boundary condition at CL section would support the upper part of the side structure.

Fixed boundary conditions are satisfactory; however the use requires that the ship structure has a strong bulkhead at the transverse section which has shear strength in the transversal direction. In the latter case the double bottom brackets carry no loads. If there are no bulkhead or similar structures but the ship is open in the longitudinal direction, then also the double bottom brackets carry loads. In case where it there is no strong transversal bulkhead the length of the model has to be considered carefully to minimize the effect of boundary condition.

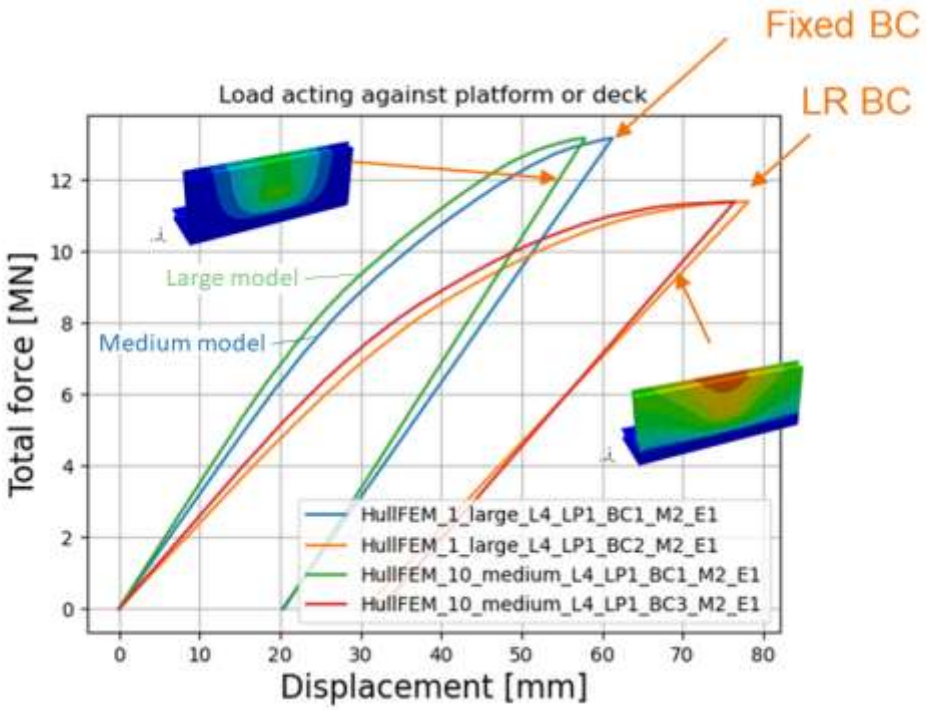

Figure 49. Displacement-force curve for Lloyds and fully fixed boundary condition for both medium and large model. Load is the web frame load as stated in Table 5.

Figure 49 shows the displacement (at the position of load) against total force for different cases. The Lloyds (LR) boundary condition has obvious problems as stated earlier. More useful in this case is to see that the medium (B) and large (C) full breadth models don't have large differences. Thus, it can be argued that the medium model is sufficiently large for the analysis. The load in this case is acting at the position of platform which results in most global deformations. The other studied load cases (web frame load acting between platforms/stringers and the smaller load patches) lead to more local deformations which means that even smaller model might be sufficient for those cases.

According to the studied cases side plating membrane in-plane boundary conditions in the ship longitudinal direction had only minor effect on the structural responses. Ice-strengthened ships have longitudinal load-carrying structural members or stringers that balance the membrane forces acting in the side plating. Moreover, in design calculations the aim is usually not to calculate the ultimate collapse load where the structures experience extremely large deformations but rather to calculate the responses at moderate deformation levels. Consequently, it is reasonable to fix the longitudinal displacement at the model fore and aft transverse sections.

6.2 Mesh size

In 5.2.2 the mesh size was discussed and in many guidelines the requirements lead to an element size of about 50x50 mm to 100x100 mm. In this study results from a model with 50x50 mm and a model with 25x25 mm element size were compared. Vessel in question was the baseline 10 000 DWT IA cargo vessel. The medium half-breadth model was used. Figure 50 shows the two meshes at the position near where the load is placed and where the deformations are largest. For frame stiffeners the 50x50 mm mesh leads to having three elements across the stiffener web.

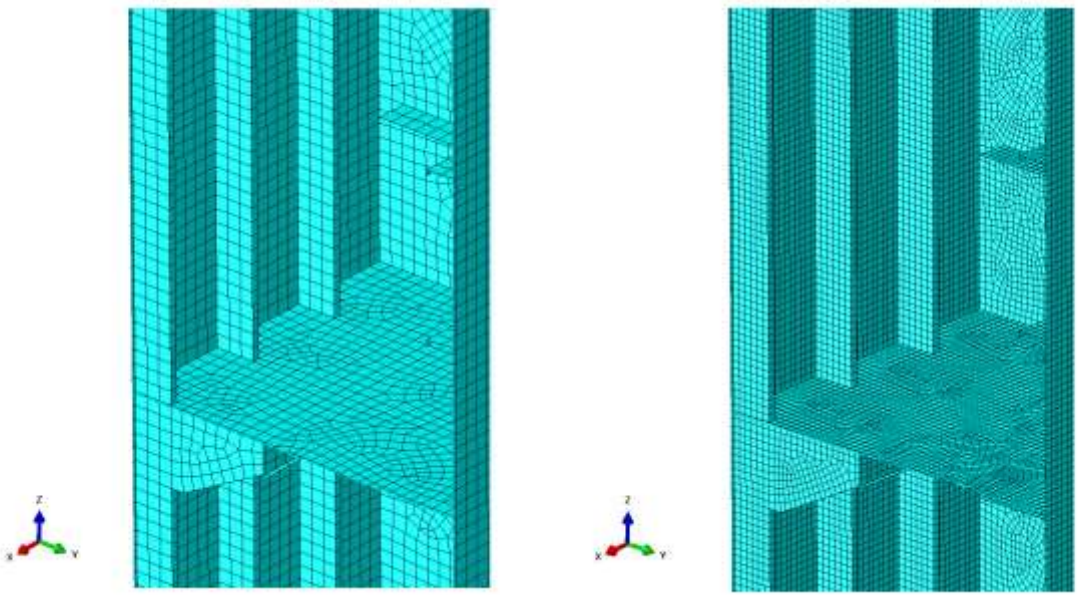

Figure 50. Mesh comparison. On the left: mesh with 50x50 mm elements. On the right mesh with 25x25 mm elements.

The results from the comparison study shows that with very high loads there are quite major differences attributed to meshes. The sensible range in this case can be estimated from Table 18 and subsequent analysis. For shell and frames (frame load case) values range from 300 to 1000 % which means load ranging from 0.47 MN to 1.6 MN. However, it should be noted that the load case with the lowest capacity drives the design, and there is no need for analysing beyond that load, which was typically between 300 and 400 % (0.47 MN – 0.63 MN). For more global webframe load (webframe load case), the loads in Table 18 ranges up to 1800 % meaning a max load of 11.9 MN. Similar to shell and frame, these highest loads were not design drivers, and for all other vessels than 10 000 DWT 1C vessel, the limiting load case had capacity around 400 to 600 %.

Figure 51 shows the overall displacement at the position of load for two different meshes (also the effect of material model is shown but that will be discussed in the next chapter). For webframe load case the analysis with 25x25 mm mesh is stopped much earlier than with 50x50 mm mesh. The reason is that with 25x25mm mesh the webframe experiences much more buckling at high loads which leads to earlier webframe collapse. The detail of this is shown in Figure 53. However, with the deformations in the range of criteria defined in chapter 5.3.3, the difference between two mesh densities is small. With more local frame load case, both meshes give similar results well beyond the expected load range.

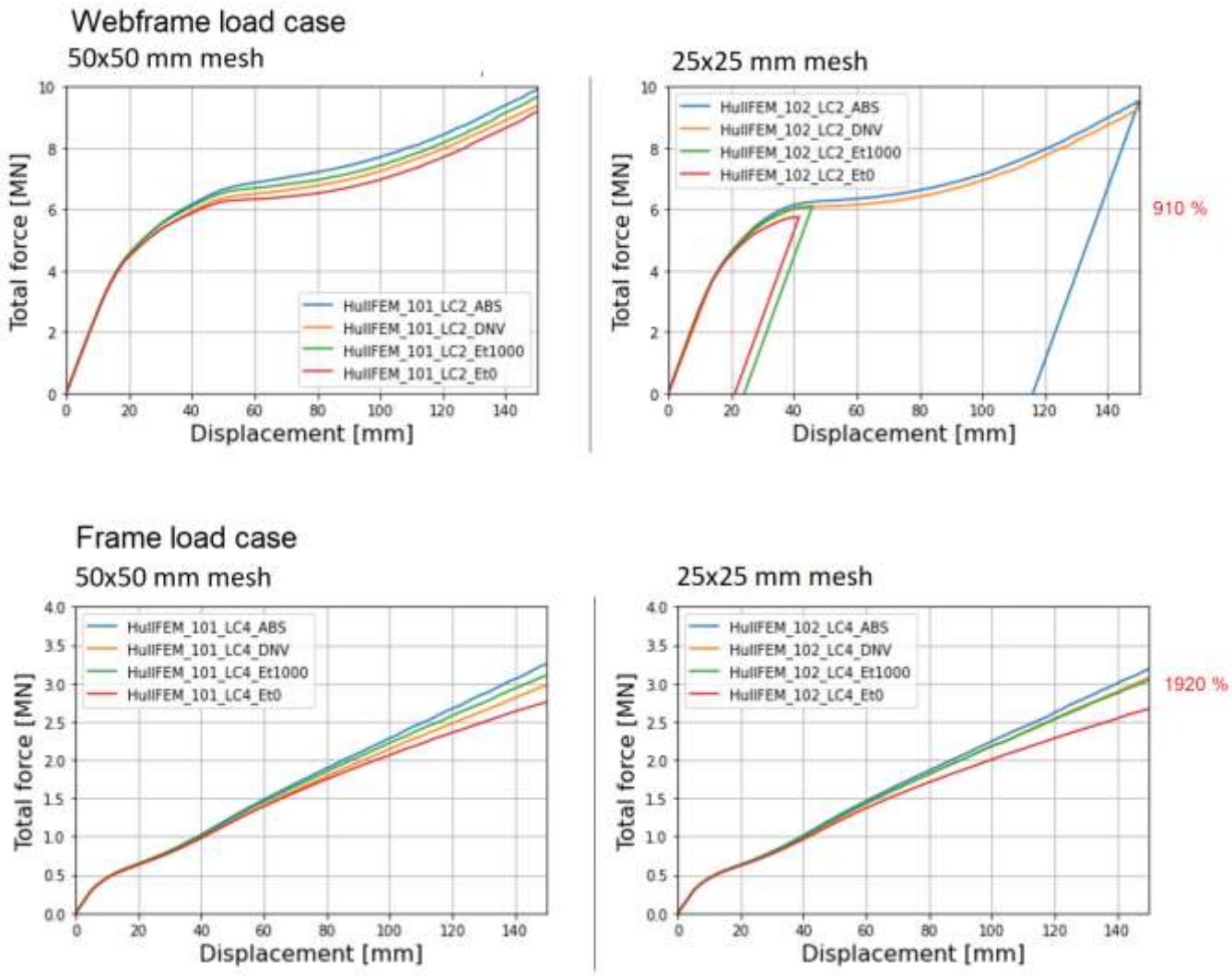

Figure 51. Displacement-force curves for two different meshes and different material models. Upper row is for webframe load case and lower row for frame load case (Table 5). Load % of nominal load also stated.

In Figure 52 the deformation is compared at 3 MN load level for the frame load case. This load level corresponds to 1870% load level which is quite much larger than the range stated earlier (300 – 400 %). It can be seen that the maximum deformation at the load point is quite similar, but some small changes are seen in the shape of the bottom part of the deformed stiffener at the position of load. However, this would not affect the overall criteria assessment.

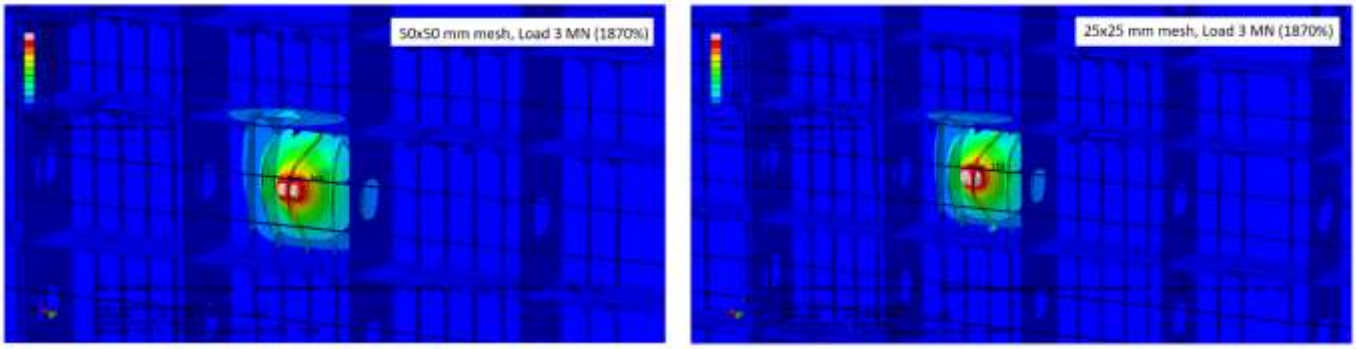

Figure 52. Comparison of deformation at 3 MN (1870%) load level. Frame load case. Same material model. Exaggerated deformation.

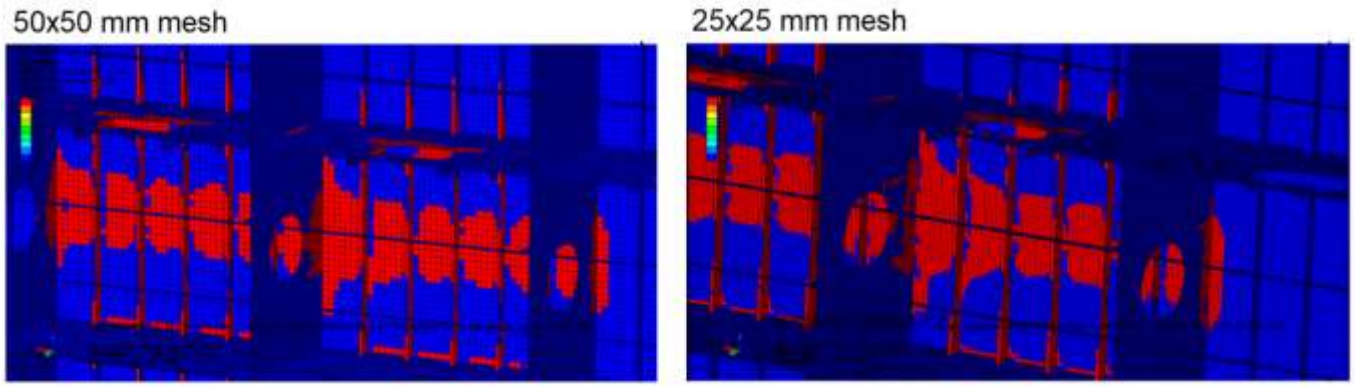

Figure 53. Contour plots of plastic regions. 50x50 mm mesh on the left and 25x25 mm mesh on the right. Web frame load case. Load level 6 MN (910 %). Material model Et1000.

Figure 53 shows the plastic regions for 50x50 mm and 25x25 mm meshes with web frame load case. The load level is rather high 6 MN (910 %). Used material models was the Et1000. Otherwise, the results seem quite similar, but some differences are seen in web frame area in the middle of the load. 25x25 mm mesh analysis stopped at this load level due to buckling of the web frame.

According to the studies made here the 50x50 mm and 25x25 mm mesh give similar results, when the loads are in the range required for the studies and thus the 50x50 mm mesh should be suitable. However, if the structure experiences major buckling the mesh density (and material model) will beginning to have an effect. If buckling cases are indeed analysed, this should be taken into account.

6.3 Material modelling

Material models listed in 5.2.3 were tested and compared. Vessel in question was the baseline 10 000 DWT IA cargo vessel. The medium (B) half-breadth model with 50x50 mm mesh is considered here. Figure 54 shows the overall displacement results. The load case is the web frame load where the required load range, as explained in the next chapter and shown in Table 18, is about 400 – 600 % from the nominal load. It can be seen that in this range all the material model work in similar way. For some reason in this case the DNV and Et1000 material analysis stop earlier than the other two models.

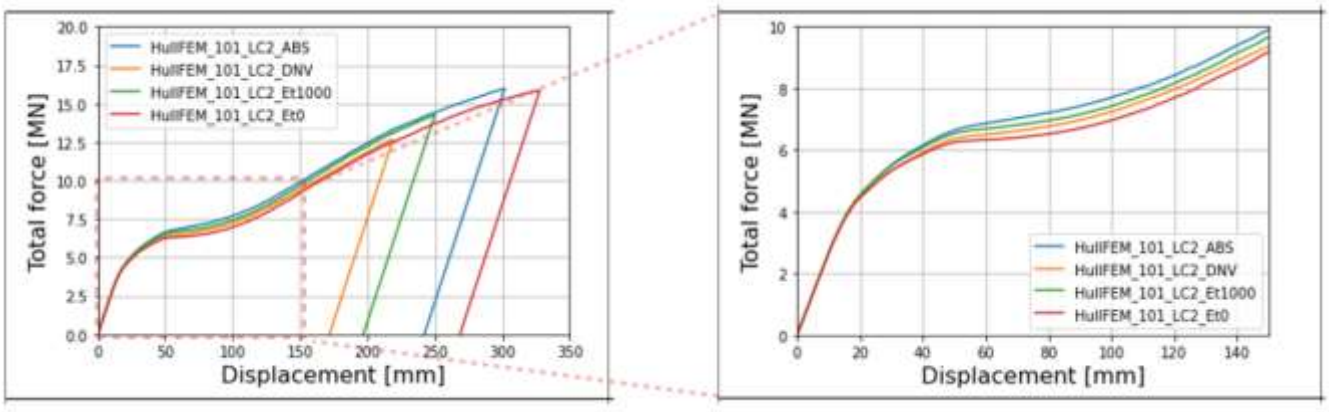

Figure 54. Comparison of four different material models. On the right the range from 0 – 10 MN is zoomed.

Figure 55 shows deformation contour plots from same positions for all material models. The load level is 5.8 MN which means a load level of 880%. This is rather high load level. However, at this load level there is no noticeable difference in the deformed shape. Figure 56 shows the same position with

contours of plastic regions at load level of 12 MN (1818 %). At this level the Et0 material model shows some differences to other material models. For the other material models results are very similar.

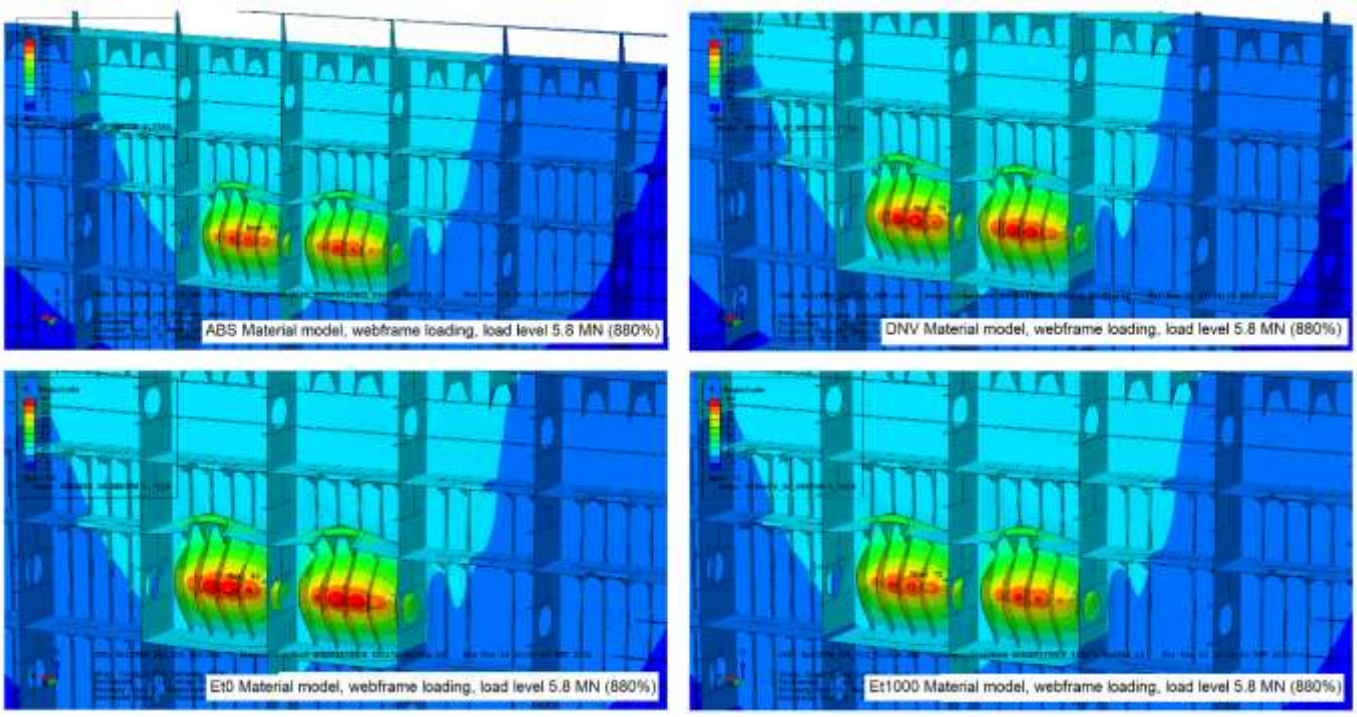

Figure 55. Deformation contour plots for all material models. Load level 5.8 MN (880 %).

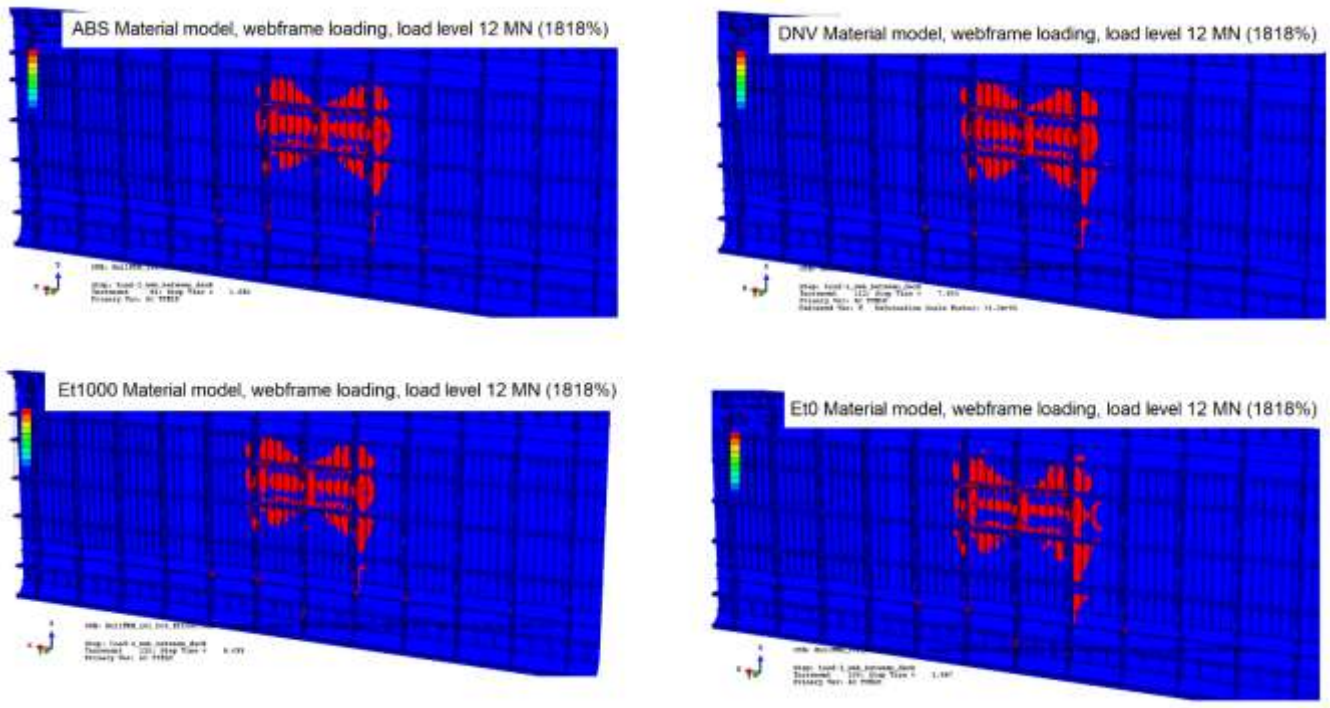

Figure 56. Contour plots of plastic regions for all material models. Load level 12 MN (1818%).

6.4 Baseline vessel, 10 000 DWT IA

The load at which the permanent deformation of the structure reaches the allowed deformation limits defined in 5.3.3 is shown in for each load case in Table 18. The load cases analysed for the baseline vessel are shown in Figure 10, Figure 11, Figure 12 and Figure 13. The load is given as percentage of the design ice pressure of the FSICR.

Table 18 Load (as percentage of FSICR design load) at which the allowed permanent deformation is reached.

Load case	Capacity					
		Frame			Stringer	
No.	Shell	Lower end	Upper end	Center	platform	Webframe
1	429 %	695 %	1000 %	397 %	1811 %	794 %
2	329 %	507 %	733 %	395 %	1897 %	1445 %
3	320 %	690 %	581 %	398 %	1814 %	1721 %
4			526 %	390 %	1866 %	1313 %
5				312 %	1004 %	629 %
6				320 %	848 %	907 %
7				304 %	1823 %	657 %
8				305 %	1817 %	1439 %
9				331 %	1873 %	1490 %
10				390 %	1226 %	1386 %
11					1122 %	637 %
12						828 %
13						1558 %

From these results, the most onerous load patch locations were chosen for the other vessels.

For shell and frames, the lowest capacity was found with load patch width of 0.6 m, due to the rule ice pressure which decreases with increasing load width above that limit and is limited to constant value for shorter load widths. However, using that limit would lead to rules that would have large discontinuity depending on frame spacing. As the load patch size for each structural element is stated in the rules to be frame spacing for transversally framed shell and frame [28], this definition is proposed to be kept for the future rules.

The limiting load cases for each structural element are shown in following figures. For shell plate, the 8 mm permanent deformation is reached at about 429 % of design load. The load – permanent deformation curve is shown in Figure 57, von Mises stress at that point in Figure 58 and permanent deformation in Figure 59. In the critical load case (Shell 1), the load patch is located vertically in middle of the plate field, and horizontally between two frames.

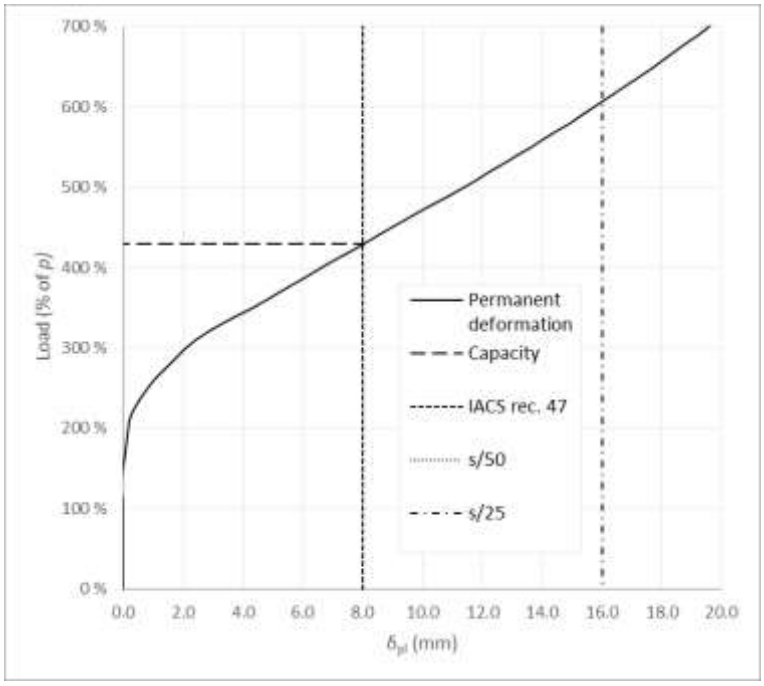

Figure 57 Load-permanent deformation for load on shell plating, 10 000 DWT IA vessel.

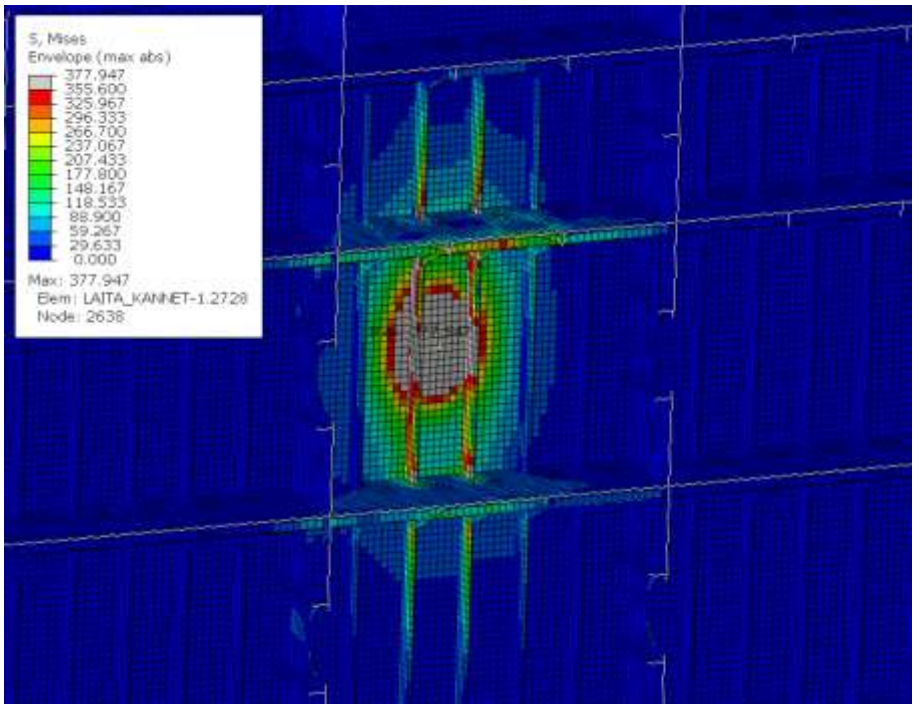

Figure 58 von Mises stress for load on shell plating, 10 000 DWT IA vessel, load 430 % of rule load.

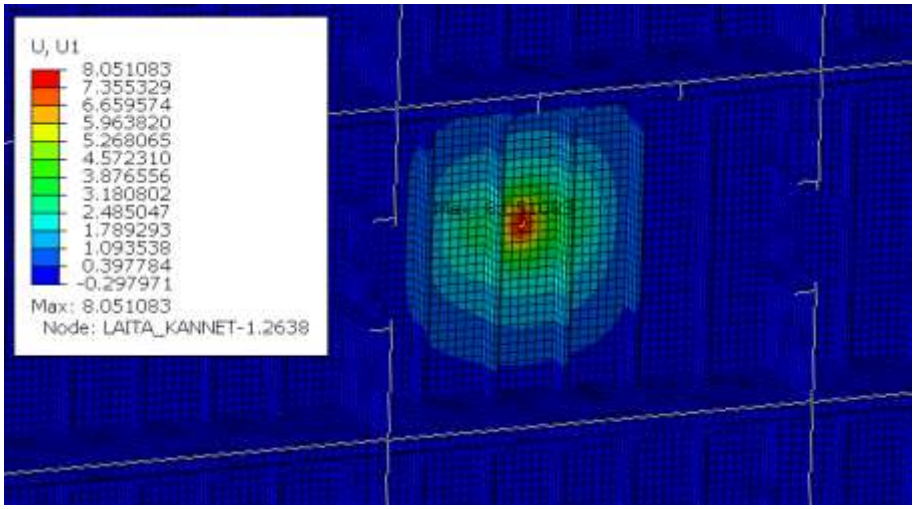

Figure 59 permanent deformation perpendicular to shell for load on shell plating, 10 000 DWT IA vessel, load 430 % of rule load.

For frame, the allowed permanent deformation of 8 mm is reached at about 390 % of design load. The load – permanent deformation curve is shown in Figure 60, von Mises stress at that point in Figure 61 and permanent deformation in Figure 62. In the critical load case (Frame centre 10), the load is located vertically to centre of effective span and horizontally centred on the frame. As can be seen from the results, out-of-plane deformation remains small compared to in-plane deformation, showing that the stability and structural arrangement requirements of the FSICR lead to a structure that behaves well under higher loads.

Interesting side note is also that for a frame adjacent to a webframe, the capacity is slightly higher than that of frame between ordinary frames, as shown by the difference between load cases 8 and 9.

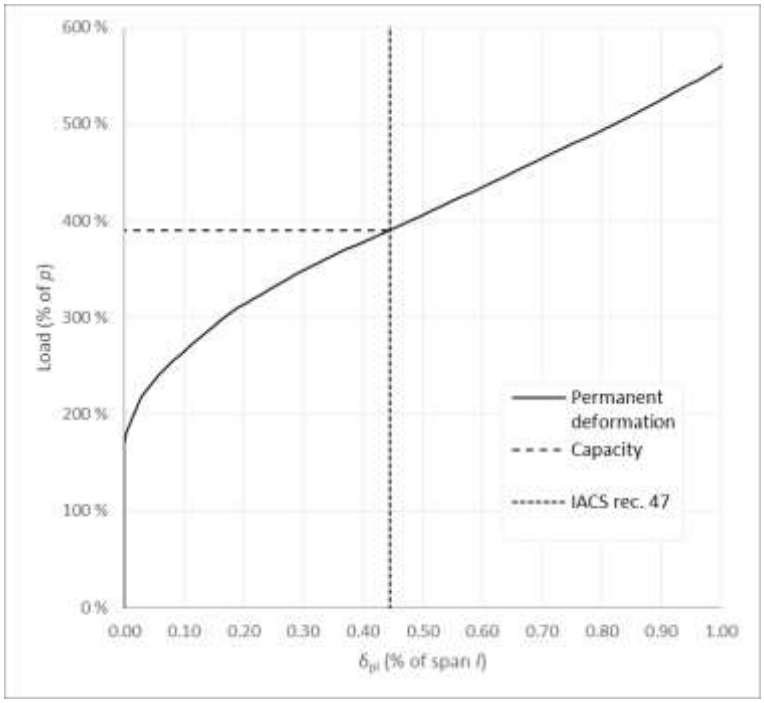

Figure 60 Load-permanent deformation for load on shell frame centre, 10 000 DWT IA vessel.

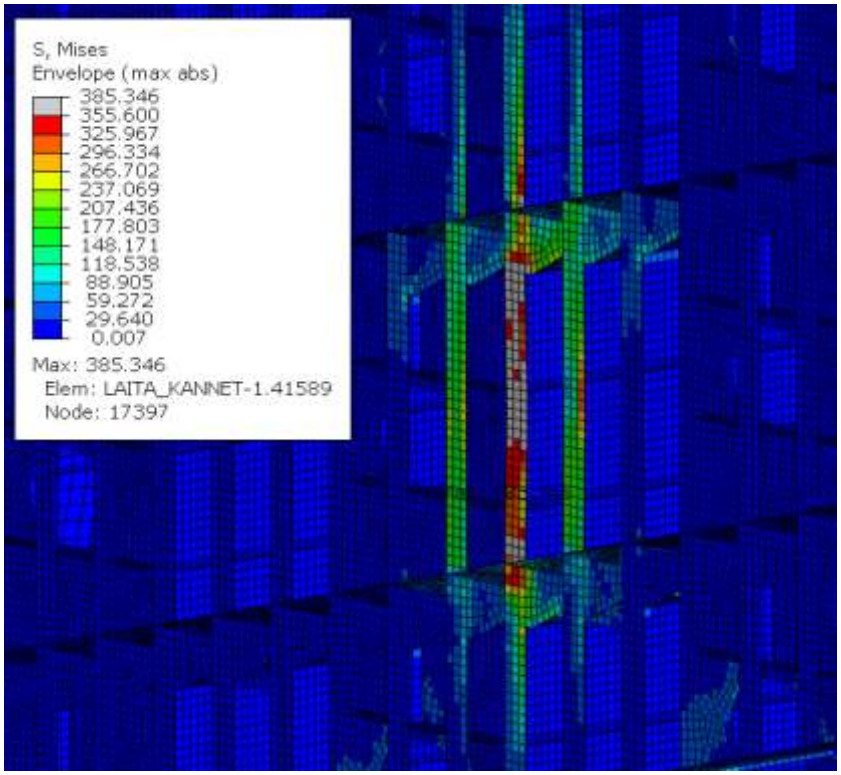

Figure 61 von Mises stress for load on frame centre, 10 000 DWT IA vessel, load 390 % of rule load.

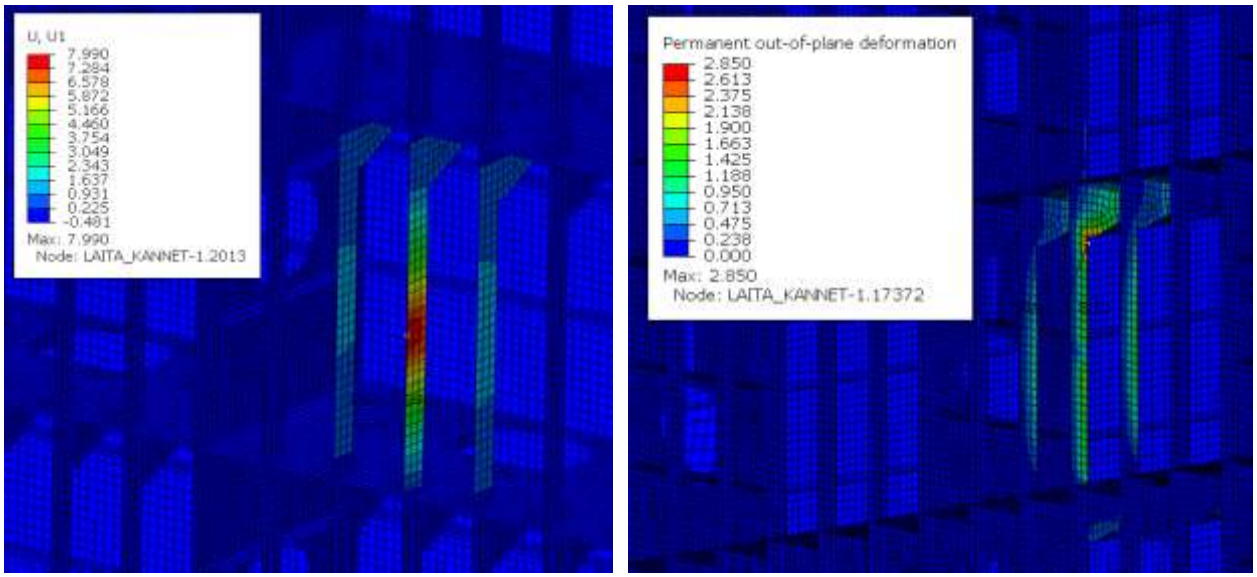

Figure 62 Permanent deformation perpendicular to shell (left) and out-of-plane (right), with load on frame centre, 10 000 DWT IA vessel, load 390 % of rule load.

For primary structures, i.e. stringer platforms and web frames, the governing failure mode is buckling, and the limit for permanent in plane (perpendicular to shell) deformation was not reached in any of the load cases before the out-of-plane (buckling) deformation limit was reached. It also turned out that the capacity of the typical arrangement with full depth plate structures through double side is not limited by bending of the primaries, but rather buckling, and the location of the first buckling was more related to structural arrangement and details of stiffening than particular load location. Therefore, it is advised that further research with open T-girder type primaries is made before conclusions are drawn on most onerous load location or minimum capacity of structures compliant with the current rules.

The load – permanent deformation curve for the limiting load case is shown in Figure 63, von Mises stress at that point in Figure 64 and permanent out-of-plane deformation in Figure 65. In this load case (Webframe 11), the limiting load is 637 % of the rule load and the load is located vertically midway between two platforms in way of manhole and horizontally centered on webframe.

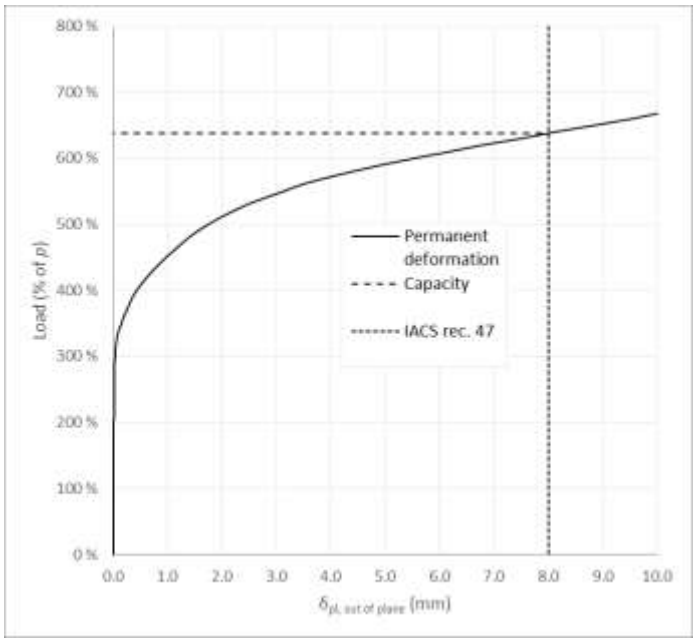

Figure 63 Load-permanent deformation for load on web frame, 10 000 DWT IA vessel.

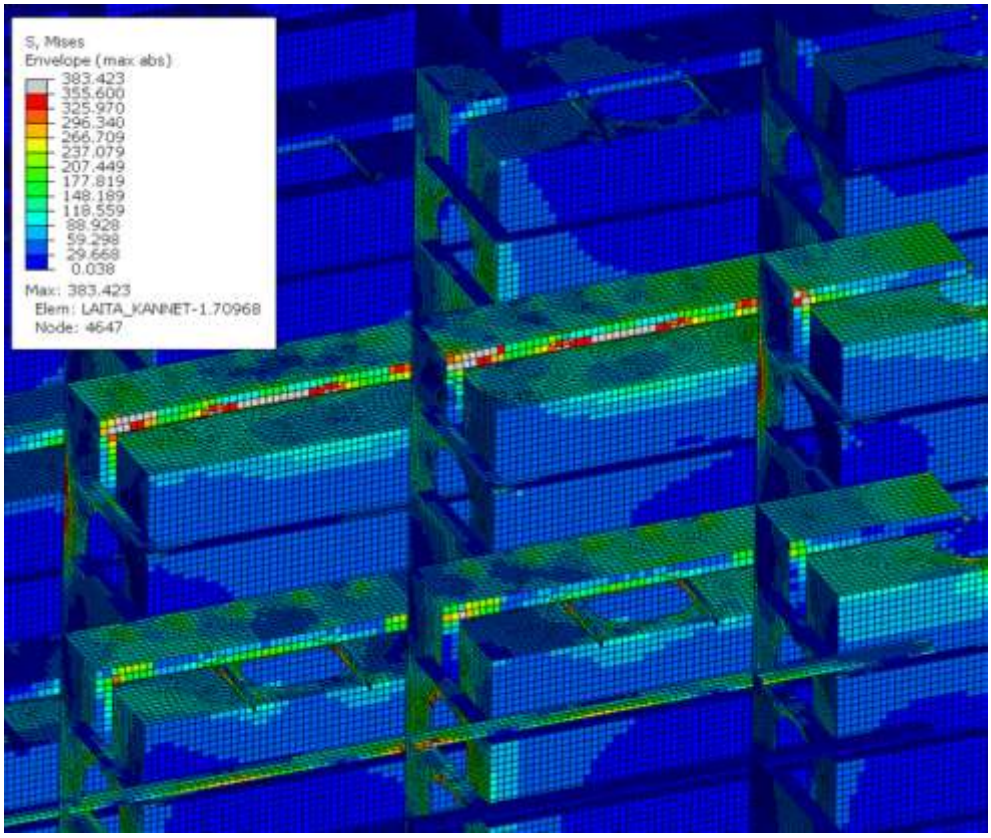

Figure 64 von Mises stress for load on web frame, 10 000 DWT IA vessel, load 640 % of rule load.

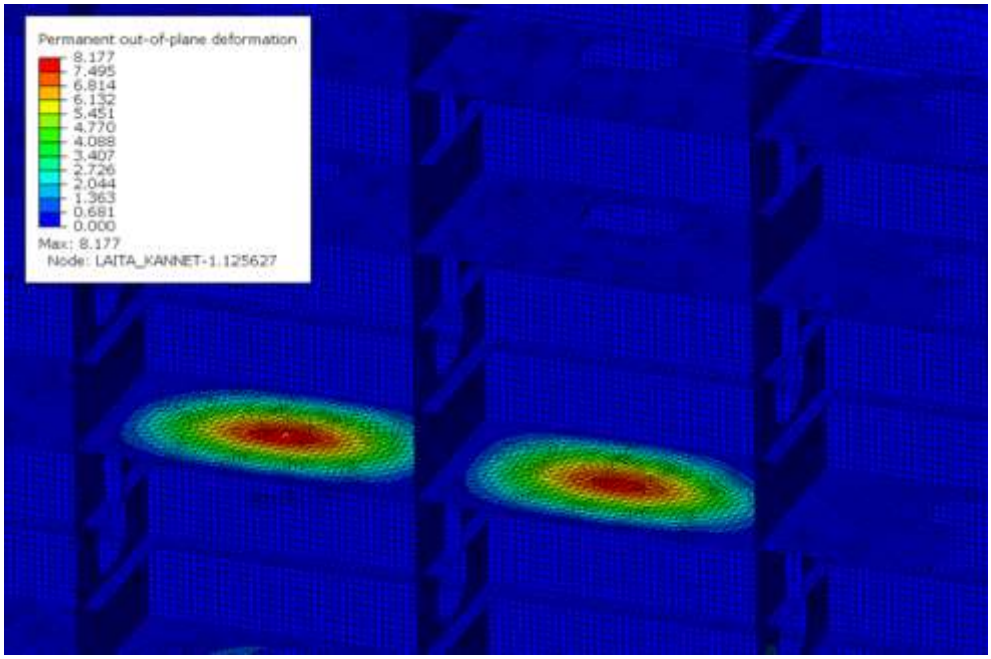

Figure 65 Permanent out-of-plane deformation for load on web frame, 10 000 DWT IA vessel, load 640 % of rule load.

Permanent deformation for each structural member is compared in Figure 66. From this, it can be observed that proper hierarchy exists between secondary and primary structures, as shell and frames deform well before stringers and web frames. It can also be seen that shell has slightly lower plastic capacity than frames, but the different is not large, showing that the 0.75 factor in the rules works as intended. Part of shell capacity exceeding that of frame may also be due to corrosion addition that is applied on shell but not on frames, and the analysis being made with gross scantlings.

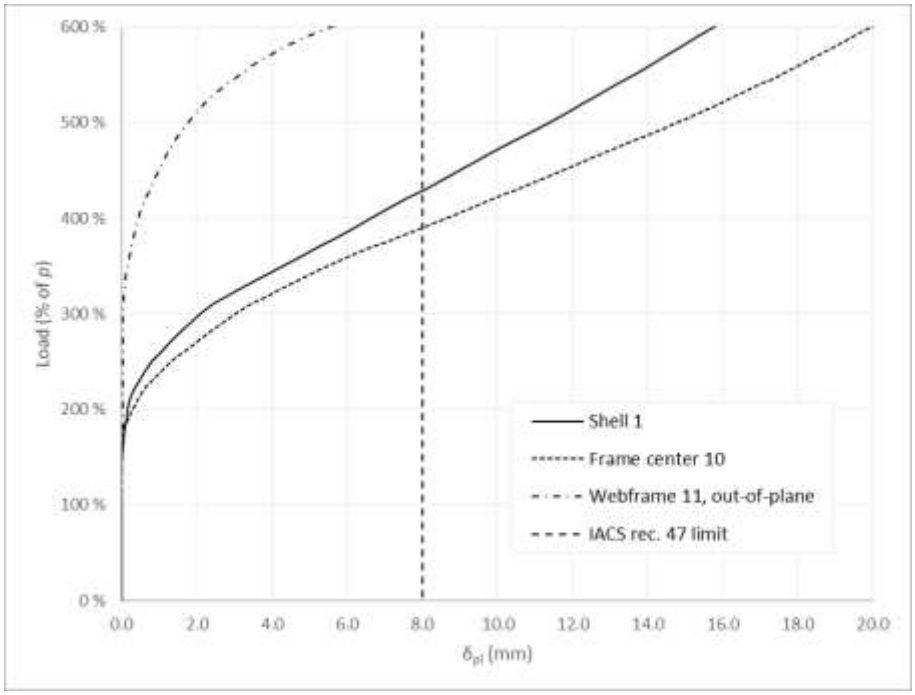

Figure 66 Comparison of load – permanent deformation curves for most onerous load case for each structural element, 10 000 DWT IA vessel.

6.5 10 000 DWT IC vessel

The load at which the permanent deformation of the structure reaches the allowed deformation limits defined in 5.3.3 is shown in for each load case in Table 19. The load cases analysed for this vessel are shown in Figure 19. The load is given as percentage of the design ice pressure of the FSICR.

Table 19 Load (as percentage of FSICR design load) at which the allowed permanent deformation is reached.

Load case	Capacity		
No.	Shell	Frame	Webframe
1	-	400 %	1011 %
2	-	390 %	2000 %
3	-		1128 %
4	-		
5	-		

The limiting load cases for all structural elements are shown in following figures.

For shell, the point at which the plastic deformation in shell panel under load patch reaches the allowed limit value of 8 mm could not be obtained using the chosen method. This is due to the frames reaching limit and giving in before the permanent deformation in the shell reaches this value. The von Mises stress in the model with load case Shell3 at the point of frame reaching the plastic limit (390% of rule load) is shown in Figure 67. As can be seen, frame cross section has reached plasticity for large part, while the plasticized region in the shell is relatively smaller.

Using Hayward method [31], the plastic capacity of the shell plate can be approximated to be about 529 % of rule ice load for load that has length of 2.4 m. For the 58 500 DWT vessel, the limiting case was shorter load patch, with length of 1.7 times frame spacing, as specified in the FSICR [28]. As Hayward method cannot calculate the permanent deformation for shorter load lengths, the Hayward load is scaled in proportion according to results of the 58 500 DWT vessel to obtain limit load of about 490 %. At this load, the von Mises stress in the model is shown in Figure 68. It seems that for this vessel, the balance between plating and framing is wrong way around, with the shell plate having much larger plastic capacity than the framing. This might be due to removal of 0.75 factor for plate pressure for longitudinal framing, that originally was there to account for the larger plastic margin of shell plate than the frames, which was made in rule update in 2010.

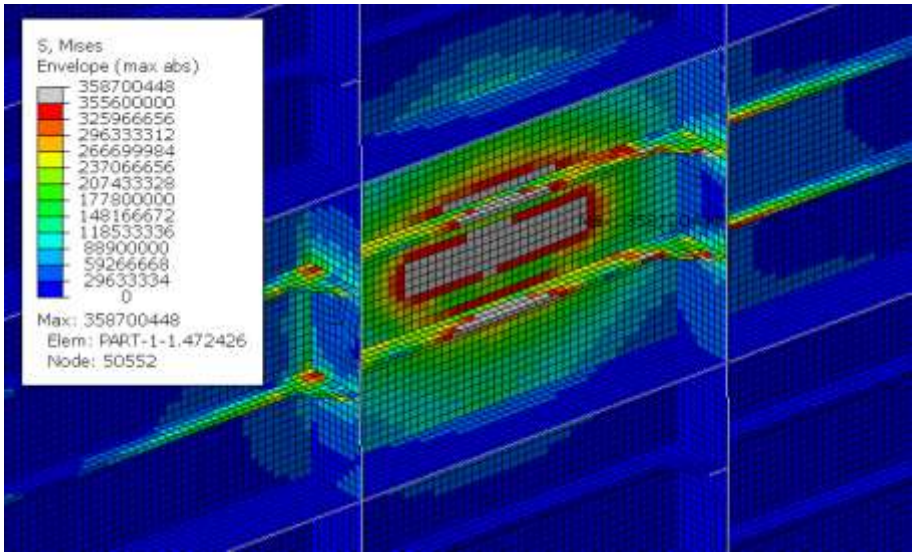

Figure 67 Load case Shell 3, von Mises stress at 390 % of the rule load (frame capacity limit).

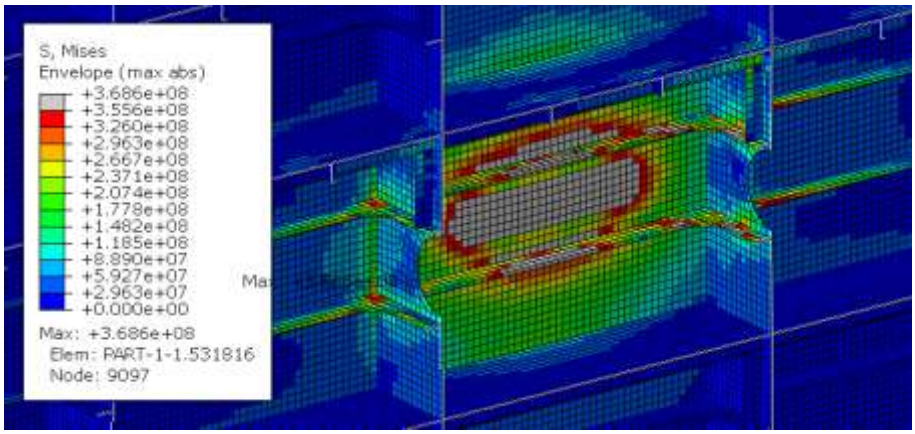

Figure 68 Load case Shell 3, von Mises stress at 490 % of the rule load (estimated shell capacity limit with Hayward method).

For frame, the 8 mm permanent deformation is reached at about 390 % of design load. The load – permanent deformation curve is shown in Figure 69, von Mises stress at that point in Figure 70 and permanent deformation in Figure 71. As shown in Figure 72, out-of-plane deformations remain relatively small and frame stability is adequate. In the critical load case (Frame 2), the load covers horizontally the full span of the frame and is vertically centred on the frame.

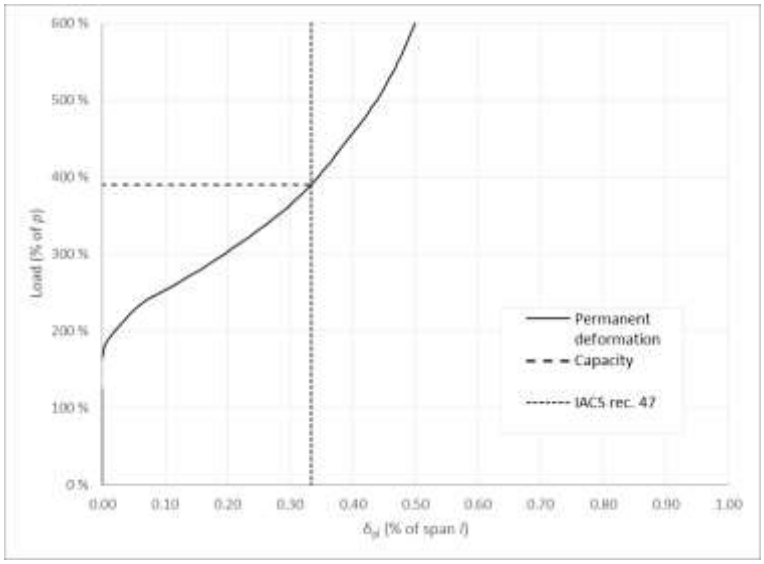

Figure 69 Load – permanent deformation curve for the critical load case for frame of 10 000 DWT IC vessel.

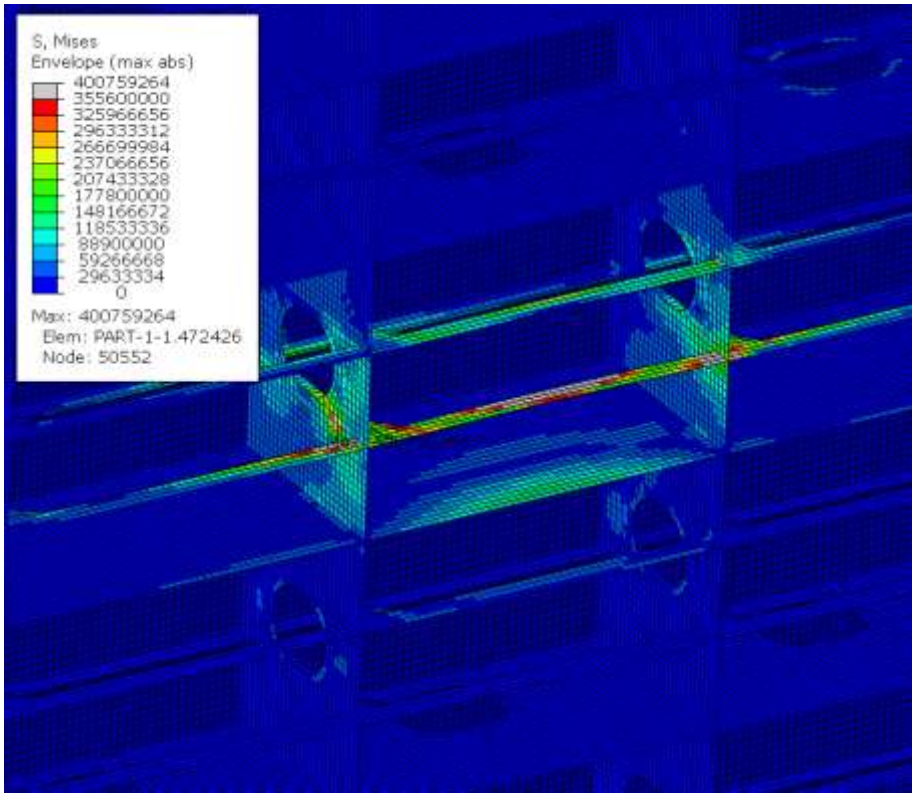

Figure 70 von Mises stress for the critical load case for frame of 10 000 DWT IC vessel, at plastic limit load (390 % of rule load).

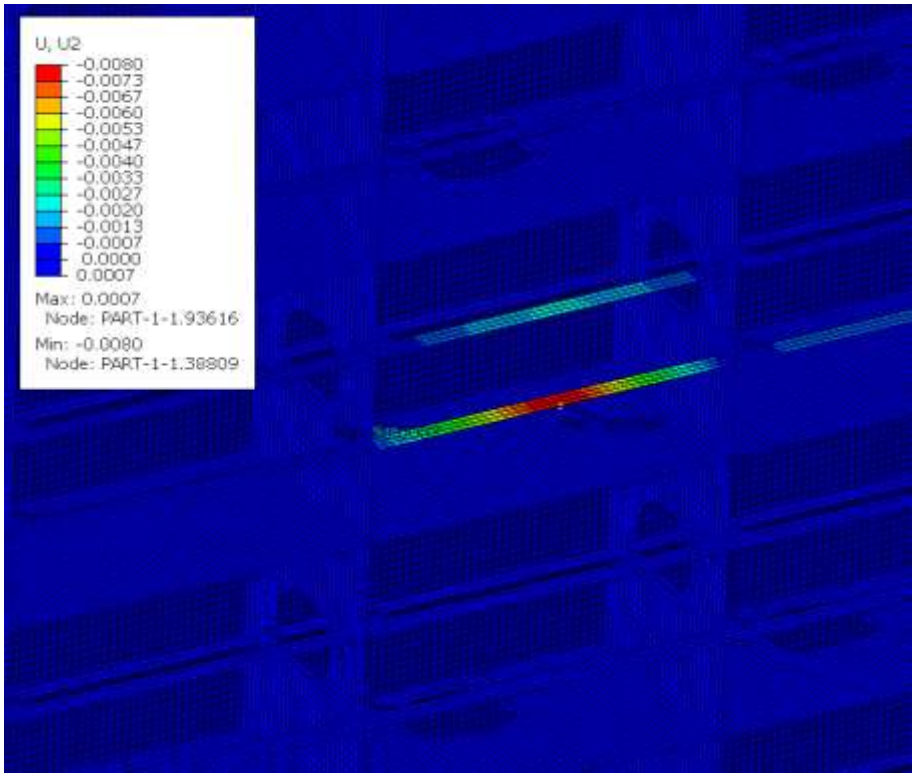

Figure 71 Permanent deformation perpendicular to shell for the critical load case for frame of 10 000 DWT IC vessel, at plastic limit load (390 % of rule load).

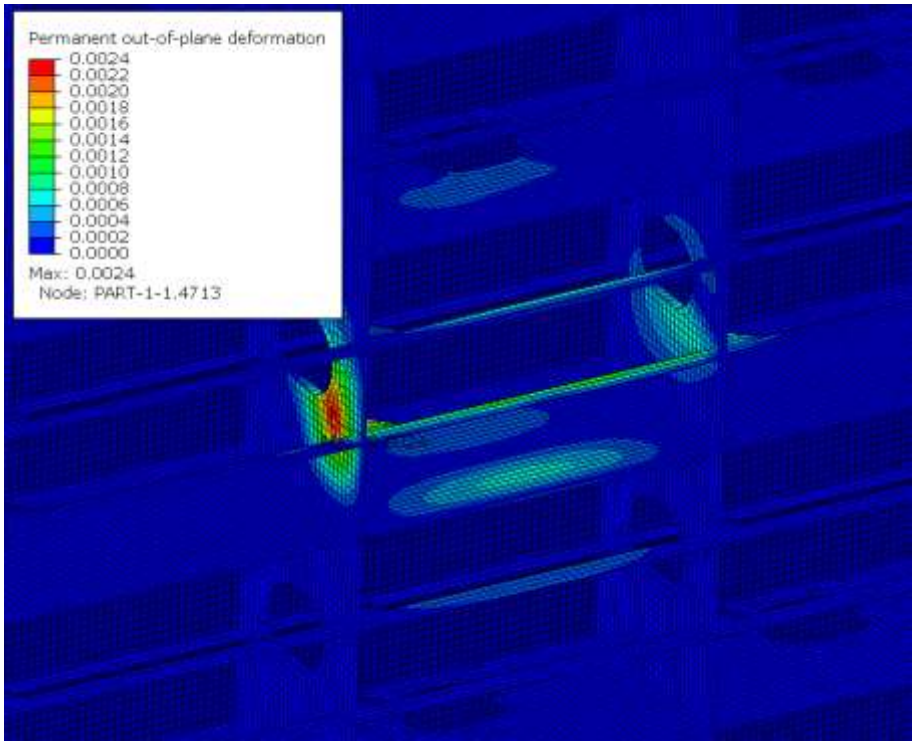

Figure 72 Permanent out-of-plane deformation for the critical load case for frame of 10 000 DWT IC vessel, at plastic limit load (390 % of rule load).

Similar to transversally framed IA baseline vessel, capacity of the primary structures is limited by stability. The load – permanent deformation curve for the limiting load case is shown in Figure 73, von Mises stress at that point in Figure 74 and permanent out-of-plane deformation in Figure 75. As can be seen from Figure 76, permanent deformation perpendicular to shell is still well below the allowed limit. In this load case (Webframe 1), the load is located vertically midway between two platforms in way of manhole and horizontally centered on webframe.

As expected, the capacity of primaries with about similar scantlings as vessels with higher ice class is higher when compared to the lower ice load of ice class IC. This is because the design of the plate structures in double side is mostly governed by the minimum thickness of 9 mm, stiffening requirements and open water loads, rather than the ice load.

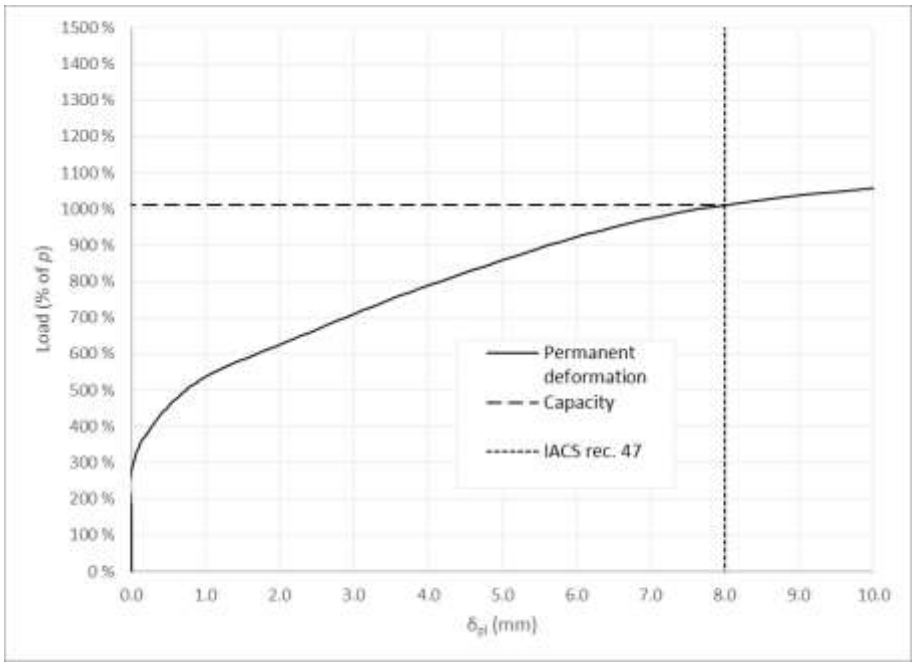

Figure 73 Load – permanent out-of-plane deformation curve for the critical load case for webframe of 10 000 DWT IC vessel.

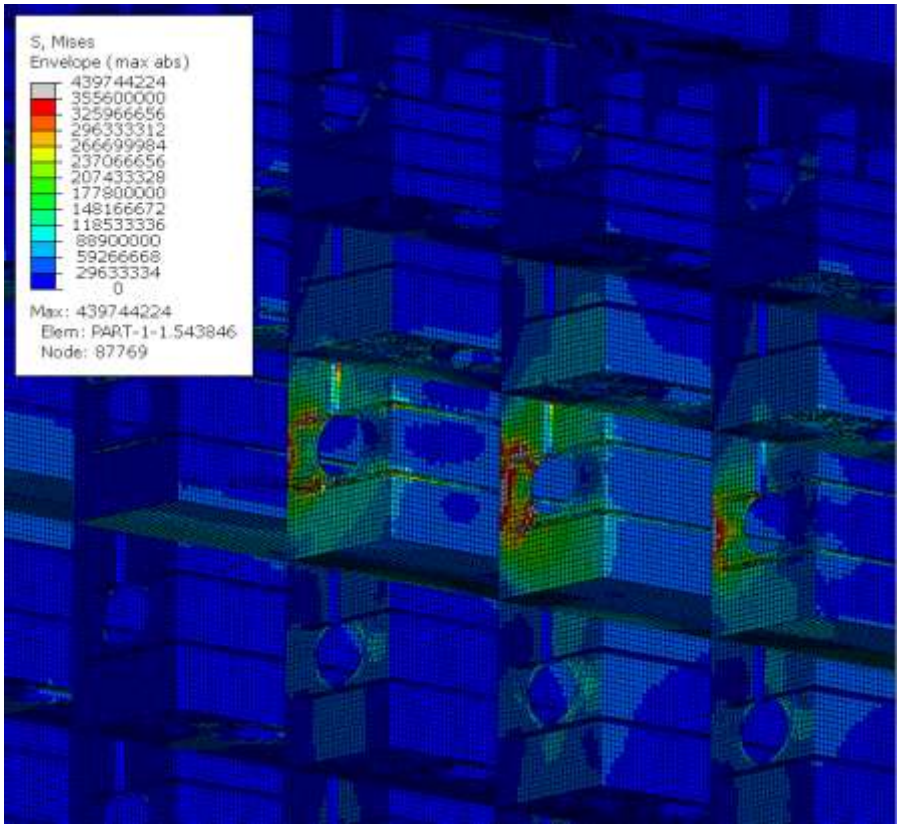

Figure 74 von Mises stress for the critical load case for webframe of 10 000 DWT IC vessel, at plastic limit load (1011 % of rule load).

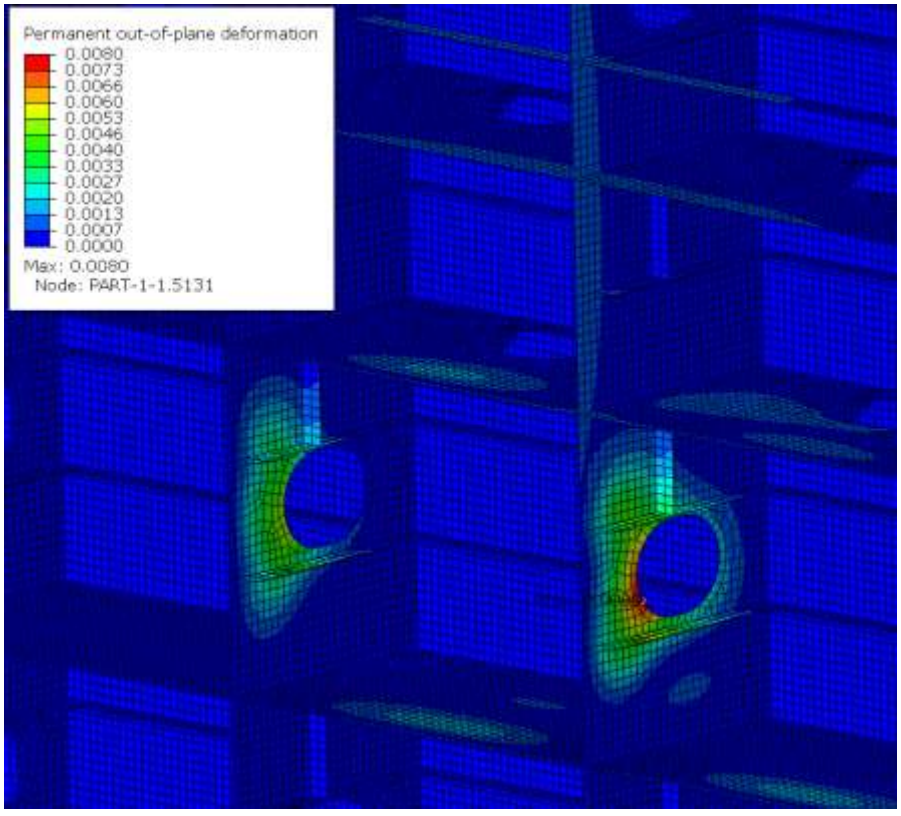

Figure 75 Permanent out-of-plane deformation for the critical load case for webframe of 10 000 DWT IC vessel, at plastic limit load (1011 % of rule load).

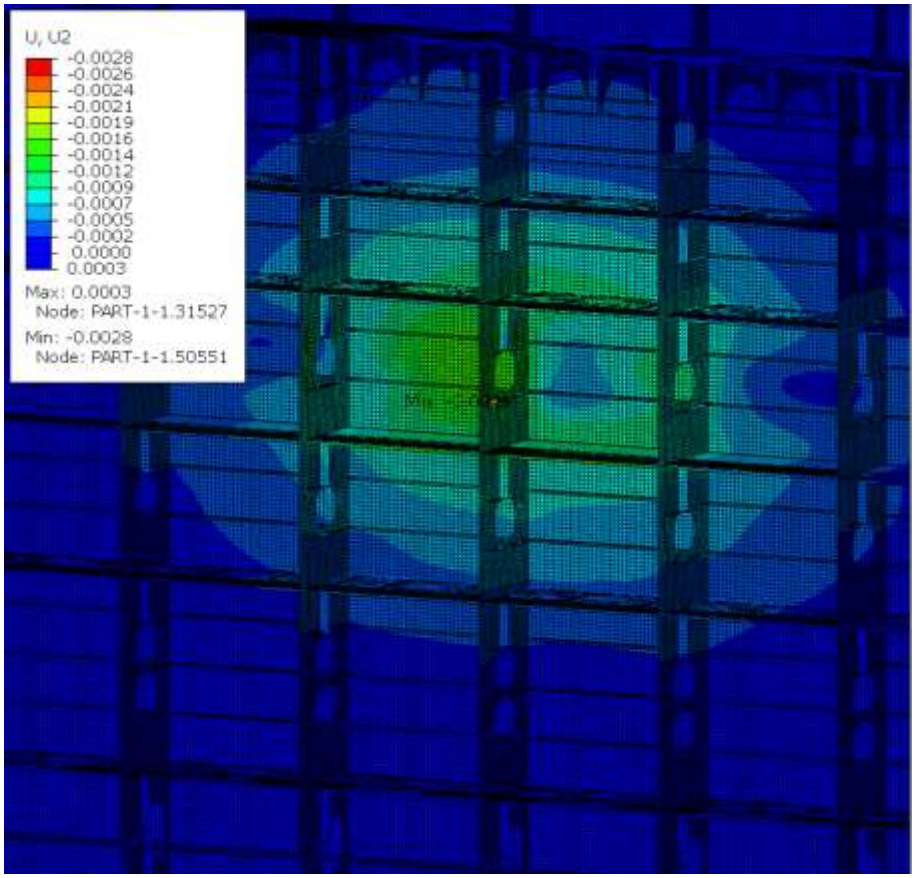

Figure 76 Permanent deformation perpendicular to shell for the critical load case for webframe of 10 000 DWT IC vessel, at plastic limit load (1011 % of rule load).

6.6 10 000 DWT IAsuper vessel

The load at which the permanent deformation of the structure reaches the allowed deformation limits defined in 5.3.3 is shown in for each load case in Table 20. The load cases analysed for this vessel are shown in Figure 26. The load is given as percentage of the design ice pressure of the FSICR.

Table 20 Load (as percentage of FSICR design load) at which the allowed permanent deformation is reached.

Load case	Capacity			
No.	Shell	Frame	Stringer platform	Webframe
1	346 %	332 %	866 %	898 %
2		259 %	874 %	543 %
3				798 %
4				545 %

The limiting load cases for each structural element is shown in following figures.

For shell, the point at which the plastic deformation in shell panel under load patch reaches the allowed limit value of 8 mm is 346 % of rule design load. The load – permanent deformation curve is shown in Figure 77. The permanent deformation perpendicular to shell at closest increment (350 %) is shown in Figure 78 and the von Mises stress in Figure 79. The structure behaves as expected. Shell and frames have about same plastic capacity, as intended by the rules.

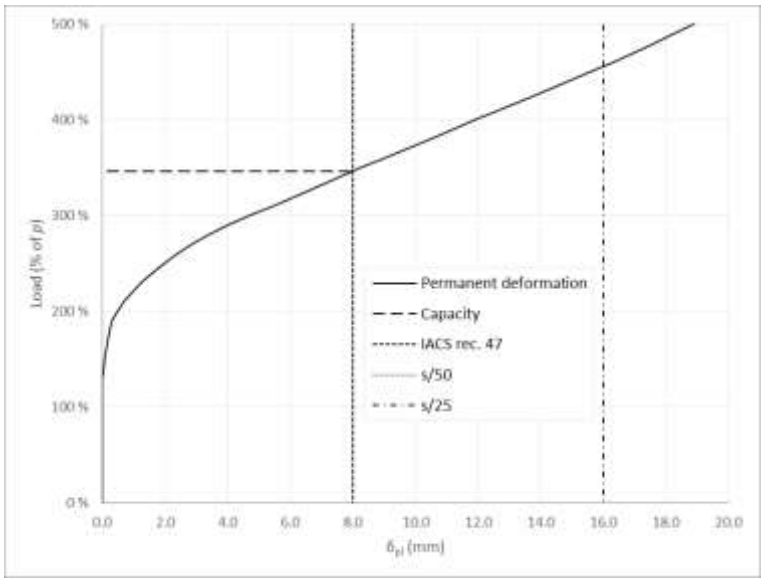

Figure 77 Load – permanent deformation for load on shell, 10 000 DWT IA super vessel.

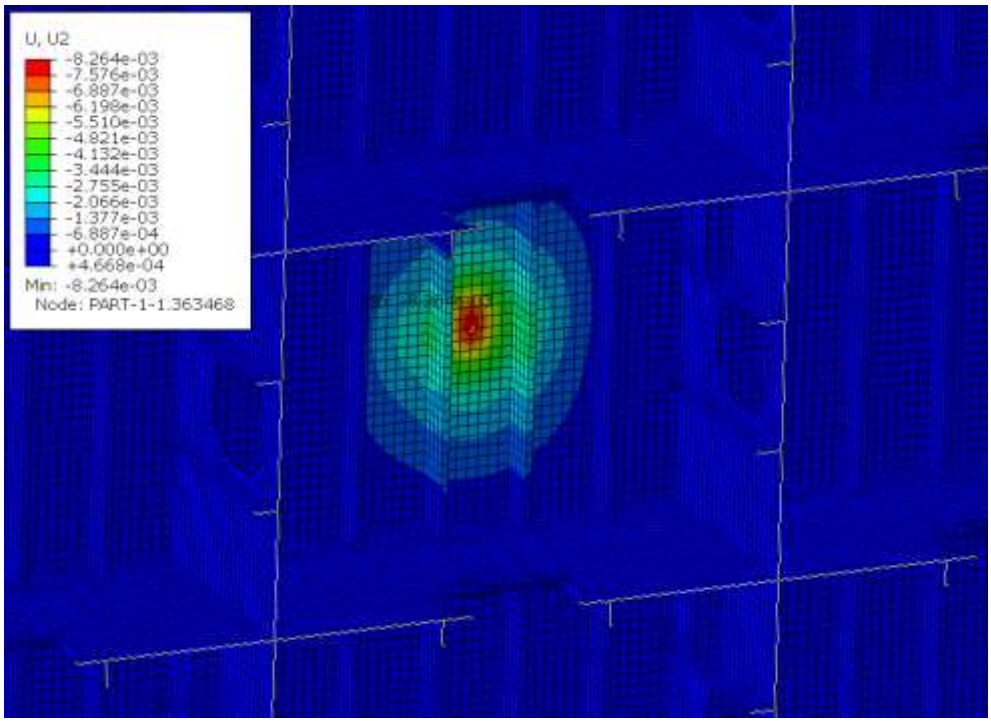

Figure 78 Load case Shell 1, permanent deformation perpendicular to shell at 350 % of the rule load.

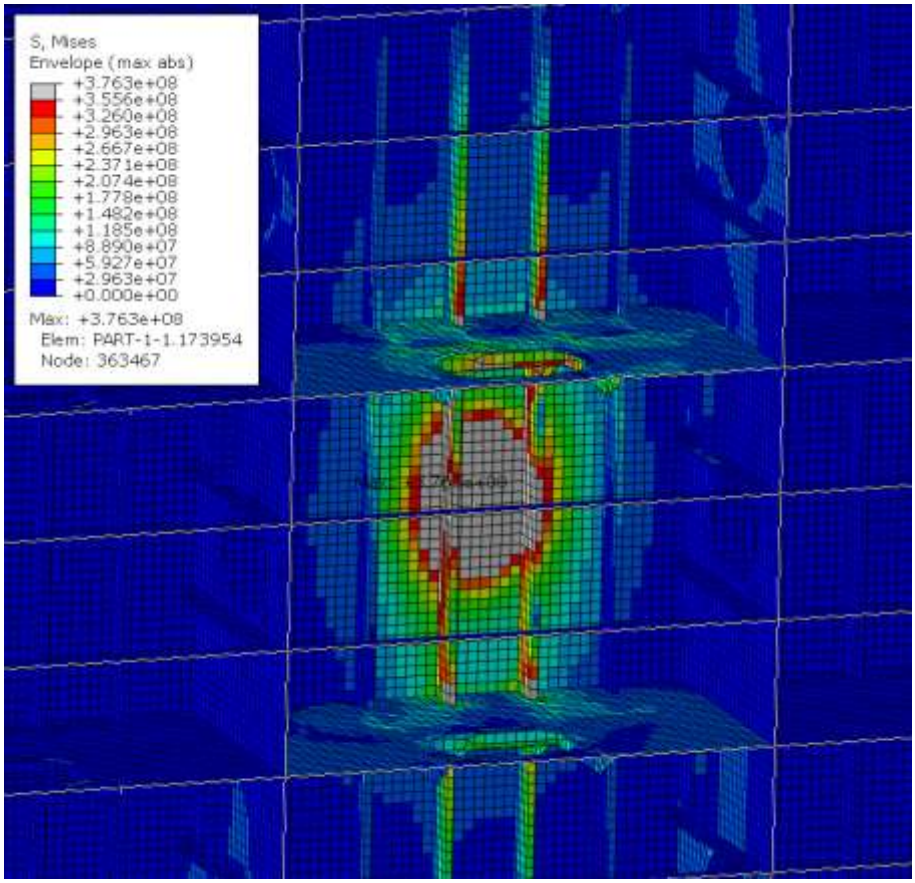

Figure 79 Load case Shell 1, von Mises stress at 350 % of the rule load.

For frame, the 8 mm permanent deformation is reached at about 332 % of design load. The load – permanent deformation curve is shown in Figure 80Figure 69, von Mises stress at that point in Figure 81Figure 70 and permanent deformation in Figure 82Figure 71Figure 70. As shown in Figure 83Figure 72, out-of-plane deformations remain below the allowed limit and frame stability is adequate. Bracket at top of the frame shows some out-of-plane deformation, and when load is increased further, will buckle. In the critical load case (Frame 1), the load is horizontally centred on the frame and vertically centred on the effective span of the frame, similar to baseline vessel.

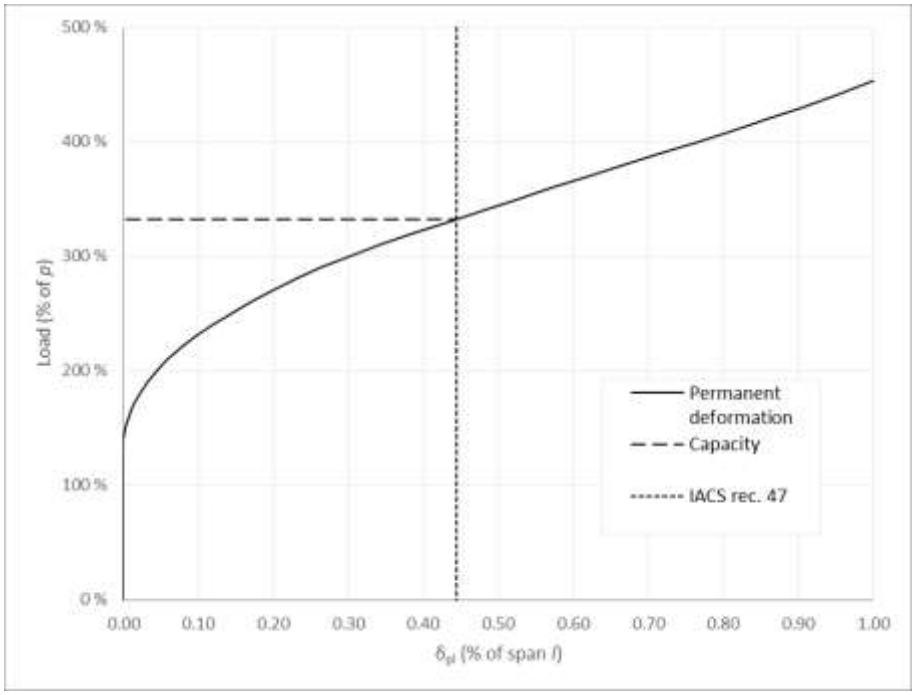

Figure 80 Load – permanent deformation curve for the critical load case for frame of 10 000 DWT IAsuper vessel.

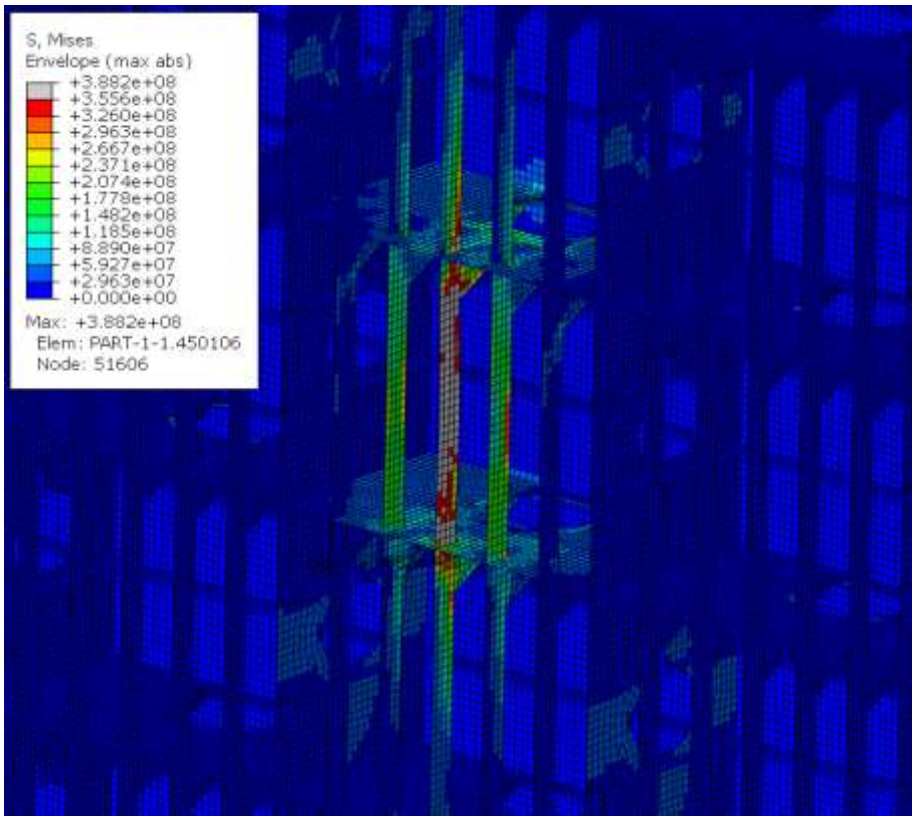

Figure 81 von Mises stress for the critical load case for frame of 10 000 DWT IAsuper vessel, at 330 % of rule load.

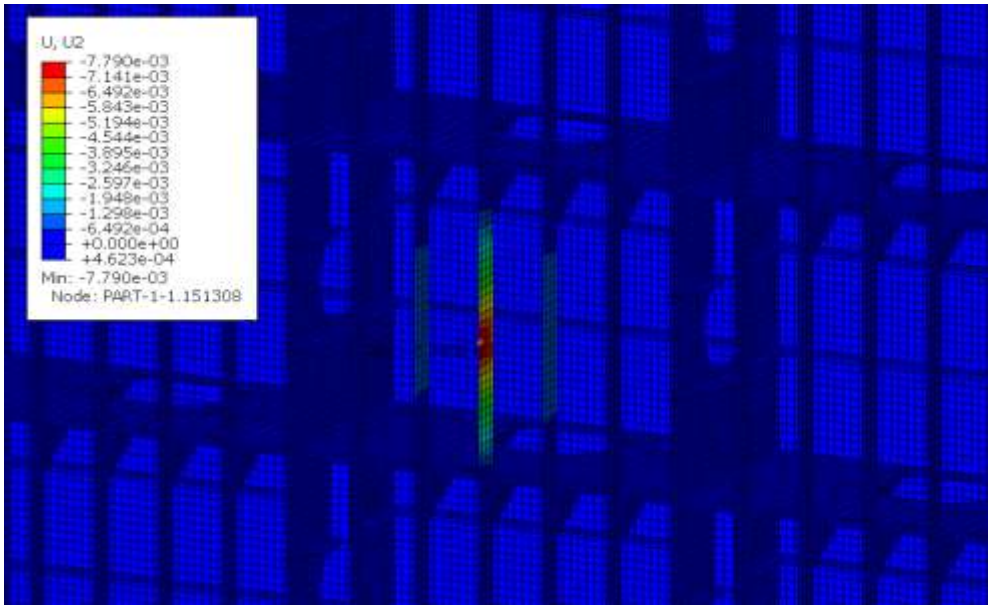

Figure 82 Permanent deformation perpendicular to shell for the critical load case for frame of 10 000 DWT IAsuper vessel, at 330 % of rule load.

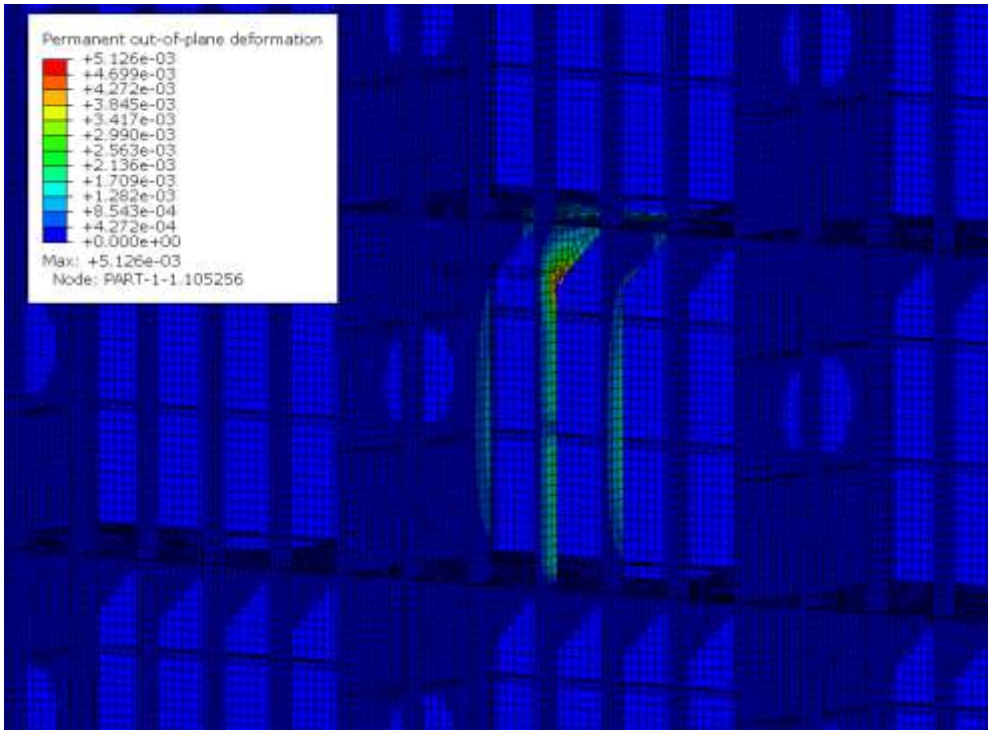

Figure 83 Permanent out-of-plane deformation for the critical load case for frame of 10 000 DWT IAsuper vessel, at 330 % of rule load.

Similar to transversally framed IA baseline vessel, capacity of the primary structures is limited by stability. The load – permanent out-of-plane deformation curve for the limiting load case is shown in Figure 84, von Mises stress at that point in Figure 85 and permanent out-of-plane deformation in Figure 86. As can be seen from Figure 87, permanent deformation perpendicular to shell is still well below the allowed limit, as well as von Mises stress. In this load case (Webframe 2), the load is located vertically midway between two platforms in way of manhole and horizontally centred on webframe.

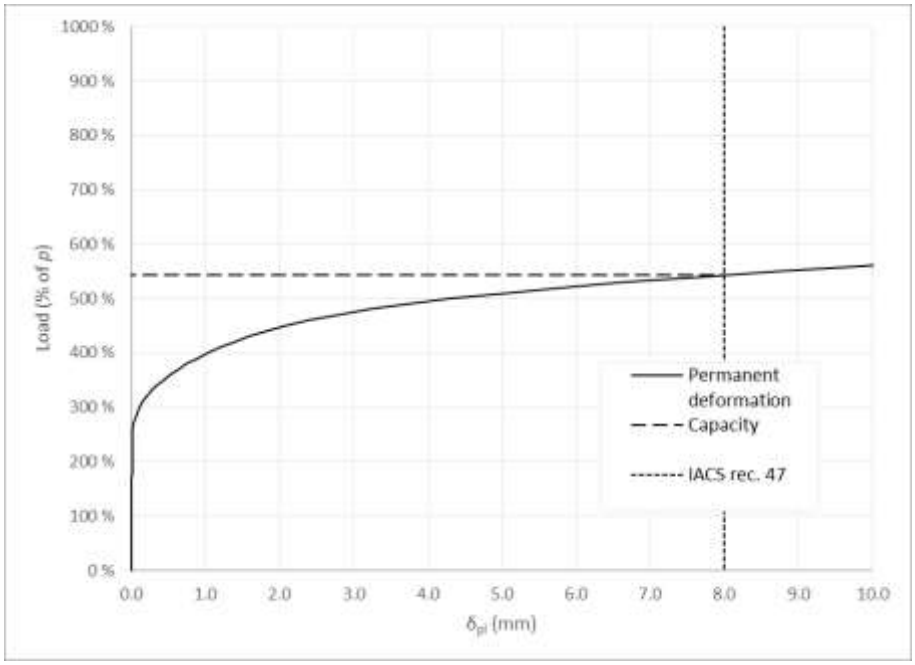

Figure 84 Load – permanent out-of-plane deformation curve for the critical load case for webframe of 10 000 DWT IAsuper vessel.

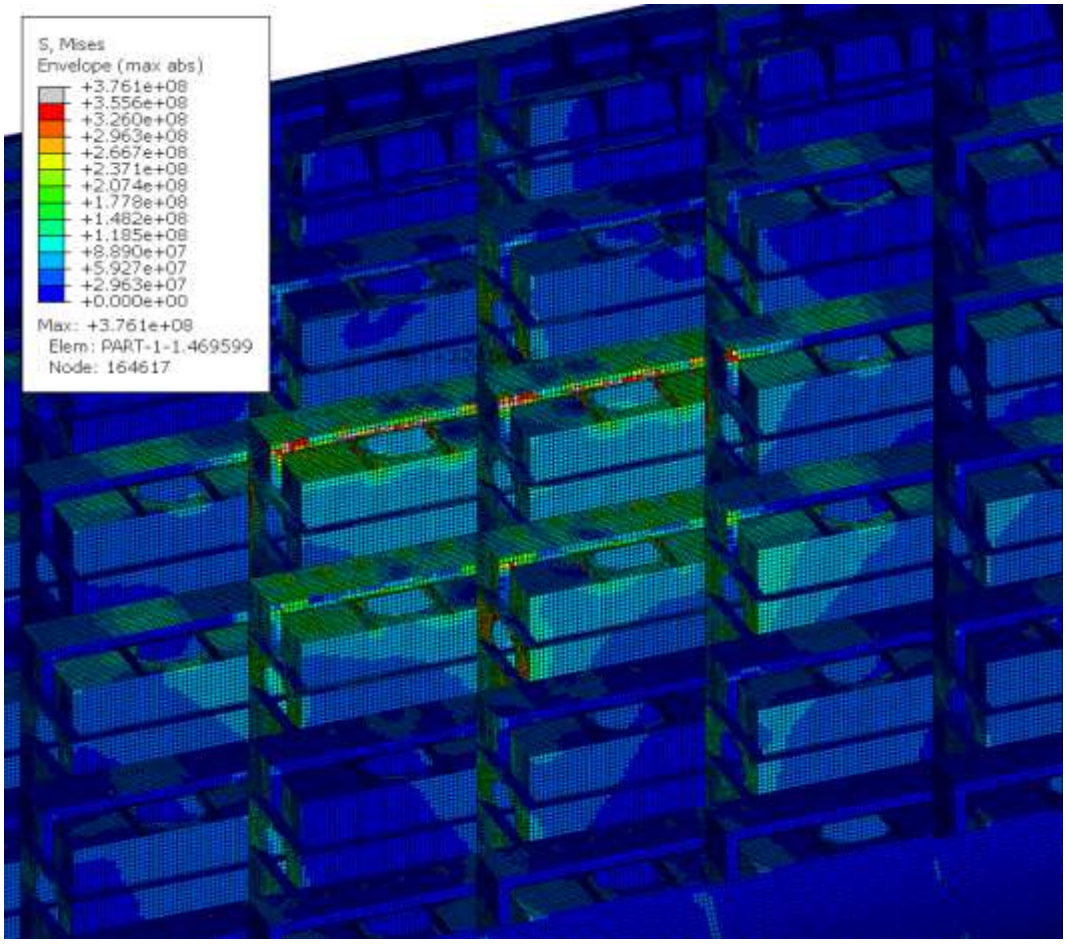

Figure 85 von Mises stress for the critical load case for webframe of 10 000 DWT IAsuper vessel, at plastic limit load (540 % of rule load).

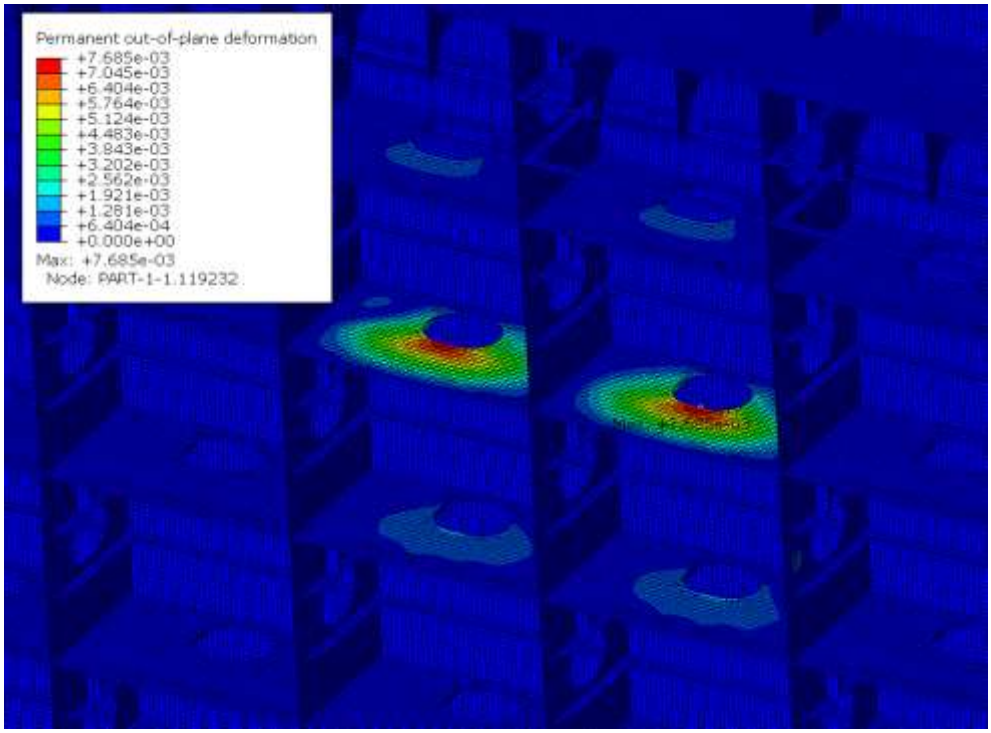

Figure 86 Permanent out-of-plane deformation for the critical load case for webframe of 10 000 DWT IAsuper vessel, at plastic limit load (540 % of rule load).

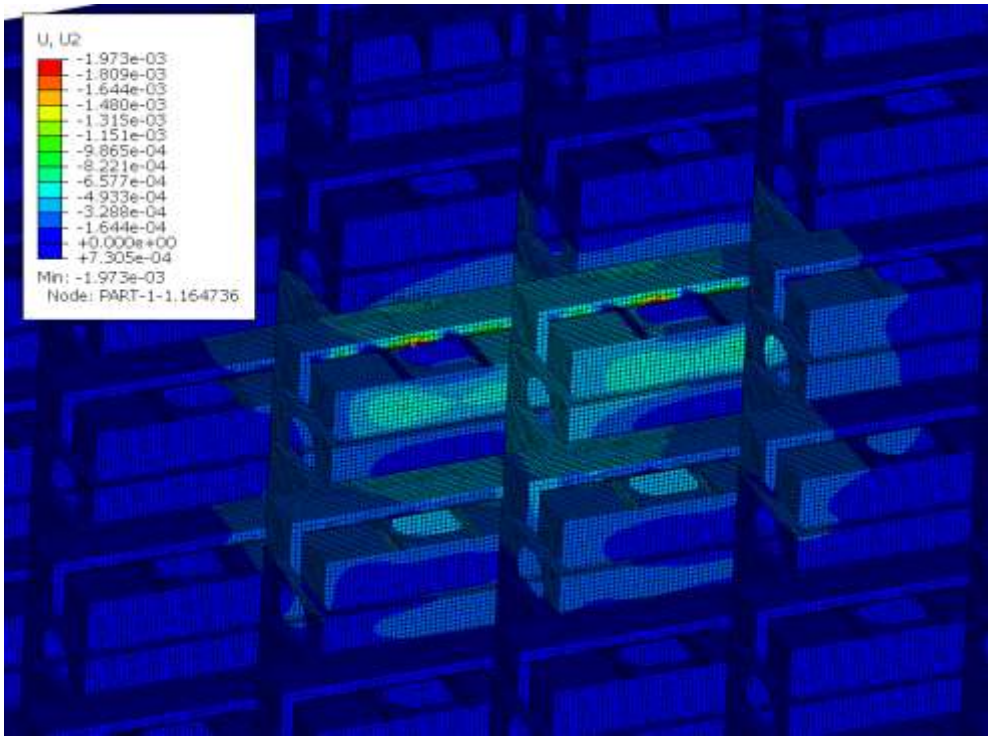

Figure 87 Permanent deformation perpendicular to shell for the critical load case for webframe of 10 000 DWT IAsuper vessel, at plastic limit load (540 % of rule load).

6.7 3 000 DWT IA vessel

The load at which the permanent deformation of the structure reaches the allowed deformation limits defined in 5.3.3 is shown in for each load case in Table 21Table 20Table 19. The load cases analysed for this vessel are shown in

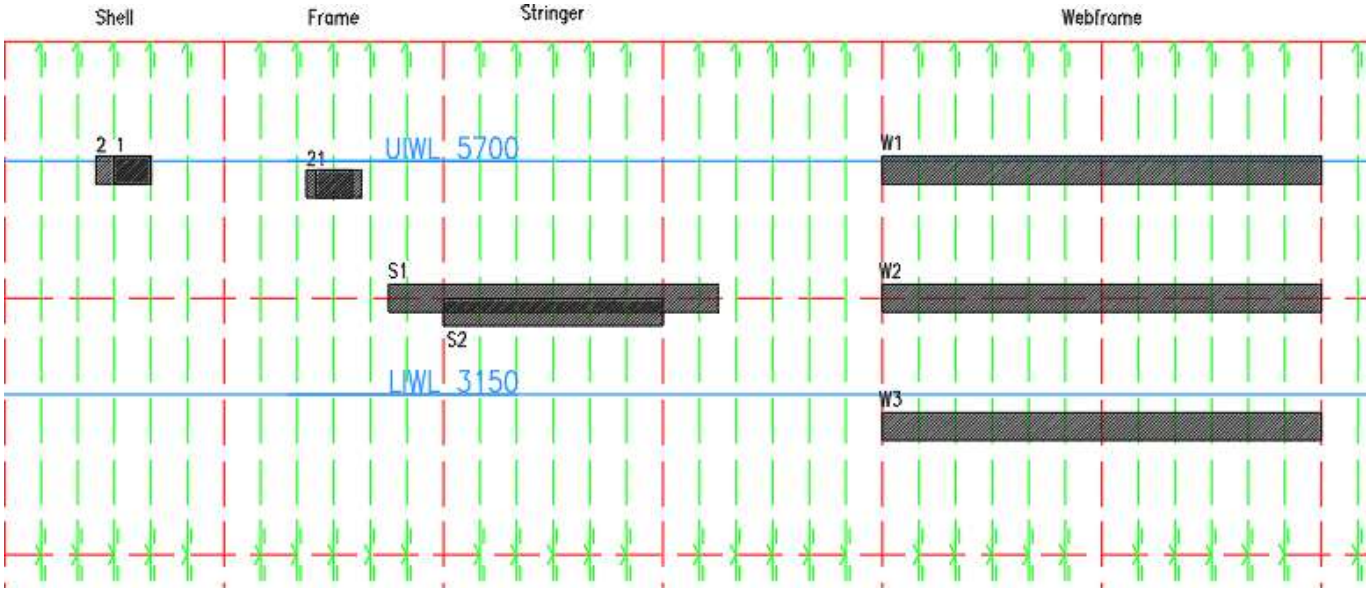

Figure 32Figure 26. The load is given as percentage of the design ice pressure of the FSICR.

Table 21 Load (as percentage of FSICR design load) at which the allowed permanent deformation is reached.

Load case	Capacity			
No.	Shell	Frame	Stringer platform	Webframe
1	362 %	344 %	815 %	472 %
2	246 %	270 %	952 %	690 %
3				524 %

The limiting load cases for all structural elements are shown in following figures.

For shell, the point at which the plastic deformation in shell panel under load patch reaches the allowed limit value of 8 mm is 362 % of rule design load. The permanent deformation perpendicular to shell at closes increment (360 %) is shown in Figure 89 and the von Mises stress in Figure 90. The structure behaves as expected. Shell and frames have about same plastic capacity, as intended by the rules.

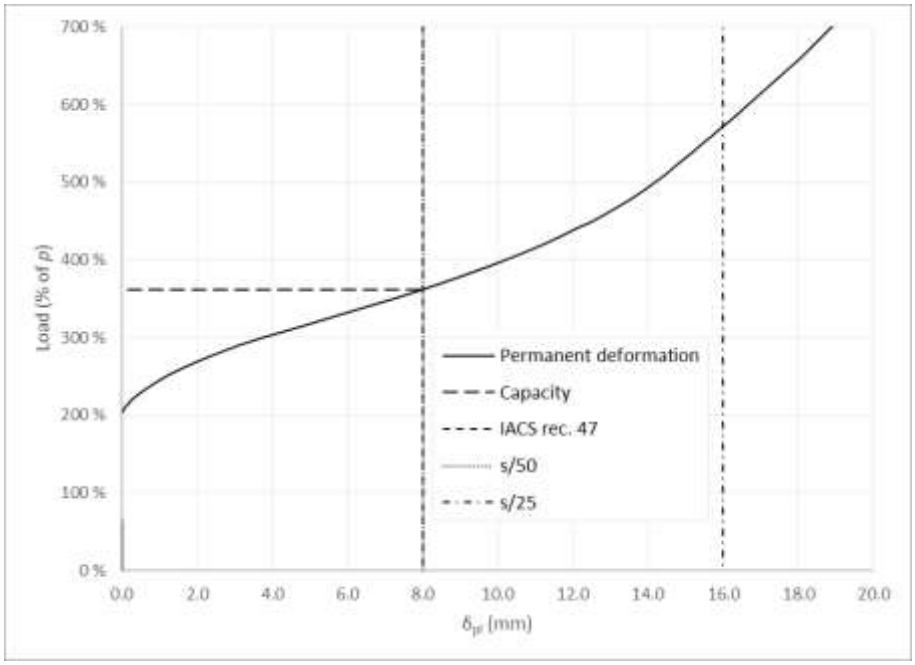

Figure 88 Load – permanent deformation curve for the critical load case for shell plate of 3 000 DWT IA vessel.

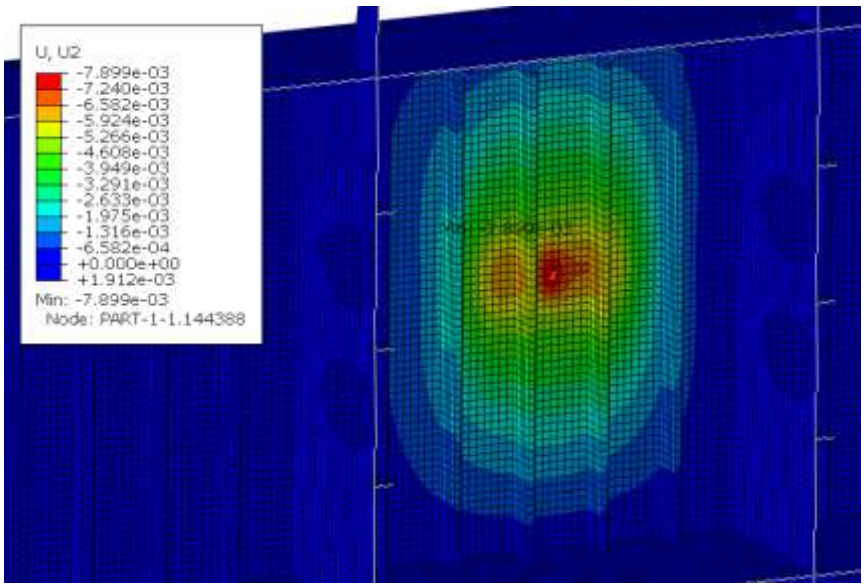

Figure 89 Load case Shell 1, permanent deformation perpendicular to shell at 360 % of the rule load.

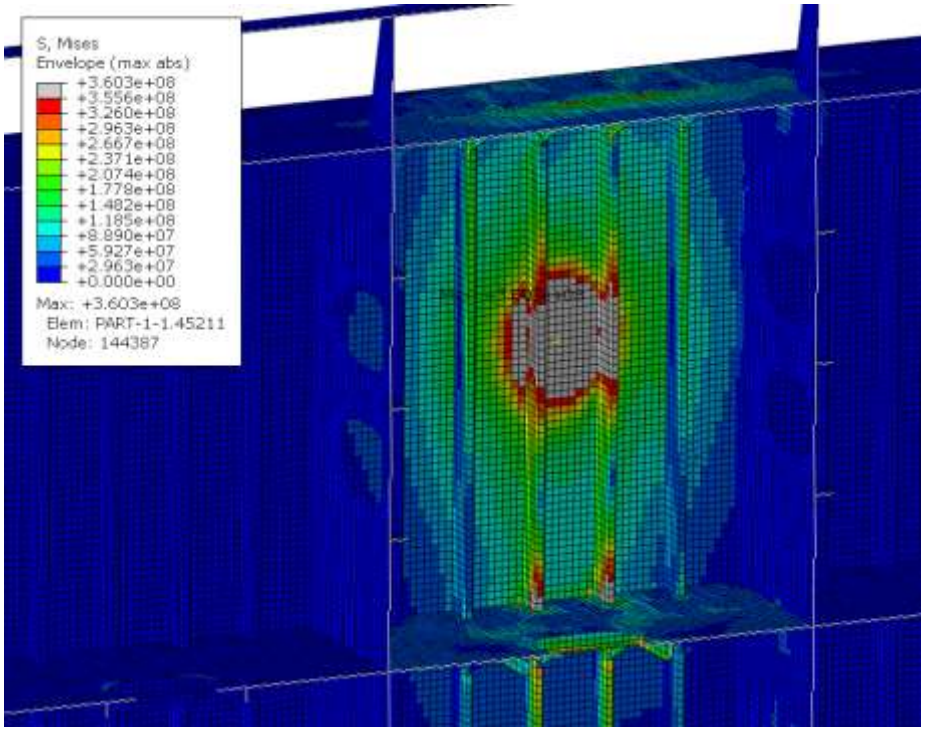

Figure 90 Load case Shell 1, von Mises stress at 360 % of the rule load.

For frame, the 8 mm permanent deformation is reached at about 344 % of design load. The load – permanent deformation curve is shown in Figure 91Figure 80Figure 69, von Mises stress at that point in Figure 92Figure 81Figure 70 and permanent deformation in Figure 93Figure 82Figure 71Figure 70. As shown in Figure 94Figure 83Figure 72, out-of-plane deformations remains well below the allowed limit and frame stability is adequate. In the critical load case (Frame 1), the load is horizontally centred on the frame and vertically centred on the effective span of the frame, similar to baseline vessel.

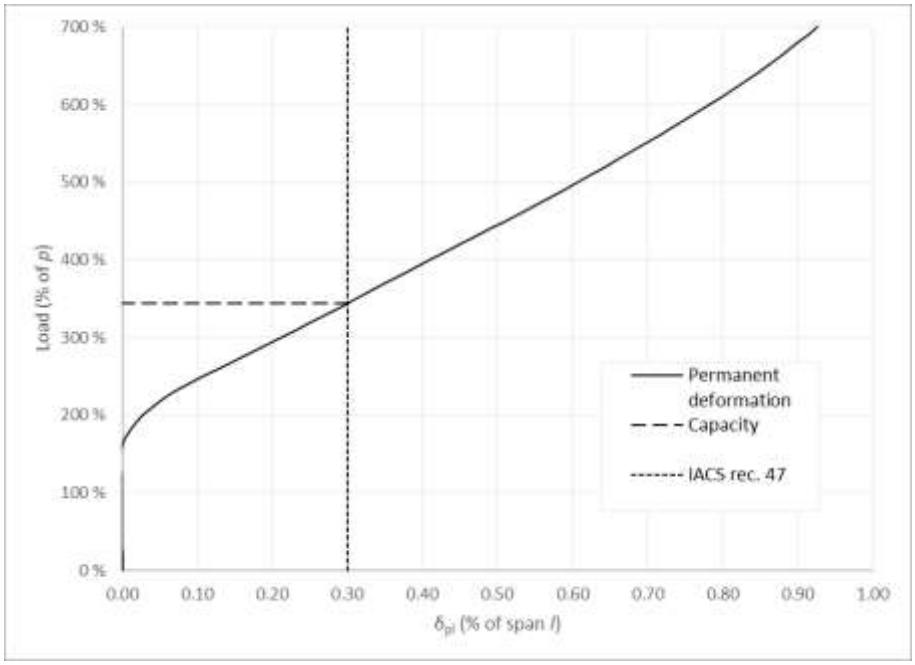

Figure 91 Load – permanent deformation curve for the critical load case for frame of 3 000 DWT IA vessel.

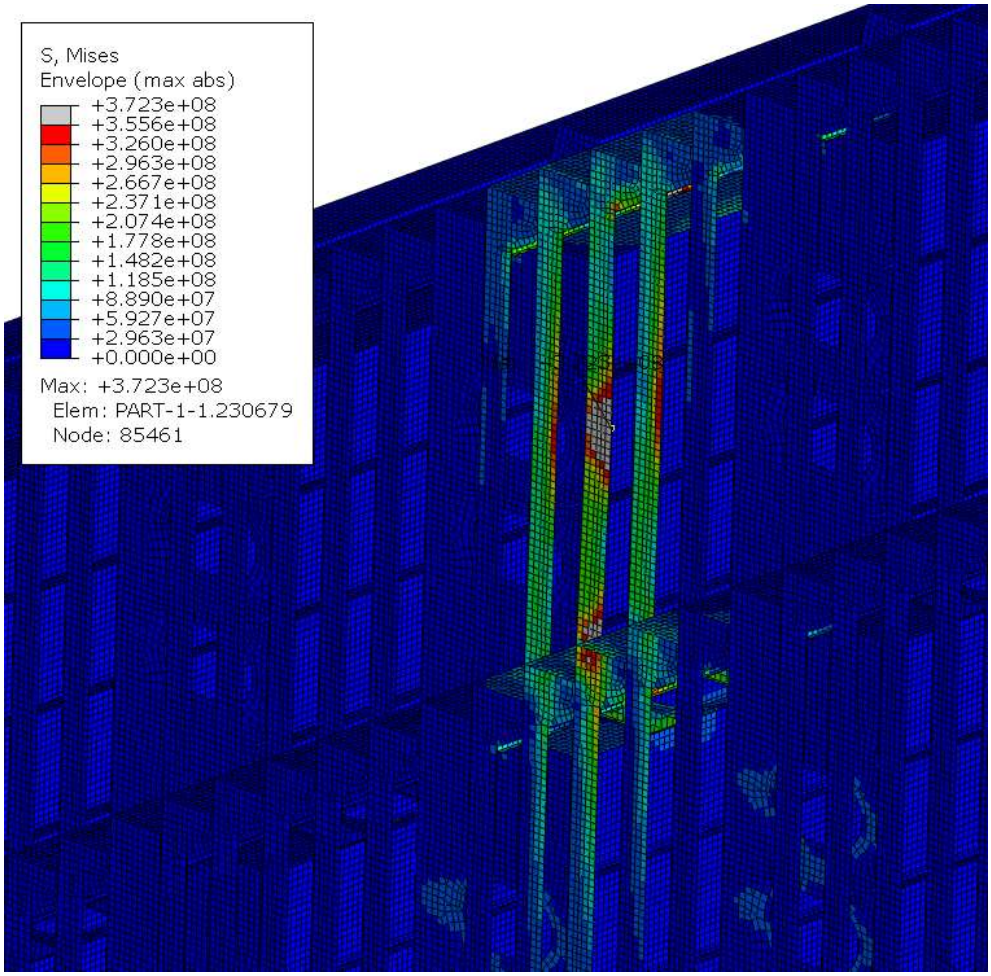

Figure 92 von Mises stress for the critical load case for frame of 3000 DWT IA vessel, at 340 % of rule load.

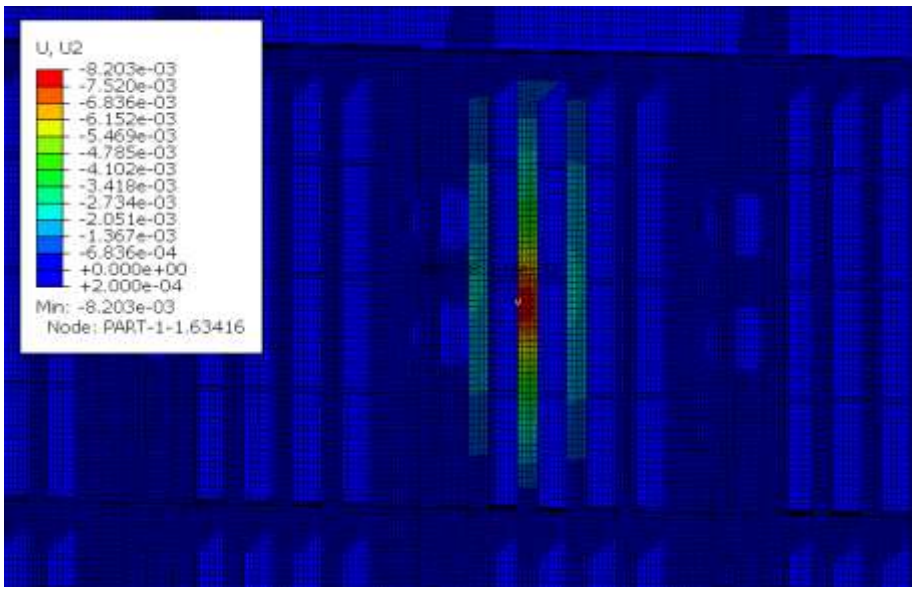

Figure 93 Permanent deformation perpendicular to shell for the critical load case for frame of 3 000 DWT IA vessel, at 340 % of rule load.

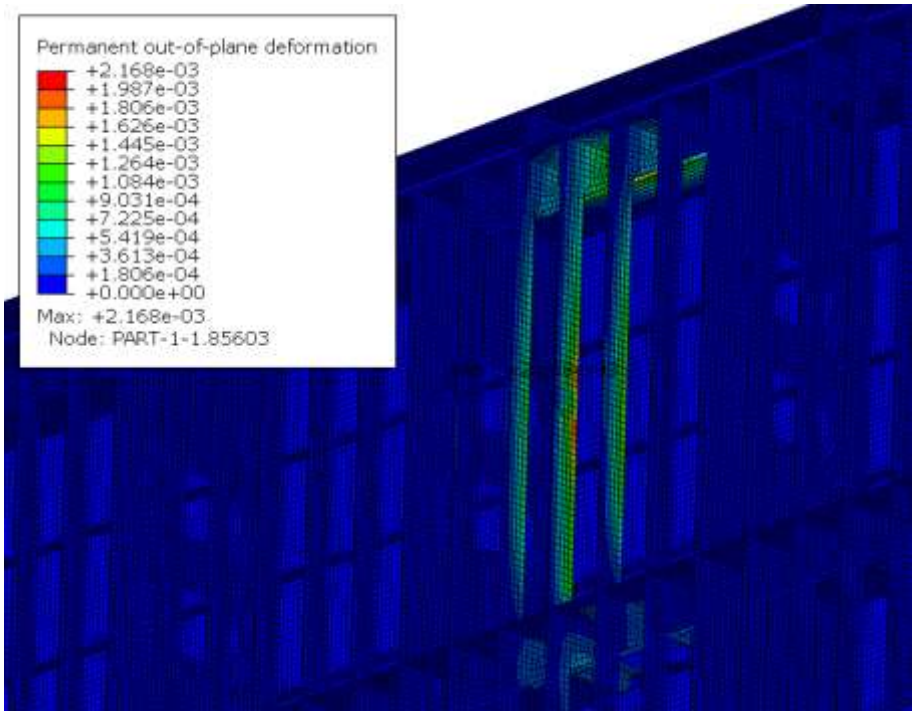

Figure 94 Permanent out-of-plane deformation for the critical load case for frame of 3 000 DWT IA vessel, at 340 % of rule load.

Similar to transversally framed IA baseline vessel, capacity of the primary structures is limited by stability. The load – permanent out-of-plane deformation curve for the limiting load case is shown in Figure 95Figure 84, von Mises stress at closest increment in Figure 96Figure 85 and permanent out-of-plane deformation in Figure 97Figure 86. As can be seen from Figure 98Figure 87, permanent deformation perpendicular to shell is still well below the allowed limit. It can also be observed from the von Mises plot that frames have plasticised and deformed to a large amount at this point, which demonstrates proper structural hierarchy, meaning that secondary structure reaches its capacity before the primary structure. In this load case (Webframe 1), the load is located vertically midway between two platforms in way of manhole and horizontally centred on webframe.

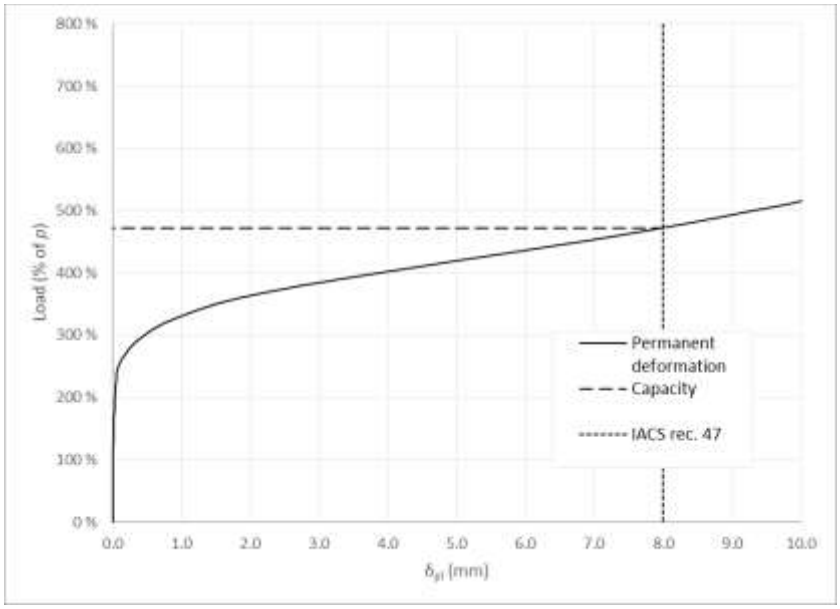

Figure 95 Load – permanent out-of-plane deformation curve for the critical load case for webframe of 3 000 DWT IA vessel.

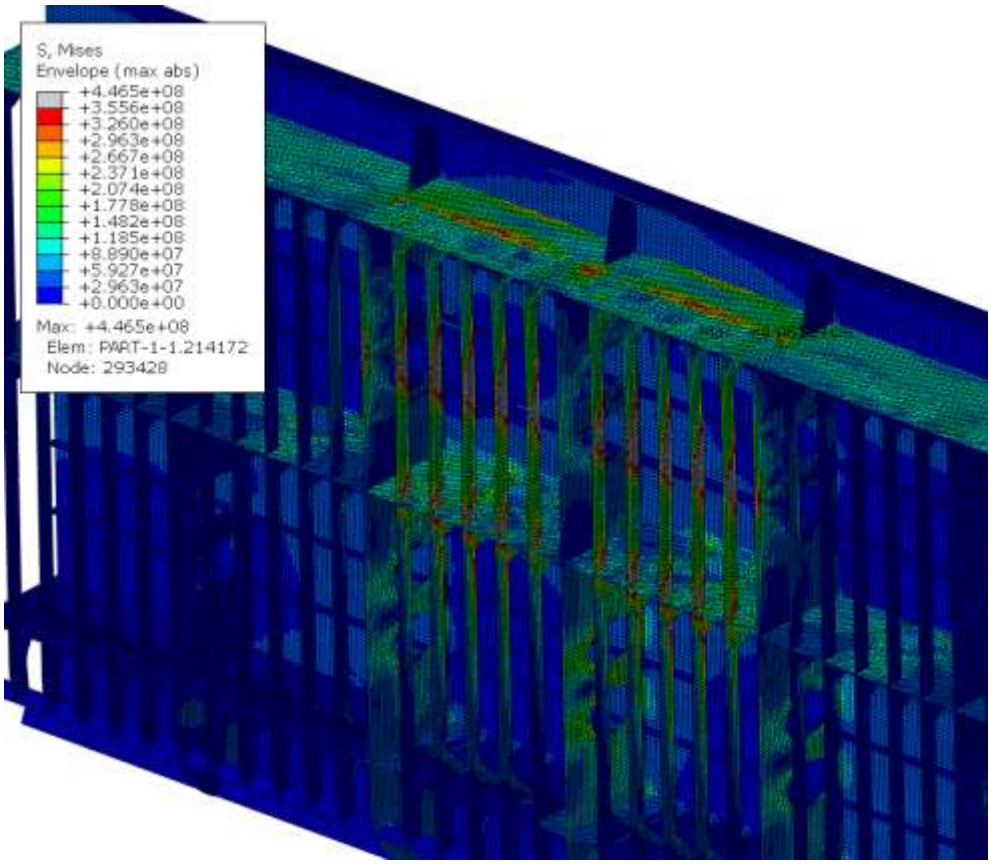

Figure 96 von Mises stress for the critical load case for webframe of 3 000 DWT IA vessel, at plastic limit load (470 % of rule load).

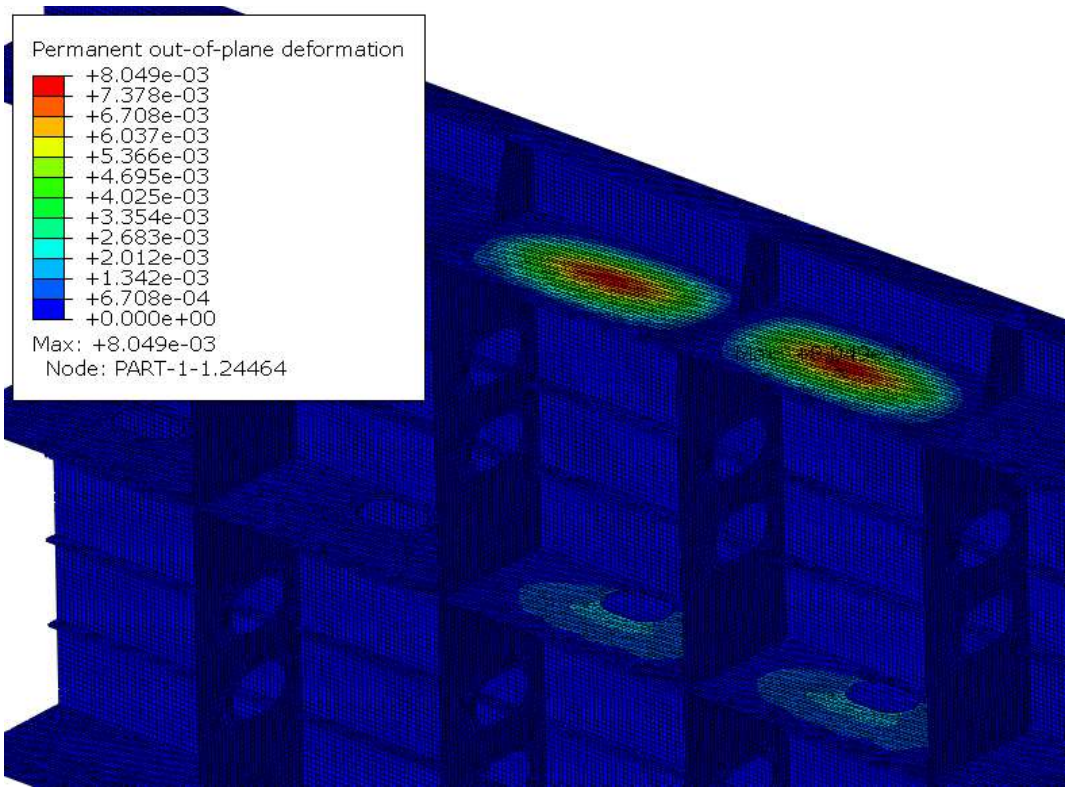

Figure 97 Permanent out-of-plane deformation for the critical load case for webframe of 3 000 DWT IA vessel, at plastic limit load (470 % of rule load).

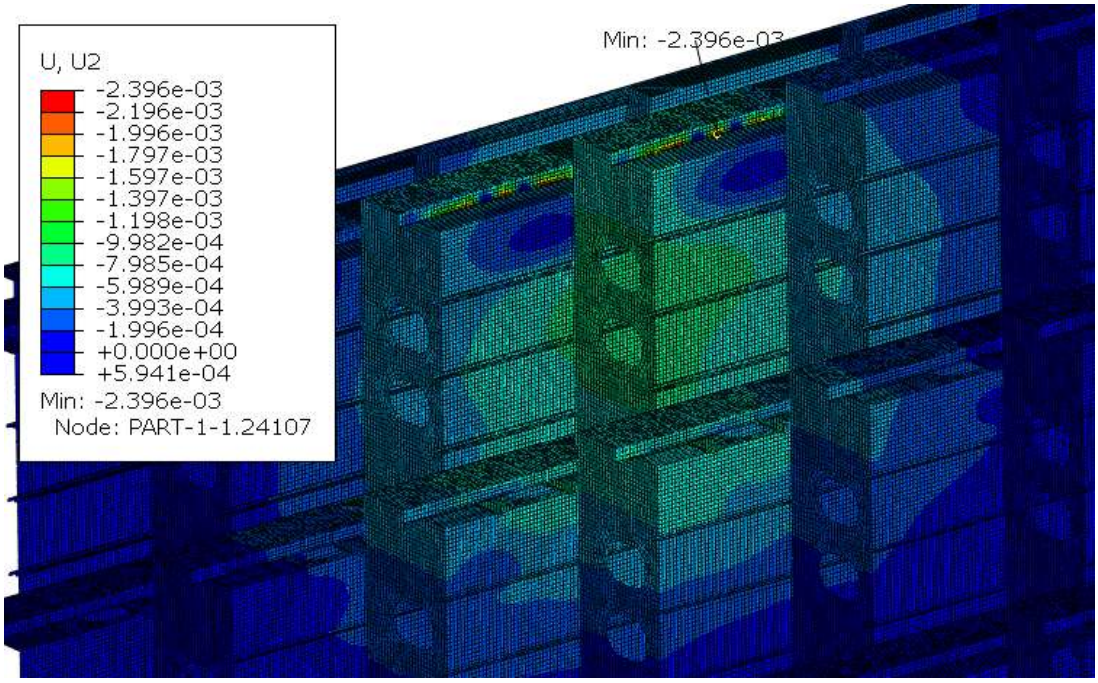

Figure 98 Permanent deformation perpendicular to shell for the critical load case for webframe of 3 000 DWT IA vessel, at plastic limit load (470 % of rule load).

6.8 58 500 DWT IA vessel

The load at which the permanent deformation of the structure reaches the allowed deformation limits defined in 5.3.3 is shown in for each load case in Table 22Table 20Table 19. The load cases analysed for this vessel are shown in Figure 39Figure 26. The load is given as percentage of the design ice pressure of the FSICR.

Table 22 Load (as percentage of FSICR design load) at which the allowed permanent deformation is reached.

Load case	Capacity		
No.	Shell	Frame	Webframe
1	363 %	285 %	547 %
2	337 %	286 %	705 %
3	364 %	295 %	382 %

The limiting load cases for all structural elements are shown in following figures.

For shell, the point at which the plastic deformation in shell panel under load patch reaches the allowed limit value of 8 mm is 337 % of rule design load, as shown in Figure 99. The load length that causes the permanent deformation limit to be reached at lowest load is 1.7 times frame spacing, which agrees with the load lengths given for structural elements in the FSICR [28]. Both increasing and decreasing the load

length from this value will increase the load at which the limit is reached. The permanent deformation perpendicular to shell at closest increment (340 %) is shown in Figure 100Figure 78 and the von Mises stress in Figure 101Figure 79.

The shell has somewhat lower plastic capacity than the frame, indicating that the strength balance between these two is somewhat off. As can be seen from Figure 101, the frames have fully plasticised at this point, and as shown in Figure 110, permanent deformation of frame exceeds that of shell plate.

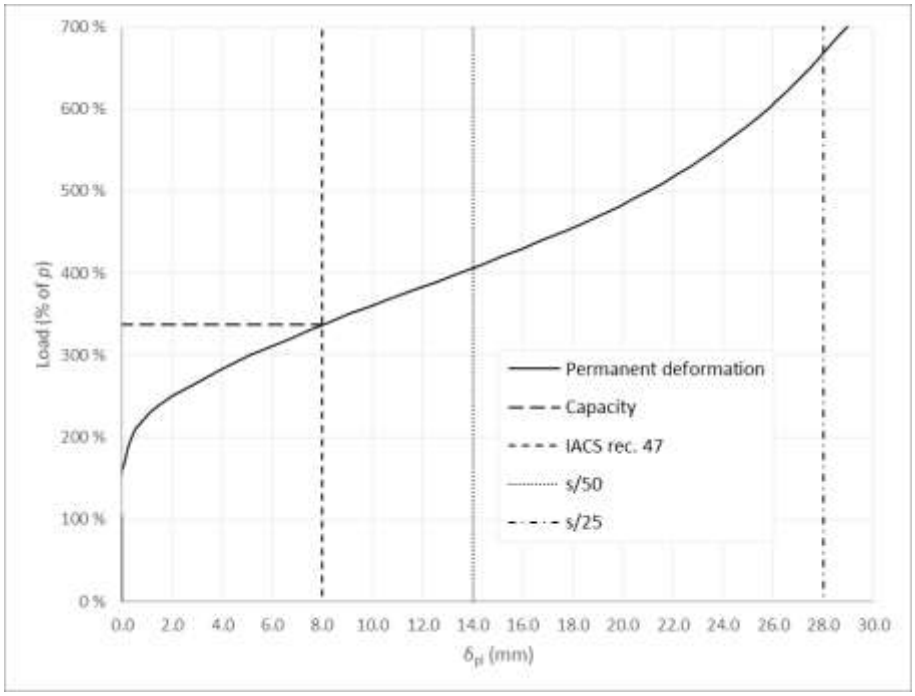

Figure 99 Load – permanent deformation curve for the critical load case for shell plate of 3000 DWT IA vessel.

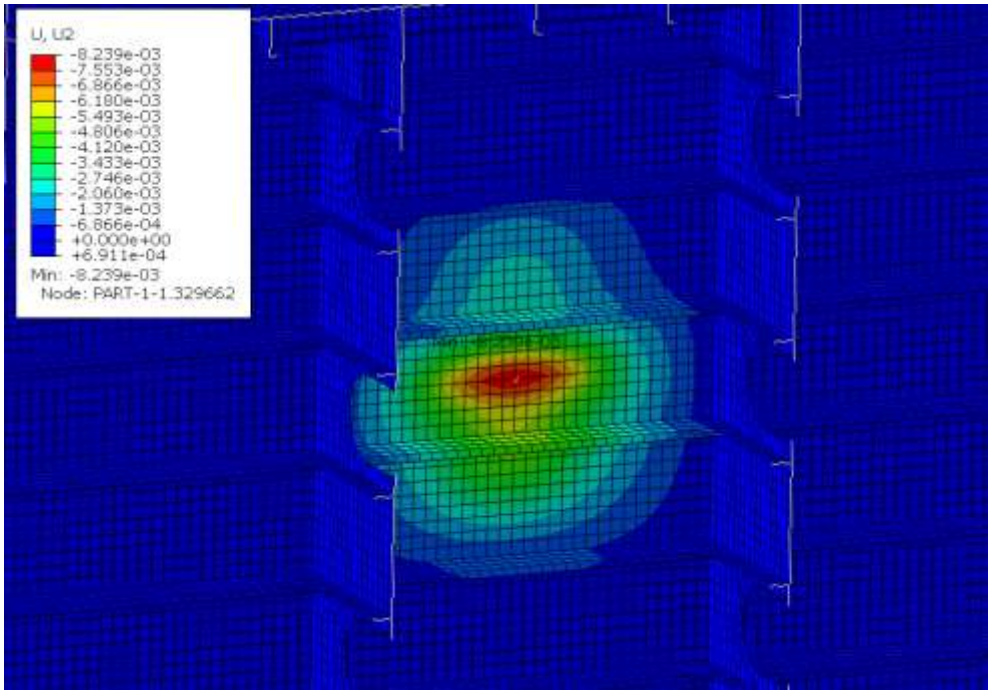

Figure 100 Load case Shell 1, permanent deformation perpendicular to shell at 340 % of the rule load.

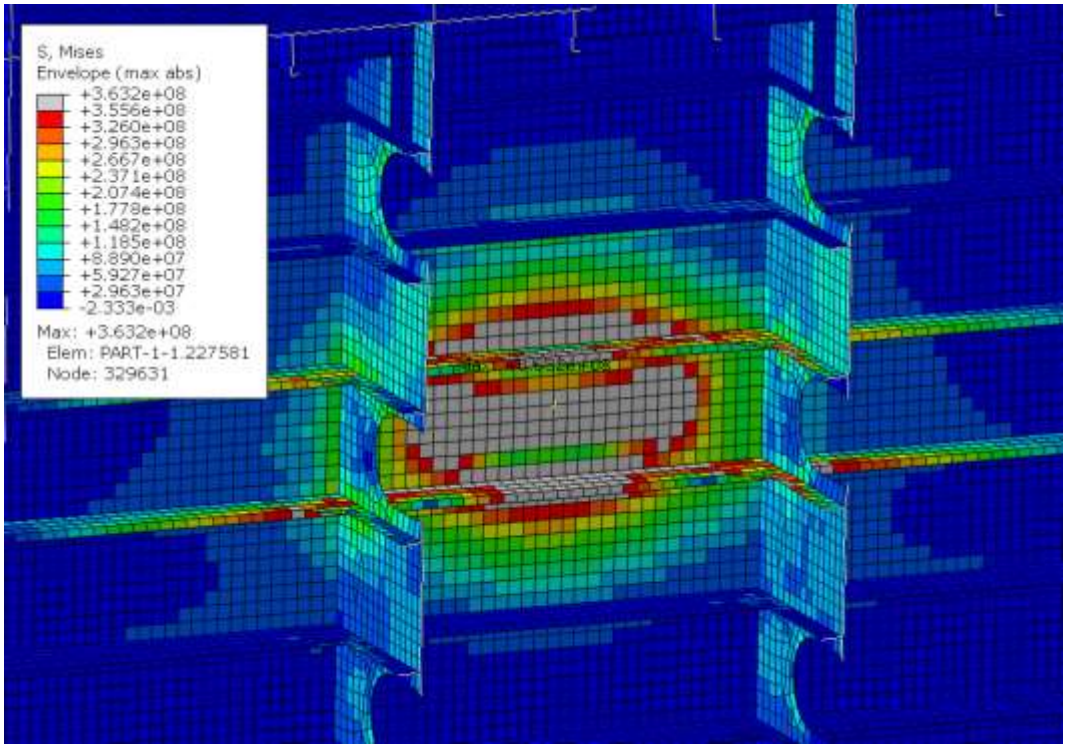

Figure 101 Load case Shell 1, von Mises stress at 340 % of the rule load.

For frame, the 8 mm permanent deformation is reached at about 285 % of design load. The load – permanent deformation curve is shown in Figure 102, von Mises stress at that point in Figure 103 and permanent deformation in Figure 104. As shown in Figure 105, out-of-plane deformations remains well below the allowed limit and frame stability is adequate. In the critical load case (Frame 1), the load is horizontally centred on the frame and vertically spans the whole frame.

Load cases Frame 2 and 3 are otherwise identical, but for Frame 3, the same phenomena as was observed for the baseline vessel is repeated; the frame adjacent to a plate structure has higher capacity due to better support for shell plate on that side.

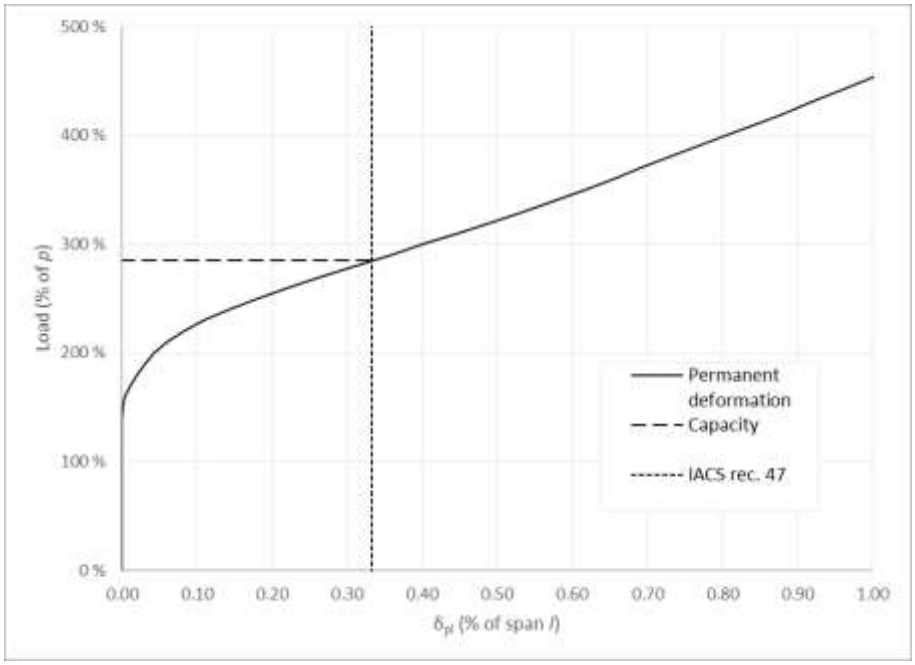

Figure 102 Load – permanent deformation curve for the critical load case for frame of 58 500 DWT IA vessel.

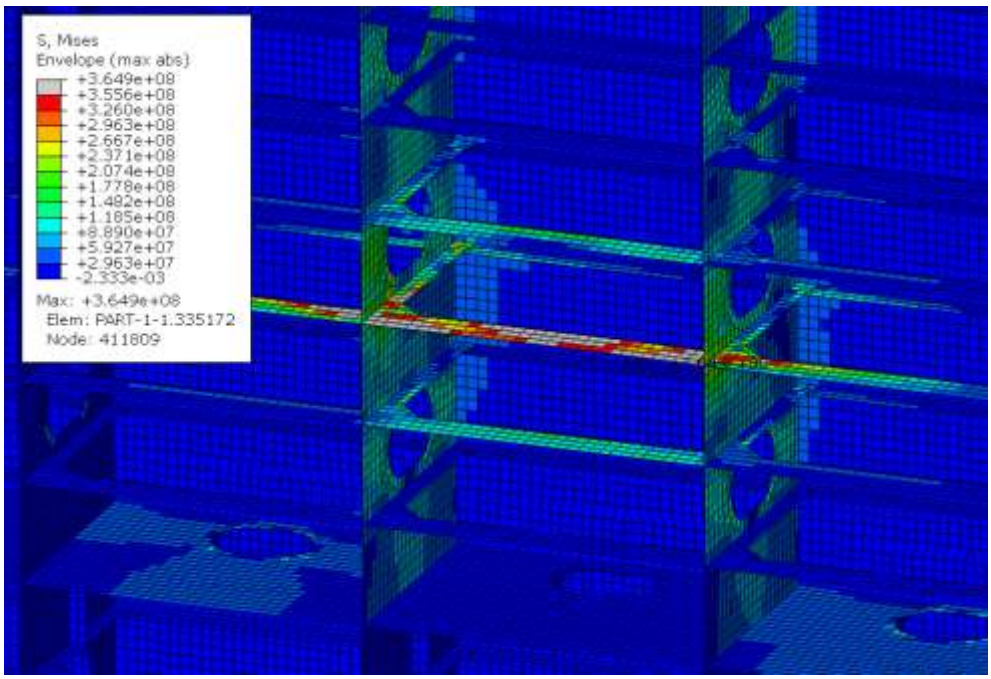

Figure 103 von Mises stress for the critical load case for frame of 58 500 DWT IA vessel, at 290 % of rule load.

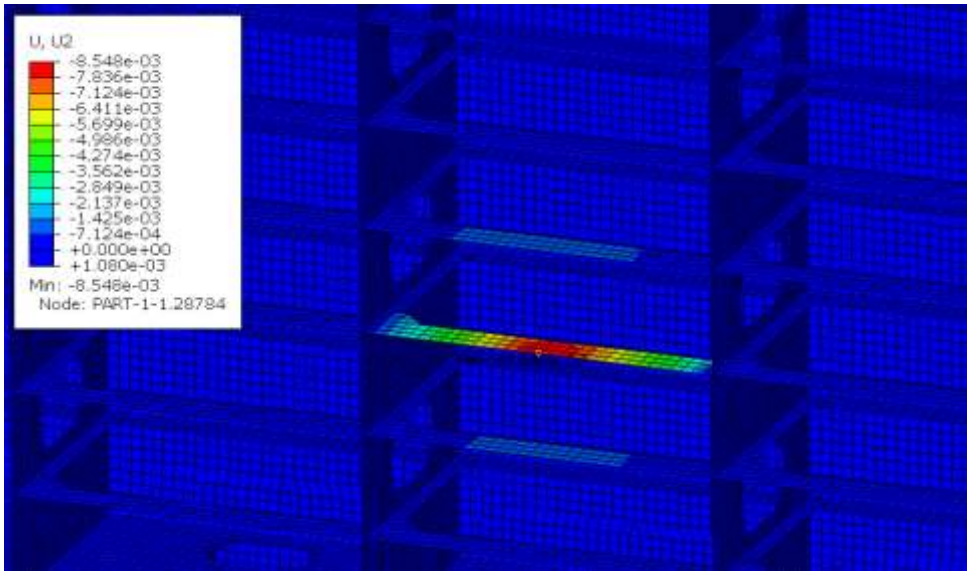

Figure 104 Permanent deformation perpendicular to shell for the critical load case for frame of 58 500 DWT IA vessel, at 290 % of rule load.

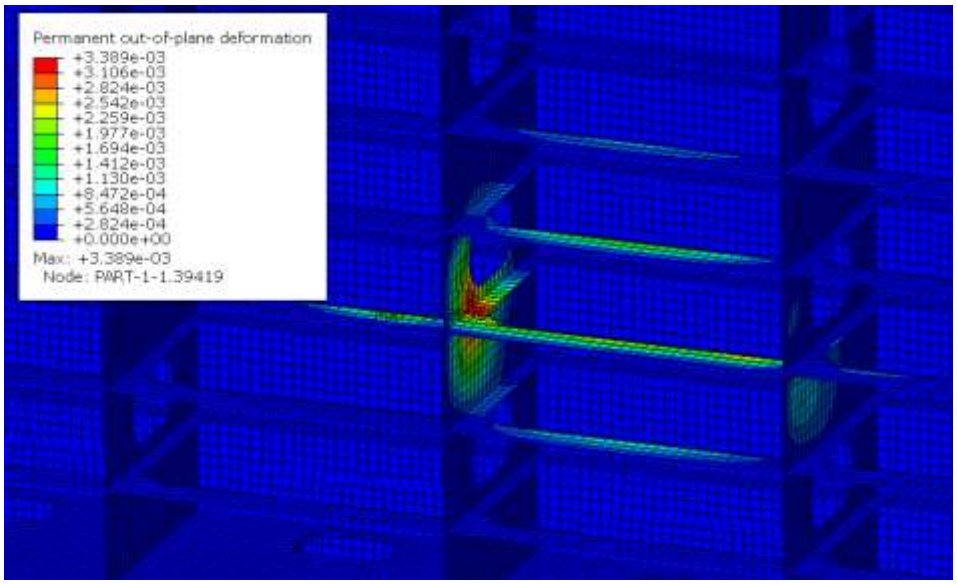

Figure 105 Permanent out-of-plane deformation for the critical load case for frame of 58 500 DWT IA vessel, at 290 % of rule load.

Similar to transversally framed IA baseline vessel, capacity of the primary structures is limited by stability. The load – permanent out-of-plane deformation curve for the limiting load case is shown in, von Mises stress at closest increment in and permanent out-of-plane deformation in. As can be seen from, permanent deformation perpendicular to shell is still well below the allowed limit. In this load case (Webframe 3), the load is located vertically midway between two platforms in way of manhole and horizontally centred on webframe.

It can be observed from Figure 110 that plastic capacity of the webframe is well above that of ordinary frames, ensuring proper structural hierarchy. For this vessel, the capacity of webframes is relatively lower than for other vessels, which is mainly due to relatively similar structure, which is mainly driven by minimum thickness requirement of 9 mm and typical buckling stiffener arrangement, but in this case asked to support the higher loads of a larger vessels. Still, the capacity of the structure is adequate.

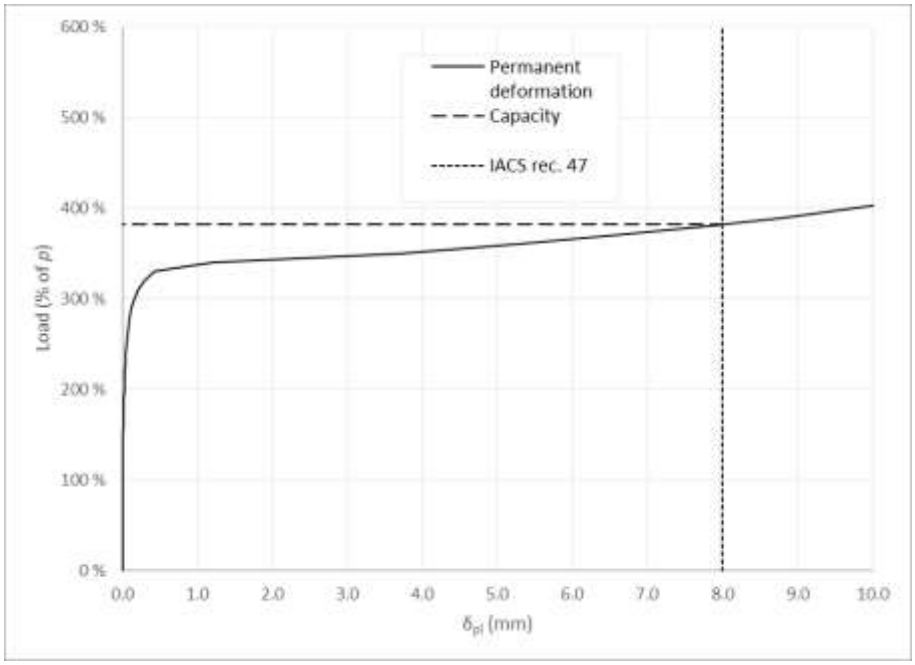

Figure 106 Load – permanent out-of-plane deformation curve for the critical load case for webframe of 58 500 DWT IA vessel.

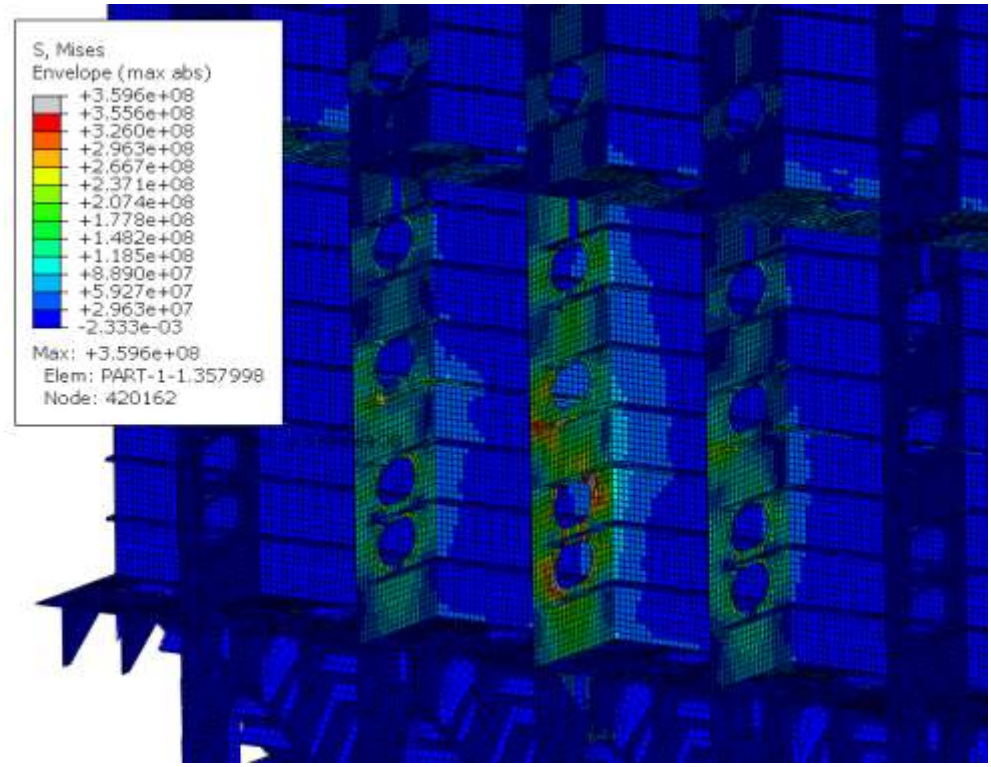

Figure 107 von Mises stress for the critical load case for webframe of 58 500 DWT IA vessel, at plastic limit load (380 % of rule load).

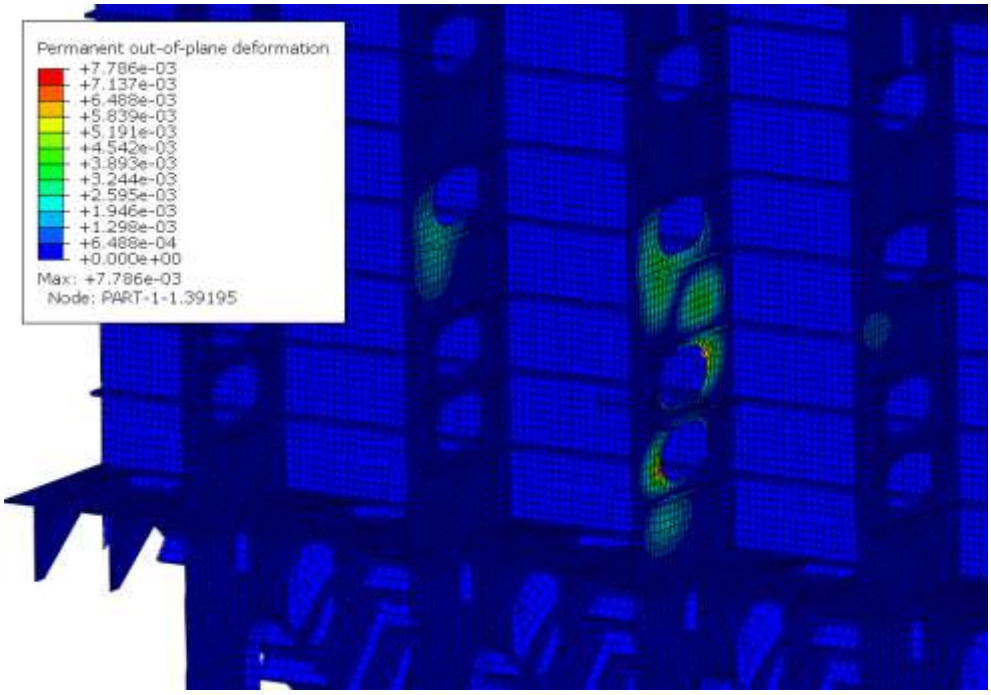

Figure 108 Permanent out-of-plane deformation for the critical load case for webframe of 58 500 DWT IA vessel, at plastic limit load (380 % of rule load).

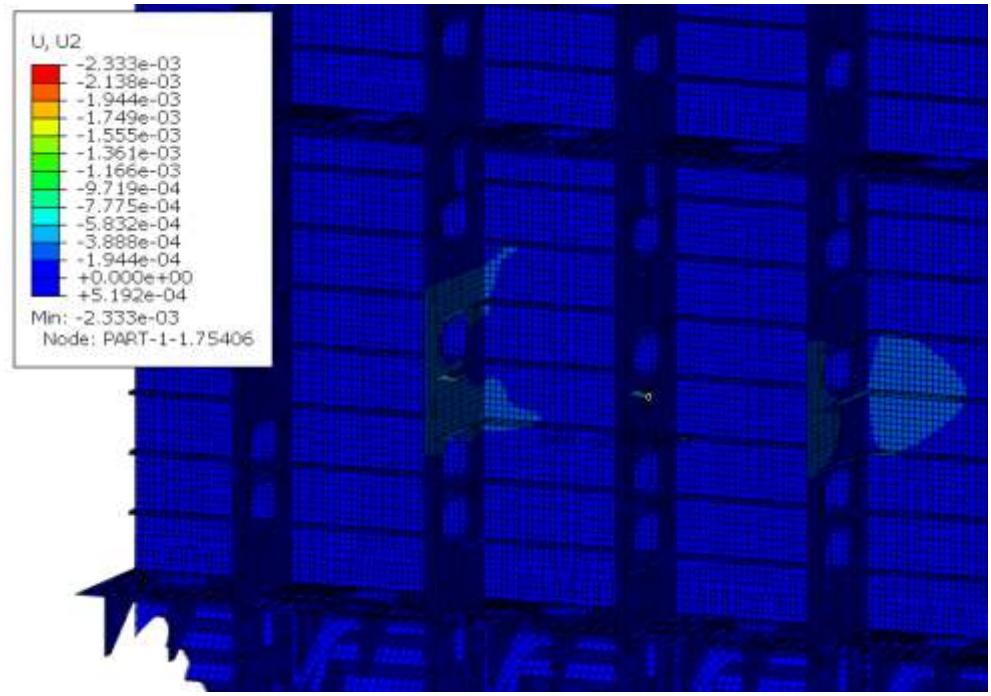

Figure 109 Permanent deformation perpendicular to shell for the critical load case for webframe of 58 500 DWT IA vessel, at plastic limit load (380 % of rule load).

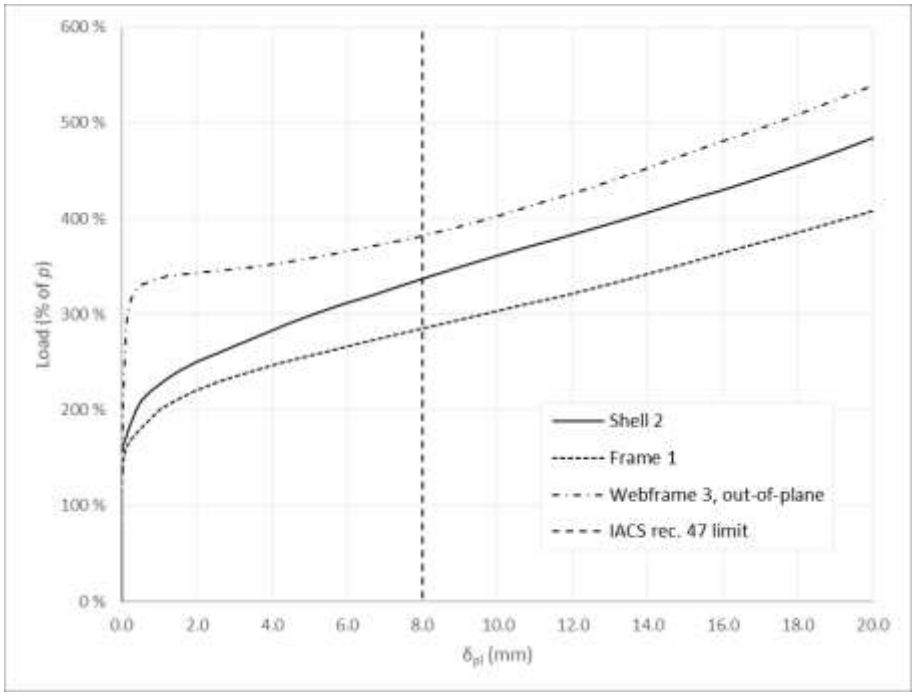

Figure 110 Comparison of load – permanent deformation curves for most onerous load case for each structural element, 58 500 IA vessel.

6.9 Discussion

Overview of the results is shown in Table 23. While there is some variation in the results, in general it can be concluded that the plastic capacity of the shell plate and framing is typically around 300 to 350 % of the rule load. It should be remembered that the rule load is made to be used for designing the structure against elastic limit (first yield), and the plastic limit used here includes permanent set of 8 mm, and thus it is expected that the plastic capacity of the structure is much higher than elastic capacity.

Table 23 Summary of plastic capacity of each structure for all studied vessels.

Ship	Framing	Shell	Frame	Primaries
3 000 DWT IA	Transv.	362 %	336 %	472 %
10 000 DWT IC	Longit.	490 %*	390 %	1011 %
10 000 DWT IA	Transv.	429 %	390 %	629 %
10 000 DWT IAsuper	Transv.	346 %	332 %	543 %
58 500 DWT IA	Longit.	337 %	285 %	382 %
** Shell capacity for 10 000 DWT IC could not be determined by FE, estimated with Hayward method*				

Part of the variation between the vessels may be due to plate thicknesses and profiles having been selected in typical shipbuilding fashion, using available standard thicknesses and profiles. Especially for bulb flats, this might lead to either a frame that just fulfils the requirement or to one that has some spare capacity, depending on how the list of standard profiles aligns with the required section modulus and shear area. This can be examined for the example vessels in scantlings summary presented in Table 3. It is recommended to do further research with exact minimum scantlings to remove this source of variation from the results before the final rules are set.

7. Conclusions and recommendations

Earlier studies and application to analysis of Polar Class vessels prove that non-linear finite element method is suitable tool for analysing the load-carrying capability of ice strengthened structures [4] [5] [6] [3]. Based on this study, it can be applied also to ships designed with Finnish-Swedish Ice Class Rules.

The advantage of this approach is that the limit state is tied directly to the goal, which is avoiding ice damages, understood here as permanent deformation that goes beyond normal building tolerances, rather than elastic capacity and assumption of certain plastic margin. Moreover, as the non-linear finite element analysis can consider buckling and load transfer between members, there is no need for strict guidance on structural details such as brackets, stiffening and end connections, giving more design freedom for the builders to seek optimal solutions.

The downside of the non-linear finite element method is obviously the required effort in both modelling and analysing the structure. Therefore, it is clear that if non-linear FEM is added to FSICR, it should be added as optional method that can be used instead of prescriptive rules, rather than to replace the current rules.

The study on mesh size was carried out with 50x50 mm mesh and 25x25 mm mesh. The 50x50 mm mesh resulted in 16 elements between frames and 3 elements across stiffener web. In cases where there is no major buckling of primary structures no notable difference was seen in the results and thus the 50x50 mm mesh should be suitable for use. However, if buckling of primary structures is analysed the mesh density has to be considered. Finer mesh with simple material models resulted in buckling with lower load levels.

Care should be taken when choosing the size of the model and the sections where the model is cut from the vessel. It seems reasonable to require a model with the double bottom to be modelled. In longitudinal direction it was found out for the test case that a 12 web frame long model worked well but 4 web frames was too small. The ship should be cut in longitudinal direction at stiff locations, for example bulkhead. At the cross section all degrees of freedom should be fixed. If no such bulkhead is present the length of model and should be carefully considered, it might need to be longer than 12 web frames. On the various vessels, it was noted that if load was closer than two webframe spacings from the boundary condition, the boundary started to have notable effect on the stress field. Thus, it is recommended that the model is limited to transverse bulkheads or if these are not available, extended at least 2 and preferably more webframe spacings from the load location.

The whole width of the ship need not to be modelled as the loading is concentrated in the side plating. A practical choice is to cut the ship along the centre line and define symmetric boundary conditions. At the centre line horizontal displacement is to be fixed as well as rotations about ship longitudinal and vertical axes.

In short, a simple fully fixed boundary condition at the rigid transverse section, such as watertight bulkhead, combined with a symmetry condition at the centre line should work well.

Material study was carried out for four different materials. Two material models (ABS, DNV) represented more detailed models with multiple parameters for the stress-strain curve. In the range of loads and deformations required in the analysis, there was not major difference between the material models. With very large deformations there can be differences but these are probably not relevant. Thus, for sake if simplicity in the rule formulation, the bi-linear model with proposed 1000 MPa plastic modulus would be suitable for this sort of analysis. This model is easy to formulate for different steel materials.

The best way to define the capacity of the structure was concluded to be to use permanent (plastic) deformation, as it is robust against mesh and modelling variations [3]. The allowed plastic deformation was tied to IACS recommended newbuilding tolerances, following the logic by [4] and [3].

For the analysed vessels, the typical capacity of shell plating before reaching the allowed deformation limit was about 350 to 360 % of the rule design load. The capacity for longitudinally framed vessels was somewhat higher than that of transversally framed vessel, as expected, as rules allow reduction of design pressure with a factor of 0.75 for shell of transversally framed vessels. It should be noted that these were calculated using gross thicknesses. With net thicknesses, the capacity would be slightly lower.

For the framing, the typical capacity was about 350 % of the rule design load. It was also found out that at the defined limit load, all frame profiles had adequate stability, and buckling and tripping were successfully limited by the current stability criteria in the rules.

For primary structures, it became evident that for a typical vessel with double side and primaries as plates through the double side, the capacity is limited by the stability, rather than bending of the members. Nevertheless, capacity of the primaries was typically about 600 % of the rule design load, with notable large variation. The large variation was because the scantlings were mainly driven by the fixed minimum thickness of 9 mm, while the ice load varied depending on the vessel. Even the lowest case of 382 % had higher capacity than the shell plate and frames, ensuring proper structural hierarchy. It seems that for a typical double side construction, the minimum thickness requirements results in a primary structure with adequate stability and capacity.

Area that would need further research before new Rules are written would be to expand this study to cover other relevant ship types, such as ferries, container vessels, RoRo vessels and tankers.

Other area which would require further research is behaviour of the primary structures, i.e. web frames and stringers / platforms. As it was found out that typical plate structures through double side have ample bending capacity and are purely limited by buckling, some further study into stiffening arrangements should be made in addition to the typical ones used in this study. In addition, it should be studied how vessels with single skin construction and open T-girder type primaries behave.

It was also noticed that the margin between elastic limit (design point in current FSICR) and plastic limit (as defined here as permanent deformation of IACS rec. 47 limit values) varies slightly depending on vessel size and ice class. For vessels with higher ice loads, the margin is smaller. The reasons for this trend should be studied and understood, so that correct design limits can be set for all vessels.

It would also be beneficial to study if there is any difference between midbody and bow. In principle, these are designed the same way. However, in bow the design load is higher, and due to hull shape, framing is not perpendicular to shell plating, which might create some new phenomena.

8. Summary

The goal of the study was to lay groundwork for implementing guidelines in the Finnish-Swedish Ice Class Rules (FSICR) for using direct calculation methods (e.g. Finite Element Method, FEM) for assessing hull structural strength in the case of ice loads.

Major part of the work was to study in practice with FE analysis how the proposed concepts on modelling and criteria would work on different sized vessels with different ice class. It was decided to focus on general / bulk cargo vessels as these are most frequent ship type operating in ice in the Baltic Sea. Three different sizes (3000 DWT, 10 000 DWT and 58 000 DWT) of vessels, corresponding to typical sizes on the Baltic Sea, were designed and modelled. From 10 000 DWT ship three different ice class (IA, IASuper and IC) versions were modelled.

The Baseline 10 000 DWT IA model worked as test model for testing how mesh size, model size, boundary conditions and different material models affect the results. From these studies, results were gathered for suitable proposals for the future guideline text.

For determining the plastic capacity of the structure, criteria were chosen to be to limit the permanent deformation of the structure to remain below limits of IACS newbuilding quality standard [1]. All chosen vessels were loaded with various load patches to understand the capacity of the structure against the chosen criteria, and to find the most onerous load patch locations and sizes. The load patches followed the FSICR. In general, the plastic capacity of the shell and framing was found to be about 350 to 360 % of elastic rule design load. For stringers and web frames, the typical double side construction resulted in structure where capacity is not limited by bending capacity, but rather by buckling, and clear conclusions of capacity of structures according to current rules could not be drawn. For this, further research with single skin type vessels is recommended.

Finally, some recommendations for future rule formulation are given. However, further research is required before the final rule formulation can be given.

9. References

[1] International Association of Classification Societies (IACS), Recommendation No.47 Shipbuilding and repair quality standard, IACS, rev. 8, 2017.

[2] J. Pearson, R. Hindley and J. Crocker, “Icebreaker grillage structural interaction and the characteristic stiffness curve,” in *SNAME World maritime technology conference*, Providence, Rhode Island, 2015.

[3] V. Valtonen, J. Bond and R. Hindley, “Improved method for non-linear FE analysis of Polar Class ship primary structures,” *Marine Structures,* vol. 74, 2020.

[4] American Bureau of Shipping (ABS), Rules for building and classing marine vessels - Part 6 Chapter 1 Strengthening for navigation in ice, ABS, 2022.

[5] Lloyd's Register, *Guidance Notes for Non-Linear Analysis for the Primary Support Structures for Polar Class Vessels,* 2022.

[6] Det Norske Veritas (DNV), Guidance Notes for Non-Linear Analysis for the Primary Support Structures for Polar Class Vessels, DNV, January 2022.

[7] V. Valtonen, “Impacts of nonlinear vs. linear finite element analysis on ice-strenghtened primary structures,” in *Proceedings of the 25th International Conference on Port and Ocean Engineering under Arctic Conditions, POAC*, Delft, the Netherlands, 2019.

[8] American Bureau of Shipping (ABS), GUIDANCE NOTES ON ICE CLASS, 2014.

[9] K. Riska and J. Kämäräinen, “A review of ice loading and the evolution of the Finnish-Swedish ice class rules,” *SNAME Transactions,* 2012.

[10] P. Kujala, Damage statistics of ice-strengthened ships in the Baltic Sea 1984-1987, Winter Navigation Research Board, Research report No.50.

[11] S. Hänninen, Incidents and accidents in winter navigation in the Baltic Sea, winter 2002-2003, Winter Navigation Research Board, Reserach report No. 54.

[12] Finnish Board of Navigation, Rules for Assigning ships separate ice-due classes "Finnish-Swedish ice class rules", 1971.

[13] Finnish Board of Navigation, Rules for Assigning ships separate ice-due classes "Finnish-Swedish ice class rules", 1985.

[14] Finnish Maritime Administration, Finnish-Swedish ice class rules, 2002.

[15] Finnish Maritime Administration, Ice class regulations 2008 (Finnish-Swedish ice class rules), 2008.

[16] Transport Safety Agency TraFi, Ice class regulations 2010 "Finnish-Swedish ice class rules 2010", 2010.

[17] J. Adams, An Extended Inverse Method for the Determination of Ice-Induced Loads on Ships, Master's thesis, Aalto University, 2018.

[18] M. Määttänen, P. Marjavaara, S. Saarinen and M. Laakso, “Ice crushing tests with variable structural flexibility,” *Cold Regions Science and Technology,* vol. 67, no. 3, pp. 120-128, 2011.

[19] I. Perälä and M. Tikanmäki, “Study on the Current Winter Navigation Challenges Related to EEDI regulations at the Bay of Bothnia,” Winter Navigation Research Board, Report No. 111, 2020.

[20] Väylävirasto, “Saimaan kanavan sulkujen pidentäminen, hankearviointi,” Väyläviraston julkaisuja 31/2020, 2020.

[21] J. Alanko, Laivan yleissuunnittelu, Turku, 2007.

[22] Dassault Systemes - SIMULIA, Abaqus user's manuals, elements, SIMULIA, 2021.

[23] American Bureau of Shipping (ABS), Guidance notes on nonlinear finite element analysis of marine and offshore structures., ABS, 2021.

[24] Det Norske Veritas AS (DNV), Determination of Structural Capacity by Non-linear FE analysis Methods. Recommended Practice DNV-RP-C208, DNV, 2013.

[25] European Committee for Standardization, EN-10025. Hot rolled products of structural steels. Part 2, 3, 4 and 6, 2004.

[26] European Committee for Standardization, EN-10225. Weldable structural steels for fixed offshore structures – Technical delivery conditions., 2009.

[27] D. P. Walter, Formulas for Stress, Strain, and Structural Matrices, Second Edition, John Wiley & Sons, Inc., 2004.

[28] Traficom, Ice Class Regulations and the Application Thereof, Traficom, 2021.

[29] Russian Maritime Register of Shipping, Rules for the classification and construction of sea-going ships, part II hull, RMRS, 2022.

[30] Det Norske Veritas (DNV), Rules for classification of ships - Part 6 Additional class notations - Chapter 6 Cold climate, DNV, July 2022.

[31] R. Hayward, Plastic response of ship shell plating subjected to loads of finite heigth, Master's Thesis, Memorial University of Newfoundland, 2001.

[32] American Bureau of Shipping, Guidance notes on Ice Class, ABS, February 2014.